THE INTERACTION BETWEEN HUMAN VISION AND EYE MOVEMENTS IN HEALTH AND DISEASE

Richard Joel Sylvester

Institute of Cognitive Neuroscience
Wellcome Trust Centre for Neuroimging
Institute of Neurology
University College London

Prepared under the supervision of:
Professor Geraint Rees
Professor John Driver

Submitted to UCL for the Degree of PhD

DECLARATION

I, Richard Sylvester, confirm that the work presented in this thesis is my own. Where information has been derived from other sources, I confirm that this has been indicated in the thesis.

Part of the work presented in Chapters 3, 5 and 7 has been published as the following papers.

Sylvester,R., Haynes,J.D., and Rees,G. (2005). Saccades differentially modulate human LGN and V1 responses in the presence and absence of visual stimulation. Current Biology. *15*, 37-41.

Sylvester,R., Rees,G. (2006). Extraretinal saccadic signals in human LGN and early retinotopic cortex. Neuroimage. 30(1):214-9.

Sylvester,R., Josephs,O., Driver,J., Rees,G. (2007) Visual FMRI responses in human superior colliculus show a temporal-nasal asymmetry that is absent in lateral geniculate and visual cortex. Journal of Neurophysiology. 97(2):1495-502.

ACKNOWLEDGEMENTS

Above all, I would like to thank my supervisor Geraint Rees for his encouragement, guidance, patience and for his invaluable ability to remain positive and enthusiastic in almost any situation. In addition I am very grateful to my second supervisor Jon Driver, whose ability to get to the crux of a problem and then design a workable experiment to test it was crucial in the construction of this thesis.

I would also like to thank the members of the Rees lab – David, Sue, John, Phillip, Bahador, Davina, Rimona, Elaine, Claire, Christian and Ayshe for all their help and advice, and also for the many evenings spent discussing a range of relevant (and trivial) issues in the Queen's Larder. In addition without the input of many people at the ICN including Eliot, Stephan, Neil and Christian my time there would have been less productive (and less interesting). Klass and Will were both instrumental in helping with the DCM analysis. Thanks also to all the ICN and FIL support staff – Michelle, Karen, Dominic, Marcia, Amanda, Jan, David, Ric, Rachel, Chris, Lambert and Martin for all their help. Special thanks to Eric, for providing much needed practical support in overcoming a myriad of technical issues.

Thanks also to the Wellcome Trust and the Guarantors of Brain for funding me.

I would also like to thank my family and friends. In particular, Emma, for her unfailing support and many ideas for imaging studies that I did not have time to carry out. Also thanks to Eddie for his willingness to lie in the scanner for many hours of testing. Thank you to Max, who has been a great distraction during the writing stage of this thesis. Finally thanks to my parents for making it all possible.

ABSTRACT

Human motor behaviour depends on the successful integration of vision and eye movements. Many studies have investigated neural correlates of visual processing in humans, but typically with the eyes stationary and fixated centrally. Similarly, many studies have sought to characterise which brain areas are responsible for oculomotor control, but generally in the absence of visual stimulation. The few studies to explicitly study the interaction between visual perception and eye movements suggest strong influences of both static and dynamic eye position on visual processing and modulation of oculomotor structures by properties of visual stimuli. However, the neural mechanisms underlying these interactions are poorly understood.

This thesis uses a range of fMRI methodologies such as retinotopic mapping, multivariate analsyis techniques, dynamic causal modelling and ultra high resolution imaging to examine the interactions between the oculomotor and visual systems in the normal human brain. The results of the experiments presented in this thesis demonstrate that oculomotor behaviour has complex effects on activity in visual areas, while spatial properites of visual stimuli modify activity in oculomotor areas. Specifically, responses in the lateral geniculate nucleus and early cortical visual areas are modulated by saccadic eye movements (a process potentially mediated by the frontal eye fields) and by changes in static eye position. Additionally, responses in oculomotor structures such as the superior colliculus are biased for visual stimuli presented in the temporal rather than nasal hemifield.

These findings reveal that although the visual and oculomotor systems are spatially segregated in the brain, they show a high degree of integration at the neural level. This is consistent with our everyday experience of the visual world where frequent eye movements do not lead to disruption of visual continuity and visual information is seamlessly transformed into motor behaviour.

CONTENTS

LIST OF FIGURES

LIST OF TABLES

CHAPTER 1 : GENERAL INTRODUCTION

1.1 Introduction

Over recent decades there has been remarkable progress towards an understanding of the neural processes that underpin human cognition and behaviour. The prevalent approach, utilised with great success, has involved the study of brain systems (and functions) in relative isolation. While this method has enabled mapping of brain structures according to their predominant function, it has often failed to address how closely related behavioural processes are neurally integrated. The successes and limitations of this method are clearly illustrated by considering the study of human vision and eye movements. The visual system has predominately been investigated by measuring its response to the systematic manipulation of basic visual properties (such as colour, contrast or motion) while other factors affecting visual input such as eye movements are controlled. This method eliminates 'confounding' effects of eye movements by either presenting visual stimuli very briefly or requiring subjects to maintain central fixation. In contrast, the oculomotor system has largely been investigated by measuring its response to systematic manipulations of oculomotor behaviour in an impoverished visual environment. This approach has resulted in a detailed understanding of the neurophysiology of both the visual and the oculomotor systems, but relatively little information about how they interact.

However, outside of the strictly controlled environment of vision science experiments, successful human behaviour requires that vision and eye movements are highly integrated. For instance, normal vision is characterized by frequent saccades, blinks and changes in the locus of fixation, while oculomotor behaviour usually takes place in a complex and rich visual environment. Some human behavioural studies have indeed demonstrated profound perceptual effects of eye movements on vision (and similarly profound effects of vision on oculomotor behaviour) and in non-human subjects the neural basis of these interactions has been explored. But, the neural mechanisms that subserve successful integration of the visual and oculomotor systems in the human brain

are not well defined. This thesis is concerned with investigating these mechanisms to generate an understanding of human vision that reflects the importance of interactions between the visual and oculomotor systems.

1.2 The role of eye movements in human vision

In order to appreciate why the visual and oculomotor systems require such close neural integration, one must first consider why eye movements are ubiquitous in human vision. The most important reason for eye movements is readily apparent from examining the anatomical organisation of the retina and early visual system. The structure of the retina is not homogenous; the fovea is highly specialised for detailed processing of visual information. Although the foveal region represents the central 1º of the visual field, it contains the vast majority of cone photoreceptors that are required for high acuity colour vision (Figure 1.1).

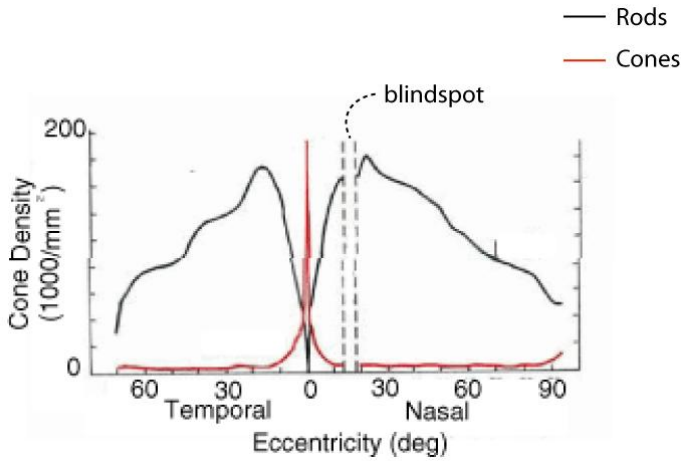

Figure 1.1. Density distribution of cones and rods on the human retina with respect to eccentricity
Cones which carry information about detail and colour are concentrated on the portion of the retina, the fovea, that represents the central portion of the visual field (from Wandell, 1995).

In addition, despite containing the highest density of photoreceptors, other retinal cells at the fovea are displaced towards the periphery leading to a significant thinning of the retinal surface over the fovea (figure 1.2). This creates the foveal pit, which enhances the optical quality of the image reaching the foveal photoreceptors compared to the image

reaching photoreceptors in other parts of the retina. Therefore high acuity processing of visual information anywhere outside the central few degrees of vision is not possible.

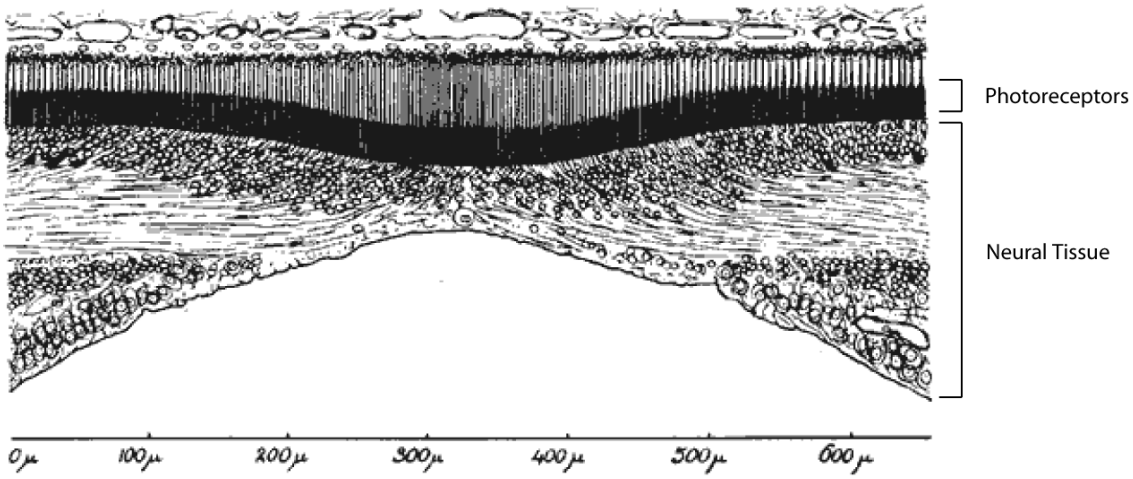

Figure 1.2. Cross-section of the human retina at the foveal region demonstrating the foveal pit. Note that the surface of the retina thins at the point where the concentration of photoreceptors is greatest. Measurements are given in microns. 1 degree of visual angle is approximately 300 microns (from Polyak, 1957).

Following transduction of visual information by retinal photoreceptors, the visual signal then proceeds via ganglion cells along the optic nerve to the visual areas of the brain. One of the defining features of the visual projection is that spatial relationships are maintained and a retinotopic map of the visual world is reproduced at each level of the early visual system. However, there is evidence that the visual projections undergo a spatial transformation so that projections away from the central regions are given uniformly decreasing weighting further magnifying the foveal representation (Azzopardi and Cowey, 1996;Connolly and Van Essen, 1984;Malpeli and Baker, 1975;Perry and Cowey, 1985;Van Essen et al., 1984). This is illustrated by the increased foveal representation seen in macaque V1 compared to LGN (see Figure 1.3). Studies of human LGN and V1, while less clear, suggest a significant proportion (around 50-80%) of the surface volume of LGN and V1 represent the central 15° of the visual field (Dougherty et al., 2003;Schneider et al., 2004).

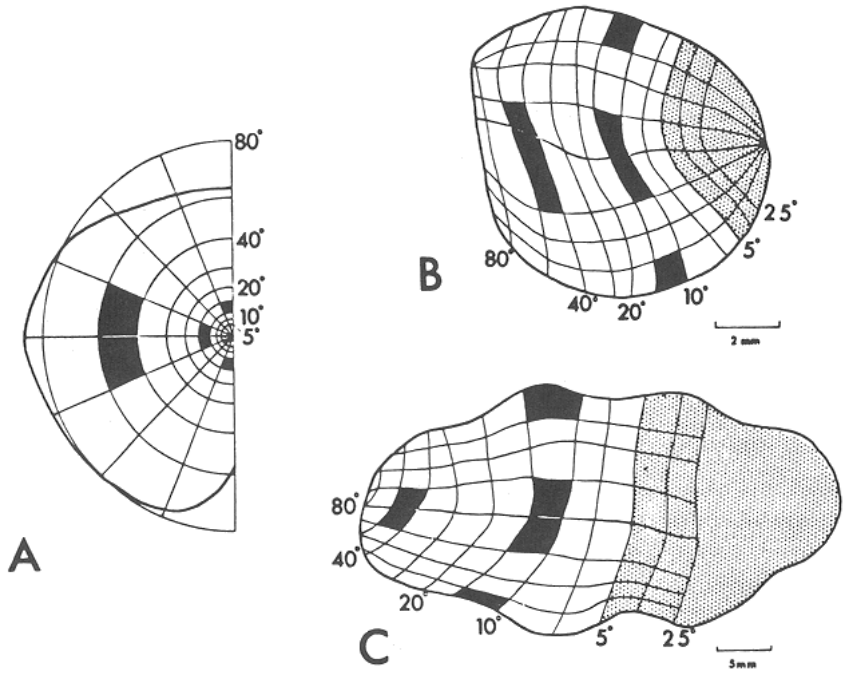

Figure 1.3. The mapping of the visual field (A) on the LGN (B) and V1 (C) in the macaque monkey. Note that the representation of the central 5 degrees (shaded areas) in the visual field occupies about 20% of the LGN and 40% of the cortex (from Connolly and Van Essen, 1984).

The major advantage of this method of organising the visual system is a reduction in the 'hardware' required to process visual information. If the density of photoreceptors in the whole of the retina was matched to that at the fovea, the diameter of the optic nerve would be hugely increased and the brain would have few neurons left to process other sensory modalities let alone higher cognitive functions. However, the disadvantage of this system is that visual acuity rapidly decreases when objects are even a small distance away from the fovea (Figure 1.4).

Figure 1.4. A letter chart that accurately represents the perceptual consequences of the variation in visual acuity with retinal eccentricity.

When the centre is fixated each letter is ten times its threshold legibility. Clearly the size that a letter must be to be legible rapidly increases with the retinal eccentricity that letters are presented at (adapted from Anstis, 1974).

Although only the foveal portion of the visual scene can undergo detailed processing by the visual system, humans are clearly capable of seeing fine detail anywhere in the visual field. Viewing non-central parts of the visual field using high acuity colour vision requires efficient foveation of the location of interest and this is primarily achieved through eye movements. Eye movements can be classified according to whether they are involved in gaze-holding or gaze-shifting. Gaze-holding eye movements enable the visual image to be held on the fovea during head movements and include the vestibular-ocular reflex (driven by vestibular output) which acts to move the eyes an equal but opposite amount in the opposite direction to head movements and optokinetic nystagmus (driven by full field motion across the retina) which allows tracking of objects while in motion while the head remains still. Gaze-shifting eye movements are concerned with making sure that targets of interest are foveated and include saccades and smooth pursuit. Saccadic eye movements are key to shifting gaze so that specific locations in the visual

field are brought onto the fovea (although in subjects with congenital opthalmoplegia, this can be successfully achieved using head movements, see Gilchrist et al., 1997). While vergence and smooth pursuit eye movements allow foveation of objects moving in depth or across the visual field respectively.

Thus the critical role of eye movements is to rapidly and accurately bring and hold locations of interest onto the fovea. To successfully achieve this crucial function, the oculomotor system clearly requires detailed visual information (which one would expect to be derived from the visual system). In addition, in order to minimise disruption to visual perception and allow successful visually guided action, the visual system also requires detailed information about ongoing oculomotor behaviour (which one would expect to derive from the oculomotor system). Consequently one might expect that the visual and oculomotor systems interact at multiple levels. Although this interaction is poorly defined in man, the integration of these two systems can be illustrated by considering their anatomical organisation and the response properties of their components in non-human primates.

1.3 The anatomy of interactions between vision and eye movements

The primate visual system has a complex and highly interconnected structure (Felleman and Van Essen, 1991) illustrated in figure 1.5. However, this hierarchy can be simplified into two parallel processing pathways: a ventral stream projecting from the primary visual cortex (V1) to the inferotemporal cortex, and a dorsal stream projecting from V1 to the posterior parietal cortex (Ungerleider and Mishkin, 1982). In this proposed scheme (shown in figure 1.6), the two streams mediate different components of visual processing, with the ventral stream handling information about an object's features (the ‘what’ pathway) and the dorsal stream mediating information about its spatial location (the ‘where’ pathway).

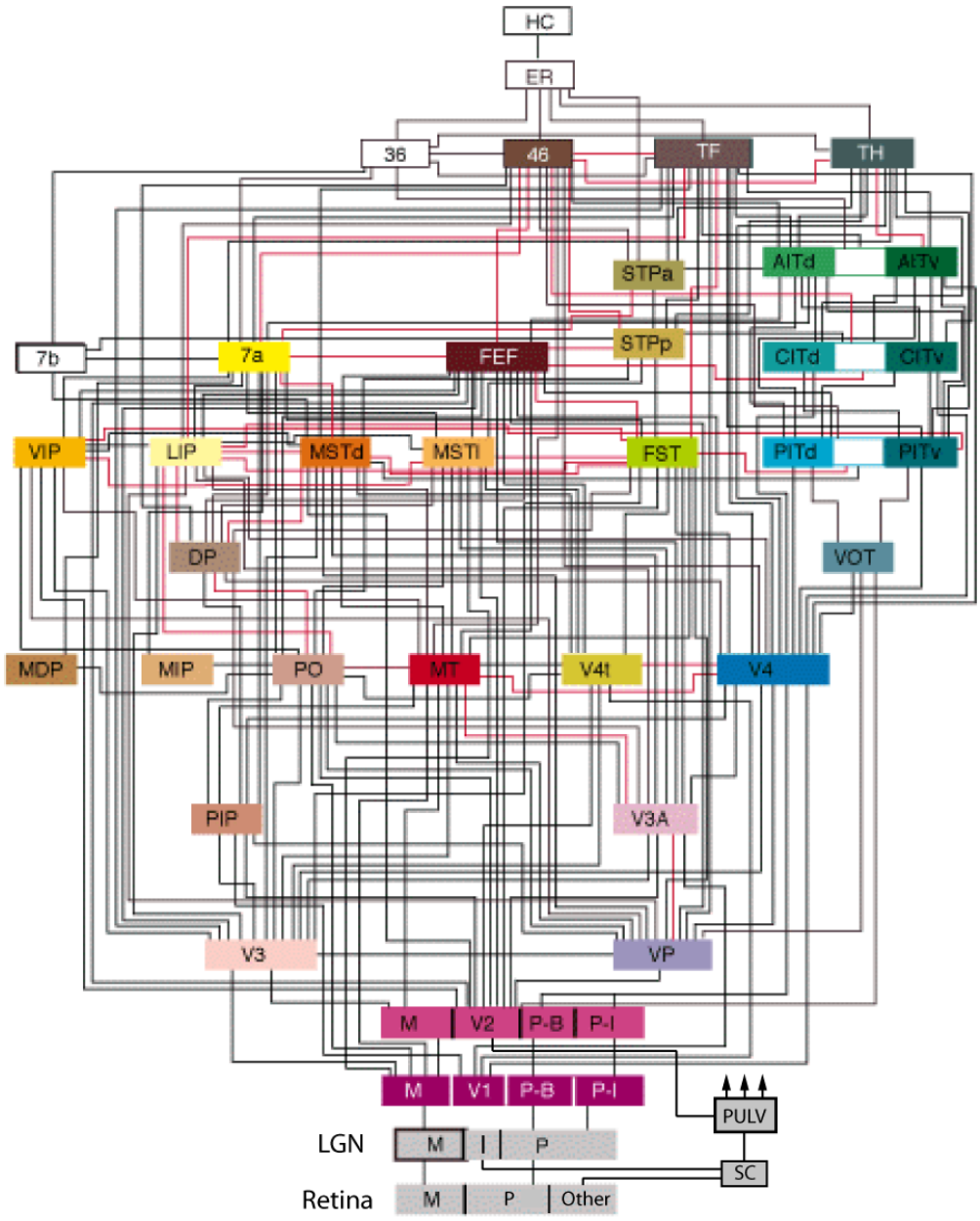

Figure 1.5. The hierarchy of visual areas in the macaque, based on laminar patterns of anatomical connections (adapted to include subcortical regions from Felleman and Van Essen, 1991).

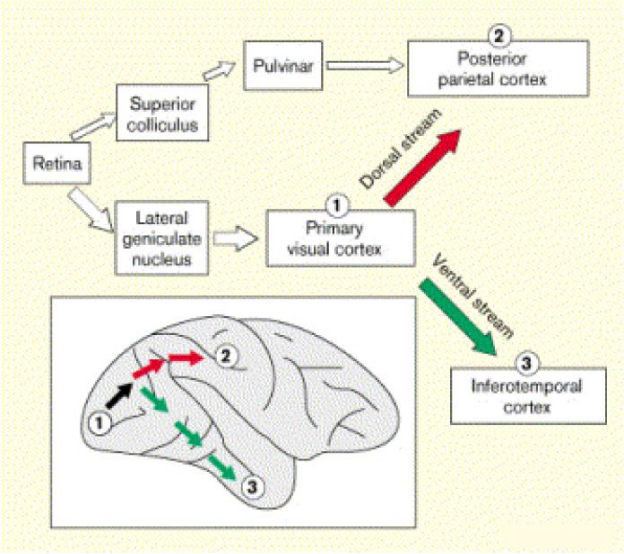

Figure 1.6. The dorsal and ventral streams of the primate visual system.

The diagram of the macaque brain (inset) shows the approximate routes of the cortico-cortical projections from the primary visual cortex to the posterior parietal and the inferotemporal cortex, respectively (from Goodale, 1998).

This theoretical framework assumes a predominantly sensory role for the visual system, but the dorsal stream in particular seems to have a key role in visuomotor control. For example, visually sensitive cells in the posterior parietal cortex have been implicated in visual fixation (Andersen and Mountcastle, 1983), pursuit and saccadic eye movements (Andersen et al., 1987), visually guided reaching (Snyder et al., 1997) and the manipulation of objects (Murata et al., 1996). This has led to proposals that the dorsal and ventral streams reflect vision for action and vision for perception respectively (Milner and Goodale, 1995).

As neurons in dorsal stream structures respond to oculomotor activity while visual stimulation remains constant, one might expect them to have close links to the oculomotor system. Indeed, brain areas involved in saccade generation such as the posterior parietal cortex (PPC) and superior colliculus (SC) (see Figure 1.7) are also either part of or directly connected to the dorsal stream.

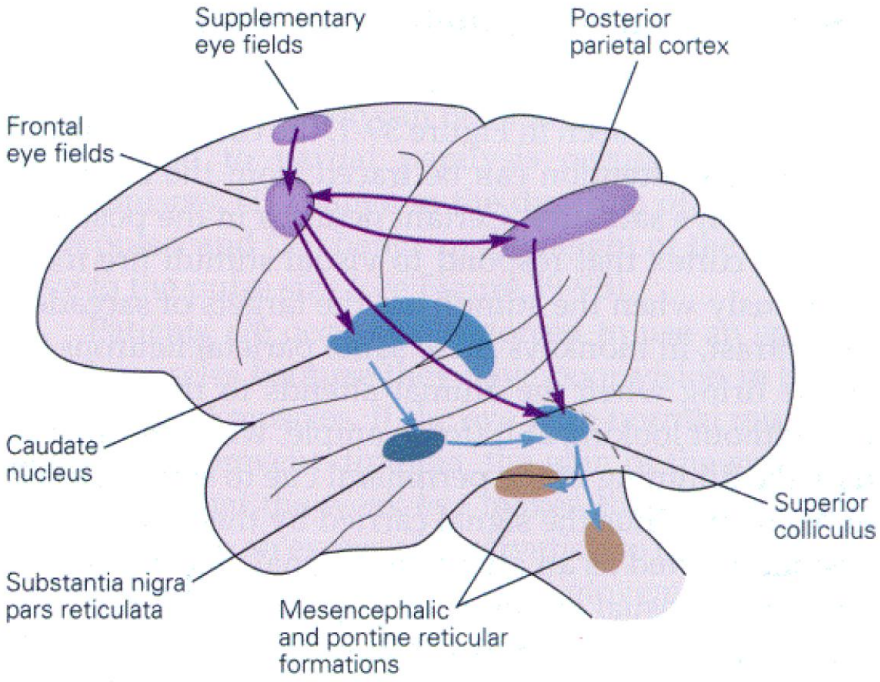

Figure 1.7. Schematic diagram of the primary structures involved in the neural control of saccades.

These structures (and also the frontal eye fields - FEF) have extensive connections with retinotopic early visual areas, and are involved in transforming visual signals into oculomotor commands (Schall and Thompson, 1999;Snyder et al., 1997).This is reflected in the response properties of neurons within these structures. In both human and non-human primates, the PPC (Bruce and Goldberg, 1985;Sereno et al., 2001), the SC (Cynader and Berman, 1972;Schneider and Kastner, 2005) and also the frontal eye fields (Colby et al., 1996;Hagler, Jr. and Sereno, 2006) respond robustly to visual stimulation and show a degree of retinotopic organisation in addition to activity associated with oculomotor behaviour. In addition these structures may also influence visual processing through direct modulation of activity in early visual areas. Before considering this possibility, I will review the mechanisms underlying saccade generation in human and non-human primates. This will allow a fuller description of the functions of the SC, PPC and FEF, but will also illustrate the more general role of visual information in guiding oculomotor behaviour.

1.4 Saccade generation – Visual influences on oculomotor behaviour

The neural mechanisms underlying saccadic eye movements are of great relevance to this thesis as many of the experiments presented later use saccades to investigate oculomotor influences on visual processing, but also because saccade generation fundamentally requires the integration of visual and oculomotor information. Therefore I will review the mechanisms of saccade generation and in particular the processes that illustrate interactions between the visual and oculomotor systems.

Generating saccadic eye movements requires involvement of both subcortical and higher cortical brain structures, reflecting the multiple levels of control needed. At the lowest level, brainstem structures control the eye muscles that generate the forces required to rapidly and accurately move the eyes to a new fixation point. At the intermediate level, the SC is involved in creating commands that allow saccades to be made to specific locations in space. Finally, higher level cortical areas including the PPC and FEF are involved in the planning and execution of object centred movements and the selection of targets for upcoming saccades.

The mechanisms by which eye muscles are controlled are least relevant to this thesis, but require a brief explanation in order to understand the later levels of saccade control (see Carpenter, 1988 for a more detailed review). The rapid changes in force required for short lasting saccades are generated by a burst of activity in oculomotor motor neurons during a saccade and a reduction in this rate to maintain fixation. This change in firing rate is under the control of two types of neuron located in the brainstem. Burst units fire rapidly during saccades in a particular direction, while tonic units show activity that changes from one steady level to another to reflect eye position. Tonic units are driven by burst units (via a neural integrator), while burst units are under the control of omnipause cells (again located in the brainstem). At rest, omnipause cells fire continuously; but they pause for the duration of a saccade, thus determining its size. This sophisticated mechanism allows highly accurate, rapid saccades to be generated using a set of slowly responsive mechanical effectors (the eye muscles).

The specific location in space to which a saccade is made requires the integration of visual information with oculomotor commands. There is considerable evidence that this occurs in the SC. Macaque SC is anatomically arranged to enable transformation of visual (or other sensory) information into orienting behaviours (overt and covert). Histological staining reveals that the superior colliculus is a laminated structure, which can be anatomically and functionally subdivided into superficial and deep layers (King 2004). The superficial layers have a purely sensory role (Robinson and McClurkin, 1989) as they receive visual inputs directly from the retina via the retinotectal pathway (Schiller and Malpeli, 1977) and indirectly via corticotectal feedback projections from striate (Wilson and Toyne, 1970) and extrastriate cortex (Fries, 1984). In contrast, the underlying deep layers, sometimes subdivided into intermediate and deep zones, have both sensory and motor functions. Neurons in the deep layers can respond to auditory, tactile or visual stimuli and many receive converging modality-specific inputs that endow them with multisensory response properties. The deep layers output directly to oculomotor brainstem nuclei and are involved with initiating saccades (Sparks and Hartwich-Young, 1989). The intermediate layers contain a range of cell types including fixation cells which are active during fixation and inhibit saccades (Munoz and Wurtz 1993a, 1993b), build-up and burst cells (Munoz and Wurtz 1995a, 1995b) whose function in relation to saccade generation has already been discussed. Thus the superficial and deep layers of SC have well segregated functions mediated by independent inputs and outputs. This is illustrated differing effect of cooling of primary visual cortex on visual responses in superficial and deep SC cells (Schiller et al., 1984). Visual responses are abolished in deep layers but unaffected in the superficial layer. This functional segregation is analogous to the sensorimotor transformation that occurs in from the parietal visual areas to the FEF.

Neurons in the superficial areas are arranged in a systematic retinotopic map (Cynader & Berman 1972) and their responses are fairly invariant to specific stimulus characteristics such as colour and shape (Cynader and Berman 1972;Goldberg and Wurtz, 1972). As far as can be ascertained, human SC seems to follow a similar anatomical pattern (Hilbig et al., 1999;Laemle, 1981;Tardif et al., 2005) and also shows a degree of retinotopy

(Schneider and Kastner, 2005). In primitive visual systems, such as those of reptiles and amphibians, the tectum (analogous to mammalian SC) receives retinal projections from the contralateral eye only. This may reflect an anatomical adaptation to favour orientation shifts to stimuli located in the visual periphery in animals lacking binocular vision (a distinct advantage in rapidly responding to danger). Intriguingly, similar orienting biases (to the periphery of vision – the temporal hemifield) can be demonstrated in human subjects when stimuli are viewed monocularly (Rafal et al., 1991) suggesting that the more complex visual systems retain this bias in the SC. Testing this claim is one aim of the experiments presented in this thesis.

Neurons in the superficial layers of macaque SC have small receptive fields while those in the intermediate and deep layers have large receptive fields that taper off at the edges so that a visual target generates a diffuse 'hill' of neural activity in the deep layers (Waitzman et al., 1991). As outlined above, the deep layers have a predominantly motor function and stimulation of many deep neurons evokes an eye movement to a specific location in visual space (corresponding to the area represented by superficial layer neurons above them (Wurtz and Goldberg, 1972). Neurons at the rostral pole of the SC (corresponding to the fovea) project to omnipause cells and show similar activity patterns, firing rapidly while a target is being fixated, and pausing during a saccade (Munoz and Wurtz, 1993).

Although it is not entirely clear how the SC uses this neural machinery to generate saccades to specific locations in space, one model proposes the following elegant mechanism (Guitton, 1992). As a target appears in the visual periphery, it activates a corresponding collicular region (via the superficial and deep layers), but inhibits the fixation cells in the foveal region. This leads to omnipause cell inhibition and the saccade begins. Meanwhile, an efference copy is sent back to the SC, where it moves the hill of neural activity towards the fixation region, in correspondence with the simultaneous movement of the eye itself. When it finally reaches the fixation region, omnipause cells are activated, and the eye stops. Therefore, within the superior colliculus sensory information is utilized to guide oculomotor behaviour through the integration of sensory

and motor maps of visual space. Although the SC may create the command needed to move the eye to any particular location, it requires input from parietal and frontal occulomotor areas for other crucial components of the process of saccade generation. These include the integration of multimodal sensory information to allow planning and execution of saccades in object-centred space and the control of choice of saccade target. Within the parietal and frontal lobes specific regions show greater activation in association with different movements. The areas most associated with oculomotor behaviour are the FEF and lateral intraparietal area (LIP) in monkeys and their human homologues. Although I will consider the function of these areas independently, there may well be a degree of overlap in their role in saccade generation.

Primate FEF is involved in a range of oculomotor behaviours including intentional saccades, smooth pursuit and fixation. There is little doubt that the FEF has a crucial role in saccade generation. Low-intensity electrical stimulation of monkey FEF (Bruce et al., 1985) and TMS over the FEF in humans elicits saccades. The FEF is part of a network of human brain areas (including the PPC and supplementary eye fields) that is activated during saccades and fixation (Anderson et al., 1994;Berman et al., 1999;Darby et al., 1996;Luna et al., 1998). Furthermore, activity in presaccadic movement related neurons in the macaque FEF is sufficient to specify whether and when saccades will be produced (Hanes et al., 1998;Hanes and Schall, 1996), while the magnitiude of presaccadic BOLD activity in human FEF correlates with saccade reaction time (Connolly et al., 2005). In addition, reversible inactivation studies show that FEF is necessary to produce saccades (Sommer and Tehovnik, 1997). Lesions of the FEF in both human and non-human primates produce a similar range of deficits. These include deficits in generating saccades to briefly presented targets, in the production of saccades to two or more sequentially presented targets, in the selection of simultaneously presented targets, and in the execution of smooth pursuit eye movements (Tehovnik et al., 2000b).

FEF has clear connections to the motor portions of the SC (Segraves and Goldberg, 1987;Sommer and Wurtz, 2001;Sommer and Wurtz, 1998) but also has direct connections to brainstem saccade generator structures (Segraves, 1992) including the

rostral interstitial nucleus of the medial longitudinal fasciculus and the paramedian pontine reticular formation (Huerta et al., 1986). Therefore FEF can influence saccade generation via two pathways, one indirect via the deep layers of the SC (Hanes and Wurtz, 2001) and the other through directly influencing brainstem saccade generators. However, the FEF also has reciprocal connections with many visual cortical areas (Huerta et al., 1987;Schall et al., 1995;Stanton et al., 1995), the thalamus and the visual portion of the SC (Huerta et al., 1986;Sommer and Wurtz, 1998). These connections mean that human and non-human primate FEF respond robustly to visual stimulation and show a degree of retinotopic organisation in addition to activity associated with oculomotor behaviour (Colby et al., 1996;Hagler, Jr. and Sereno, 2006). This extensive convergence of afferents from the thalamus and cortical visual areas means that individual neurons in the FEF receive signals representing the colour, form, depth and direction of motion of objects in the image. Such convergence has led to proposals that the FEF contains a salience map of visual space that enables selection of targets for gaze shifts regardless of the visual properties of the target (Thompson and Bichot, 2005).

Area LIP also receives input from several visual areas, and is interconnected with the FEF and the SC (Blatt et al., 1990;Lynch et al., 1985). LIP neurons fire both when a salient visual stimulus is detected and during preparation and performance of a saccade (Gnadt and Andersen, 1988), suggesting involvement in target selection and saccade planning or execution. However there is contradictory evidence concerning the relationship between LIP activity and saccades. Some studies suggest that the activity of LIP neurons does not predict where or when a saccade will occur (Goldberg et al., 2002). This led to proposals that LIP activity represents a dynamic map of the locus of visual attention (Bisley and Goldberg, 2003a). For example, LIP neuronal activity significantly correlates with the level of attention at a specific location, but not with whether a saccade is actually attended or performed to that location (Bisley and Goldberg, 2003a). However, more recent studies (Janssen and Shadlen, 2005) suggest that LIP activity does predict saccadic reaction times, albeit not as well as FEF or SC activity (Everling and Munoz, 2000). Inactivation of macaque LIP produces deficits in saccadic target selection whereas saccade programming and execution remain unaffected (Wardak et al., 2002).

Additionally, the representation of visual space in both monkey and human LIP is modified in a way that is dependent on the metrics of upcoming saccades (Duhamel et al., 1992;Merriam et al., 2003), such predictive remapping may help to maintain a spatially accurate representation of the visual field despite a moving eye and a resulting change in the eye-centred frame of reference. Furthermore, higher cognitive processes such as decision making, reward expectancy and perception of time have also been related to activity of LIP neurons (Dickinson et al., 2003;Platt and Glimcher, 1999;Roitman and Shadlen, 2002).

It is clear that many of the processes underlying the generation and execution of saccadic eye movements require the successful integration of visual and oculomotor information. These range from functions carried out by low level structures such as directing eye movements to specific locations in space, to higher level functions such as saccade target selection. Therefore it is not surprising that each level of the oculomotor system receives visual input and this modulates oculomotor activity and subsequently behaviour. As discussed earlier, the influence of oculomotor information on visual processing is also likely to be important. For example, in compensating for visual disruption due to eye movements and mediating coordinate transformations from retinotopic to craniotopic space (c.f. remapping of visual responses in PPC). In the next section, I will review specific evidence showing that oculomotor activity directly influences neural activity in visual brain areas.

1.5 The neurophysiology of interactions between vision and eye movements

A range of experiments have shown that oculomotor behaviour can modulate neuronal responses in monkey early visual areas. For example, visually evoked neuronal activity in LGN, V1 and later visual areas is modified during saccades (Duffy and Burchfiel, 1975;Ramcharan et al., 2001;Reppas et al., 2002;Thiele et al., 2002). One possible explanation for these findings is that modulation of visually evoked activity during oculomotor behaviour is merely due to differences in the spatiotemporal characteristics of the pattern of light reaching the retina during eye movements compared to rest. However,

similar modulation still occurs when visual conditions are carefully matched between eye movement and rest conditions (Reppas et al., 2002) and visual activity is also influenced by alterations in the direction of static gaze (Campos et al., 2006;Rosenbluth and Allman, 2002;Trotter and Celebrini, 1999;Weyand and Malpeli, 1993) where this confound is far less pronounced. Together these results suggest that oculomotor behaviour itself can influence activity of neurons in visual areas, but the relevance of these findings to visual perception and the mechanisms that drive such effects are unclear.

Although the oculomotor system is likely to influence visual activity through a range of mechanisms, its effects can be broadly categorised as either compensating for disruptive consequences of eye movements (c.f. studies of saccadic effects on visual cortex activity cited above) or facilitating visual processing at sites in the visual field that are not currently foveated (but may well be foveated by an upcoming eye movement). The effects of these influences on visual perception have been studied using human psychophysical methods and will be considered in the next section. I will now concentrate on what is known about the underlying neural mechanisms and specifically on the second category of influences – facilitation of visual responses. The rational for considering the mechanisms underlying these facilitatory processes is based on the pre-motor theory of attention (Rizzolatti et al., 1987), which proposes that overt and covert shifts in attention have the same neural substrate (activity in oculomotor structures leading to an increase in visual processing power at a region in visual space that is currently non-foveal). Moving the eyes clearly leads to a new region of visual space being foveated and therefore facilitation of visual processing at this site. However, visual perception can also be enhanced by attending to non-foveal sites without moving the eyes. Indeed, neurophysiological studies in monkeys and functional imaging studies in humans have established that this covert attention enhances representations in visual cortex (Kastner et al., 1998;Luck et al., 1997;Moran and Desimone, 1985;Rees et al., 1997;Reynolds and Desimone, 2003). In addition, prior to saccade initiation, neurons in visual areas show facilitation of visual processing at the site of an upcoming saccade. This is illustrated by a study that mapped out the spatiotemporal receptive field of

macaque V4 neurons perisaccadically, finding that receptive fields shrunk and shifted towards the target of a saccade prior to saccade initiation (Tolias et al., 2001 - figure 1.8).

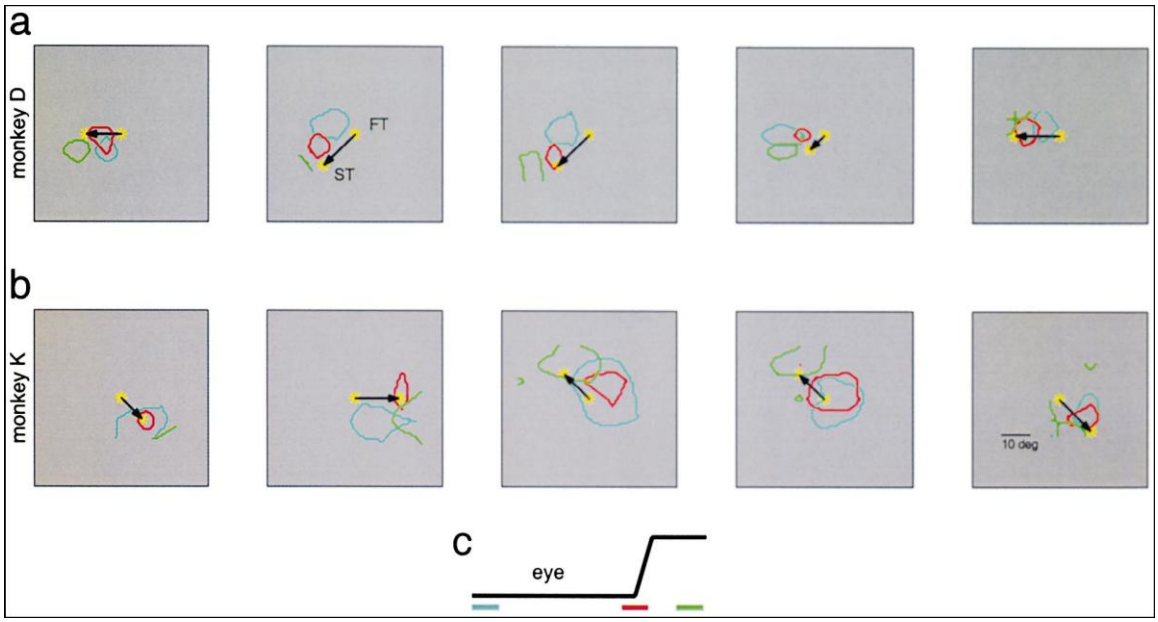

Figure 1.8. The location of V4 neurons presaccadic, perisaccadic and postsaccadic receptive field
A/B. Each plot shows the receptive field (RF) structure for a single V4 neuron (mapped using a probe stimulus). The edges of the presaccadic RF (shown in blue), the perisaccadic-RF (shown in red), and the postsaccadic-RF (shown in green) are drawn for each neuron. The perisaccadic RF shrinks and is shifted towards the saccade target. FT (fixation target). ST (saccade target).
C. The time-bins at which the presaccadic RF, perisaccadic-RF and postsaccadic-RF were calculated, shown schematically relative to the eye trace (Tolias et al., 2001).

Thus both covert and overt shifts of attention can lead to modulation of receptive field structure that is consistent with enhancement of visual processing at the locus of visual attention. In line with the premotor theory of attention, one possible explanation for these findings is that neural facilitation at covertly attended sites in the visual field (either prior to a saccade or without any eye movement) is directly caused by top down influences from oculomotor structures. Several studies have provided evidence that brain areas with established roles in the programming of visually-guided saccadic eye movements, such as the FEF (Moore and Fallah, 2001;Moore and Fallah, 2004), the SC (Cavanaugh and Wurtz, 2004;McPeek and Keller, 2004a;Muller et al., 2005b) and area LIP (Bisley and Goldberg, 2003b;Bushnell et al., 1981) are causally involved in covert attention. For example, Moore and colleagues found that subthreshold microstimulation of FEF neurons enhances retinotopically corresponding V4 responses to isolated stimuli, suggesting that FEF stimulation drives covert attention and its neural correlates in visual cortex (Moore and Armstrong, 2003a;Moore and Fallah, 2004). Spatial updating prior to saccades also occurs in FEF itself and this seems to be dependent on corollary discharge originating from the thalamus (Sommer and Wurtz, 2006).

These findings demonstrate that in non-human primates, under certain circumstances, there is a direct causal relationship between oculomotor activity and modulation of visual responses. There is far less evidence for similar neural mechanisms in humans. One approach to studying such questions in humans employed TMS stimulation of FEF and found modulation of BOLD responses in V1 using concurrent fMRI (Ruff et al., 2006). However, in general little is known about the neural mechanisms underlying oculomotor interactions with the visual system in man. In contrast, the effects of oculomotor behaviour on human visual perception have been extensively studied and can provide a basis for generating testable hypotheses regarding human the neural basis of integration of eye movements and vision.

1.6 Oculomotor influences on human visual perception

Although diverse effects of both dynamic oculomotor behaviour (saccades, blinks and pursuit) and changes in static eye position on human visual perception have been described, very few studies have examined their physiological correlates. As it is precisely these underlying neural mechanisms that this thesis seeks to explore, I will concentrate on findings that make specific predictions about the site of oculomotor effects on vision, or the specific nature of any effects (for instance inhibition or facilitation). This will allow the generation of hypotheses that can be empirically tested by directly measuring activity at various sites in the human visual system while varying the oculomotor behaviour of subjects.

1.6.1 Dynamic oculomotor behaviour

A range of oculomotor behaviours have been shown to influence human visual perception, but the effect of saccades has been studied most intensively. In contrast to monkey studies, where examining mechanisms of facilitation at covertly attended sites (or targets of upcoming saccades) has provided most insight, human psychophysics has concentrated on how the visually disruptive effects of saccades are avoided. During a saccade the visual image moves across the retina at high velocity, yet our perception of the visual world is stable and no blurring or motion of the visual scene is perceived. There seem to be a number of compensatory mechanisms that act to maintain visual continuity during saccades. Several groups have shown that there is a significant reduction in the sensitivity of the visual system during saccades (Bridgeman et al., 1975;Deubel et al., 1998;Honda, 1993;Honda, 1995;Ross et al., 1997 ;Morrone et al., 1997). Interestingly similar suppression of vision occurs during eyeblinks (Volkmann et al., 1980;Volkmann, 1986). In addition to a reduction in visual sensitivity, subjects mislocalize the position of stimuli presented during saccades in a way that is consistent with perisaccadic compression of visual space (Morrone et al., 2005). This may play a role in maintaining visuospatial relationships during saccades and is also seen during smooth pursuit eye movements (Brenner et al., 2001;Mateeff et al., 1981).

Detailed study of the reduction in visual sensitivity seen perisaccadically, has generated specific hypotheses regarding the underlying physiological processes. There is evidence that saccadic suppression of vision occurs after retinal processing (Diamond et al., 2000), but before high level visual information is extracted (Burr et al., 1982;Burr et al., 1994), suggesting involvement of the earliest stages of visual processing in the brain (LGN and early visual cortex). In addition, suppression is limited to visual stimuli processed by the motion processing magnocellular system (Burr et al., 1994), suggesting that activity in the magnocellular but not the parvocellular visual pathway is modulated by saccades. Finally suppression of vision occurs prior to saccade initiation (Burr et al., 1994) suggesting that an efference copy of the saccadic command (originating from structures involved in saccade generation) rather than feedback from eye muscles is the source of saccadic suppression. As outlined in the previous section, single cell recording in non-human primates has shown saccade related modulation of LGN and visual cortex activity (Duffy and Burchfiel, 1975;Ramcharan et al., 2001;Reppas et al., 2002) and V4 receptive field changes that could represent the neural correlates of saccadic suppression of vision and compression of space respectively. However, there is little direct physiological data in humans concerning activity in retinotopic visual areas during saccades and the source of saccadic suppression and the physiological basis for other psychophysical findings (such as magnocellular pathway involvement) have not been examined directly.

1.6.2 Static eye position

In addition to compensating for disruptive effects of dynamic oculomotor behaviour, perceptual consequences of oculomotor / visual interactions can have other roles. For example, successful visually guided action requires that visual signals encoded in retinal co-ordinates be combined with information about the position of the eyes in the head. This has been shown to occur in many macaque parietal cortical areas, for example area VIP where visual and tactile information are combined in head centred co-ordinates (Colby et al., 1998). However, as discussed earlier, single cell recording in monkeys has shown that early visual areas show modulation of visual responses by static gaze direction (Campos et al., 2006;Rosenbluth and Allman, 2002;Trotter and Celebrini,

1999;Weyand and Malpeli, 1993). Therefore one might expect the direction of static gaze to modulate human visual perception. There is some evidence that this is the case in both normal subjects and in subjects with abnormal visual perception following brain injury.

In normal subjects, altering gaze direction significantly modulates the strength of a number of visual aftereffects including the tilt aftereffect (Nieman et al., 2005;Nishida et al., 2003). These studies did not eliminate the possibility that any effects were due to alteration in the real world stimulus location (which was also altered when gaze was moved). However, these results are consistent with the modulation of visually evoked activity seen in monkey retinotopic visual areas, as the neural processes that cause the tilt aftereffect are likely to be located in early visual cortex (Dragoi et al., 2000;Movshon and Lennie, 1979;Saul and Cynader, 1989). In contrast to saccadic suppression, the timecourse of gaze modulation of visual perception does not favour a feedforward rather than feedback source. Indeed, one study has shown that tonic eye muscle proprioceptive activity (initiated by externally manipulating eye position) leads to consistent errors in localization of visual stimuli (Gauthier et al., 1990).

In subjects with symptoms of visual neglect and/or extinction following right sided parietal lobe damage, eye position can modulate the severity of their perceptual deficits. For example, eye position can modulate extinction, with worse detection of left field targets during eccentric fixation towards the left (Vuilleumier and Schwartz, 2001). Furthermore, left sided visual neglect can also be ameliorated for sustained periods of time following sensorimotor adaptation to prisms that artificially shift gaze to the right (Frassinetti et al., 2002;Pisella et al., 2002;Rossetti et al., 1998). These results demonstrate that visual neglect and extinction are influenced by extra-retinal factors related to eye position, although the precise site in the visual hierarchy where visual and eye position signals converge is not clear. Therefore establishing whether early visual cortex responses are modulated by eye position is important for understanding key processes in normal visual function, but also in understanding perceptual deficits following brain injury and interventions that show promise in ameliorating them.

1.7 Summary of current studies

The experiments presented in this thesis all attempt to characterize the neural basis of the interaction between the human oculomotor and visual systems. All the studies use fMRI to examine this interaction in retinotopically mapped visual areas in normal human subjects. The basis of fMRI acquisition, analysis and retinotopic mapping are summarised in Chapter 2. The experimental studies can be grouped according to whether they examine the effect of dynamic oculomotor behaviour on visual activity (Chapters 3,4,5), static eye position (Chapter 6) or visual effects on oculomotor activity (Chapter 7).

Chapter 3 presents a study that aims to characterize the effect of saccadic eye movements on activity in human LGN and early retinotopic cortex for a range of visual conditions. These visual conditions include presentation of visual stimuli primarily processed by either the magnocellular or parvocellular systems, plus total darkness. This allows two related hypotheses to be tested:

i) Visually evoked activity in LGN and early retinotopic visual cortex is suppressed by saccades.
ii) Activity related to stimuli processed by the magnocellular visual pathway alone is suppressed during saccades.

Chapter 4 presents a re-analysis of the data from the experiment presented in Chapter 3 using Dynamic Causal Modelling (Friston et al., 2003b). This method attempts to define the relationships that lead to changes in activity in a network of brain structures across different experimental manipulations. Therefore this type of analysis can start to define the sources and primary site of saccadic modulation of visual activity.

Chapter 5 presents a further study of saccadic influences on early visual activity that tests the hypothesis that saccades result in an extraretinal signal in visual areas (corollary discharge or efference copy) that can be isolated from any visually evoked activity.

Chapter 6 presents a study that examines whether visually evoked activity in early rertinotopic visual cortex is modulated by static eye position. This study also compares univariate and multivariate analysis techniques to explore whether gaze direction has a distributed representation in visual cortex.

Chapter 7 presents a study that uses fMRI to image visual responses in human SC, a technically challenging structure to image given its small size and location near many large blood vessels. This chapter then examines whether visually evoked responses in the SC show increased responses to stimuli presented in the temporal compared to nasal hemifield – as predicted by psychophysical studies in normals and subjects with damaged geniculostriate pathways.

1.8 Conclusion

Modern cognitive neuroscience aims to develop models that accurately describe the relationship between neurophysiological events in the brain and human behaviour and experience. It is becomingly increasingly clear that to successfully fulfil this aim requires sophisticated models of brain function that go beyond those that ascribe unitary functions to brain structures. The world we live in is not segregated and functionally related brain structures must interact in order to extract information and guide behaviour in such a complex environment. Using human vision as an example, visual processing does not occur in isolation, but takes place within the context of dynamic oculomotor behaviour and the physiological processes underlying visual processing and oculomotor behaviour must be closely linked. Therefore an ideal description of visual or oculomotor processing would define oculomotor effects in primarily visual brain structures and visual effects in primarily oculomotor structures. In addition, the functional role of connections between visual and oculomotor brain areas needs to be explored. Taken together, the series of experiments outlined above will allow the neural basis for the interaction between oculomotor behaviour and visual perception to be systematically examined in the human brain for the first time.

CHAPTER 2 : GENERAL METHODS

2.1 Introduction

This chapter will describe the methods that are common to all of the studies presented in this thesis. These are functional MRI (fMRI), the analysis of fMRI data using statistical parametric mapping (SPM) and the localisation of early cortical visual areas in individual subjects using retinotopic mapping. Other methods that are utilised in individual studies, such as electro-oculography, long range infrared eye tracking, multivariate analysis techniques, modelling effective connectivity and localization of subcortical structures (such as the lateral geniculate nucleus and the superior colliculus) and visual area V5/MT will be discussed in the relevant chapters describing the studies that used those techniques.

2.2 Functional MRI

2.2.1 Physics of MRI

Magnetic Resonance Imaging relies on the relaxation properties of excited hydrogen nuclei in body tissue (e.g. water and fat). When an object (typically a subject's brain) is placed in a uniform magnetic field (Bø), the spins of unpaired atomic nuclei (mainly protons) within it align parallel to this uniform magnetic field. By analogy with a spinning top under the influence of gravity, the spinning protons precess around the axis of the B0 at a frequency proportional to the strength of Bø (known as the resonance frequency). The direction of the precessing around the main field direction is random for all nuclei and the net 'transverse magnetisation' (Mø) is zero. However, if a radio frequency (RF) pulse is applied perpendicular to Bø at the resonance frequency, nuclei absorb this energy and their spins move away from their equilibrium positions. This leads to Mø aligning away from Bø, towards the new applied radio frequency magnetic field

(B_1) and gives rise to non-zero transverse magnetisation in the XY plane (M_{xy}), if the original magnetic field, Bø, is aligned to the Z-axis.

As the protons relax and realign, they emit energy which is recorded in a receiver coil surrounding the subject's brain and provides information about the structures being scanned. The nature of this information depends on the time constants involved in the relaxation processes following RF excitation. The realignment of nuclear spins with the magnetic field is termed *longitudinal relaxation* and the time (typically about 1 sec) required for a certain percentage of the tissue nuclei to realign is termed T1. T1 is affected by the composition of the environment and thus is different in different tissues, which can be used to provide contrast between tissues. T2-weighted imaging relies upon local dephasing of spins following the application of the transverse energy pulse; the transverse relaxation time (typically < 100 ms) is termed T2. T2 imaging usually employs a *spin echo* technique, in which spins are refocused to compensate for local magnetic field inhomogeneities. T2* imaging (used in fMRI) is performed without refocusing and sacrifices image fidelity in order to provide additional sensitivity for the T2 relaxation processes.

2.2.2 Formation of Images using MRI

To create an image with MRI, protons have to be distinguishable on the basis of their spatial location. As Bø is homogeneous, the frequency of emitted RF signals is not affected by the specific location of protons in a sample. In order to localise the nuclei an additional magnetic field is applied by passing currents through coils placed around the subject. This varies across the subject, causing the resonant frequencies of the nuclei to vary according to their position (the amplitude of the signal at that frequency depends on the number of protons in that particular location) and allows the encoding of position along the x-axis. Phase encoding enables encoding of position in a second dimension (along the y-axis). Resolution in the third dimension (along the z-axis) is created by exciting the sample one slice at a time, by combining the frequency gradient with an RF pulse of a particular frequency and bandwidth. Discrete increases in the frequency

encoding and phase encoding gradients divide each slice into small cubes, called voxels (volume elements). All the protons in a voxel experience the same frequency and phase encoding, and the signal from a voxel is the sum of the signal for all the protons in that voxel.

Contrast in the image is created by the differences in signal intensity from different tissues. The largest contribution to the signal comes from hydrogen atoms in tissue water (or other biological fluids such as blood), and signal intensity depends in part on the density of these nuclei. Signal intensity is also determined by T1 and T2 relaxation times, the magnetic susceptibility of the tissue (determined by other protons and electron clouds in the tissue), and the characteristics of the RF pulse. Spins from solid tissues such as bone are not detectable by MRI because their relaxation times are so fast that they have returned to equilibrium before any signal is detected.

2.2.3 Echo-planar imaging

Echo-planar imaging (EPI), allows extremely rapid acquisition of whole brain images. An image of a complete slice can be acquired in less than 100ms. The acquired data are Fourier transformed from the spatial frequency domain to the spatial domain. The transformed data are considered to lie in a two dimensional spatial frequency space, called K-space. EPI sequences acquire data from all the lines of K-space after each RF pulse, whereas other MRI sequences can only acquire data from one line per RF pulse. This means that acquisition time is far lower for EPI, making it very suitable for recording dynamic information, like in fMRI. All the fMRI experiments in this thesis use EPI sequences.

2.2.4 BOLD signal

Neuronal activity and increased local glucose metabolism are tightly coupled to a local increase in blood flow. FMRI measures neural activity indirectly by detecting changes in regional blood flow as indicated by blood oxygenation levels. The MRI signal is sensitive

to the oxygenation state of haemoglobin (Blood Oxygenation Level Dependent contrast) as deoxyhaemoglobin is more paramagnetic than oxyhaemoglobin (Pauling and Coryell, 1936). Paramagnetic substances have a more rapid transverse relaxation time, and a shorter T2* time constant, resulting in a reduced T2* weighted MRI signal. Thus deoxyhaemoglobin produces a smaller MRI signal than oxyhaemoglobin. This is what underlies the BOLD signal, as blood with more deoxyhaemoglobin will produce a reduced signal relative to highly oxygenated blood. This was first demonstrated in mice (Ogawa et al., 1990) and in cats (Turner et al., 1991) and subsequently in human visual cortex (Kwong et al., 1992).

BOLD contrast is determined by the balance between supply, determined by blood flow and blood volume, and demand, determined by the surrounding tissue's rate of glucose metabolism, and consumption of oxygen. Local increases in neural activity lead to increased glucose metabolism and increased oxygen consumption (Hyder et al., 1997). After about 100ms there is a relative deoxygenation of the blood in surrounding vessels (Vanzetta and Grinvald, 1999), coupled to vasodilatation and increased blood flow to the 500-1000ms later (Villringer and Dirnagl, 1995). As the rise in oxygen uptake is smaller than the rise in blood flow to activated brain regions (Fox and Raichle, 1986), there is an overall increase in blood oxygenation levels lasting for several seconds. This overcompensation is the basis for the increased BOLD signal seen when neural activity increases. This increase in BOLD contrast, caused by the decrease in deoxyhaemoglobin and measured in fMRI, is delayed in time with respect to the neural activity. Typically the BOLD signal peaks 4-6 seconds after the onset of neural activity. The rise and subsequent return to baseline of the BOLD signal is known as the Haemodynamic Response Function (HRF).

2.2.5 Resolution of fMRI

The limitations on the spatial and temporal resolution of fMRI are physiological and are imposed by the spatio-temporal properties of the HRF. Spatial resolution is limited to 2-5mm and temporal resolution is limited to seconds (Friston et al., 1998). The BOLD

signal originates in red blood cells in capillaries and veins surrounding the activated neural tissue, and thus is an indirect measure of tissue oxygenation and neural activation, thus the maximum spatial resolution obtainable with the BOLD signal is dependent on the local structure and density of the vasculature in a particular brain region.

2.2.6 Neural basis of BOLD signal

The specific cellular and molecular mechanisms underlying the BOLD signal are still a matter for debate. It is widely believed that increased blood flow follows directly from increased synaptic activity, as blood flow increases in proportion to glucose consumption (Fox et al., 1988) and glucose metabolism is linked to synaptic activity (Magistretti and Pellerin, 1999;Schwartz et al., 1979;Shulman and Rothman, 1998;Sibson et al., 1998). However, this does not explain the mismatch between blood flow and oxygen consumption described earlier. One proposal is that increases in brain activation are supported by glycolysis (non-oxidative glucose metabolism) (Fox et al., 1988;Fox and Raichle, 1986). In particular, astrocytes which have a crucial role in neurotransmitter recycling and surround both synapses and intraparenchymal capillaries, rely on glycolysis (Magistretti and Pellerin, 1999). However, astrocytes may rely on stores of glycogen to provide energy during transient periods of strong neuronal activity, obviating the need for increased glucose delivery (Shulman et al., 2001).

An alternative view is that the blood flow response does serve to deliver oxygen to active neurons, but the apparent mismatch between blood flow and oxygen consumption is a consequence of extraction (by passive diffusion) of oxygen from the blood being less efficient at higher flow rates (Buxton and Frank, 1997;Hyder et al., 1998;Vafaee and Gjedde, 2000). Therefore a disproportionately large change in blood flow is required to support a small change in oxygen metabolism. This view is supported by the finding that oxygen consumption increases with neuronal activity, although to a lesser extent than blood flow (Davis et al., 1998;Hoge et al., 1999) and estimates of brain metabolism show that most of the energy is used by neurons (and correlates with increased firing rates). In contrast only a small percentage of the energy is used for neurotransmitter recycling by

the astrocytes (Attwell and Laughlin, 2001). However, both the theories outlined above assume that the relationship between blood flow response and glucose consumption (or oxygen consumption) is causal, whereas the current evidence only shows correlation. Interestingly, the blood flow response is not affected by sustained hypoxia or hypoglycaemia (Mintun et al., 2001;Powers et al., 1996), suggesting that this causal assumption may be false.

The signals that cause the blood flow response are far from clear and may be multiple (Magistretti and Pellerin, 1999;Villringer and Dirnagl, 1995). The response might be triggered by lactate (released by astrocytes), implying a tight link between the fMRI signal and synaptic activity. However, there is evidence that nitric oxide, a diffusible by-product of neuronal spiking, has a role. Specifically, the blood flow response is reduced by blocking nitric oxide synthase while preserving the normal level of glucose metabolism (Cholet et al., 1997). Finally, the blood flow response might be triggered within the blood vessels themselves, in response to transient decreases in oxygenation that occur immediately after a neurons firing rate increases.

In order to compare fMRI studies with electrophysiological studies, it is clearly important to understand the relationship between the BOLD signal and patterns of activity shown by invasive recording techniques. A comparison of single unit data from monkey V5/MT (a motion responsive cortical area) with human fMRI measurements from V5/MT (the human homologue) showed that neuronal firing and BOLD responses increased linearly with increasing motion coherence (Rees et al., 2000). This is consistent with the two measures being well correlated. Furthermore, simultaneous recording of multi-unit activity (MUA) and local field potential (LFPs) from microelectrodes placed in monkey primary visual cortex while measuring BOLD contrast responses using fMRI (Logothetis et al., 2001) has broadly shown good correlation between these measures. However the correlation was variable over the brain areas studied. LFPs correlated slightly more than MUA with the BOLD response. MUA represents the spiking activity of neurons near (~200μm) the electrode tip, while LFPs reflect synchronised dendritic currents averaged over a larger volume of tissue (reflecting inputs and intracortical activity), and they often

(but not always) correlated with output spiking activity. This suggests that the BOLD response probably reflects additional components over and above spiking output. Further studies that decouple inputs and intracortical activity from spiking may shed light on this unresolved issue.

2.3 FMRI Analysis

All fMRI data acquired for the experiments in this thesis were analysed (at least in part) with Statistical Parametric Mapping software, SPM2, developed at the Wellcome Department of Imaging Neuroscience (http://www.fil.ion.ucl.ac.uk/spm/). SPM is a set of software tools implemented in MATLAB that allows preprocessing of fMRI data into a form that can then undergo statistical analysis to look at the effect of experimentally manipulated variables. The analyses were similar in all studies. First a series of spatial transformations was applied to each subject's data, to align and warp it to the anatomical space of the T1 structural image for that subject. In some (but not all) cases this data was then smoothed. Next a model of the hypothesised BOLD signal changes during all conditions in the experiment was created and the data fitted to the model using a General Linear Model. Analysis of the resulting parameter estimates was limited to defined a priori regions of interest (sub-cortical or retinotopic visual cortex in individual subjects) and tested for statistical significance across subjects. Therefore many 'standard' SPM techniques such as spatial normalization and multiple comparison correction across the whole brain are not relevant to this thesis and will not be discussed here.

2.3.1 Preprocessing

2.3.1.1 Spatial realignment

Head motion during the scan causes changes in signal intensity of a voxel over time, due to movement of the head through the fixed field of view, a serious confound. Despite head restraints, most subjects will move their heads at least a few millimetres. Realignment involves applying an affine rigid-body transformation to align each scan

with a reference scan (usually the first scan or the average of all scans) and resampling the data using tri-linear, sinc or spline interpolation. The 6 parameters of the rigid-body transformation, representing adjustments to pitch, yaw, roll, and in X, Y, Z position, are estimated iteratively to minimise the sum of squares difference between each successive scan and the reference scan (Friston, 1995). However, even after realignment significant movement related signals persist (Friston et al., 1996). This is due to non-linear effects, including movements between slice acquisitions, interpolation artefacts, non-linear distortion of magnetic field and spin excitation history effects, which cannot be corrected using an affine linear transformation. These non-linear movement related effects can be estimated and subtracted from the original data by including the estimated movement parameters from the realignment procedure in the design matrix during the model estimation stage of the analysis (Friston et al., 1996).

2.3.1.2 Coregistration to T1 structural image

After realignment the mean functional image (created during realignment) is used to estimate the warping parameters that map this mean image onto that subject's structural image. The warping is modelled as a 12-parameter affine transformation, where the parameters constitute a spatial transformation matrix. The parameters are estimated iteratively, within a Bayesian framework, to maximise the posterior probability of the parameters being correct. The posterior probability is the probability of getting the given data, assuming the current estimate of the transformation is true, times the probability of that estimate being true (Ashburner et al., 1997). Finding this solution involves jointly minimising the sum-of-squares differences between the T1 image and the deformed mean functional image (the likelihood potential), and the prior potentials, which are used to incorporate prior information about the likelihood of a particular warp. The estimated warp is then applied to all the functional images.

2.3.1.3 Spatial Smoothing

Functional images are generally spatially smoothed with a three-dimensional isotropic Gaussian kernel of 5-10 mm full width at half maximum. There are several reasons for doing this:

1) Smoothing the data makes the errors more normal ensuring the validity of parametric statistical test, which are based on the assumption that the errors are normally distributed.
2) Smoothing with a Gaussian kernel makes the data fit the assumptions of the Gaussian Random field model, which is used to make statistical inferences about regional effects, more closely (Adler, 1981).
3) Smoothing compensates for any small variations in anatomy between subjects that still exist after normalisation, reducing the variation in the localisation of activations across subjects (this is less relevant in the single subject designs used in studies presented in this thesis – where normalisation is not used).

2.3.2 Statistical Parametric Mapping

2.3.2.1 Basic approach

The approach used by SPM for analysis of fMRI data is based on the conjoint use of the General Linear Model (GLM) and Gaussian Random Field (GRF) theory to test hypotheses and make inferences about spatially extended data through the use of statistical parametric maps. The GLM is used to estimate parameters for the variables that could explain the BOLD signal time series recorded in each and every voxel individually. The resulting statistical parameters determined at each and every voxel are then assembled into three-dimensional images – Statistical Parametric Maps (SPM), that can then be contrasted with one another. Gaussian random field theory is used to resolve the problem of multiple comparisons that occurs when conducting statistical tests across the whole brain. The voxel values of the SPM are considered to be distributed according to

the probabilistic behaviour of Gaussian fields, and 'unlikely' excursions of the SPM are interpreted as regionally specific effects, caused by the experimentally manipulated variables.

2.3.2.2 GLM

The general linear model is used in SPM to partition the variance in the observed neurosphysiological response into components of interest, i.e. the experimentally manipulated variables, confounds and error, and to make inferences about the effects of interest in relation to the error variance. For each voxel the GLM explains variations in the BOLD signal time series (Y) in terms of a linear combination of explanatory variables (*x*) plus an error term (ε):

$$Y_j = x_{j1}\beta_1 + x_{j2}\beta_2 + \ldots\ldots + x_{jl}\beta_l + \ldots\ldots + x_{jL}\beta_L + \varepsilon$$

The β parameters reflect the independent contribution of each independent variable, *x*, to the value of the dependent variable, Y, .i.e. the amount of variance in Y that is accounted for by each *x* variable after all the other *x* variables have been accounted for. The errors, ε, are assumed to be identically and normally distributed. The GLM can also be expressed in matrix formulation:

$$Y = X\beta + \varepsilon$$

Where Y is a vector of J BOLD signal measurements (one per image volume) at a particular voxel (Y = [1…j…J]) and β is the vector of the parameters to be estimated (β=[$\beta_1 \ldots \beta_j \ldots \beta_J$]. X is the design matrix containing the variables which explain the observed data. The matrix has J rows, one per observation, and L columns, one per explanatory variable (*x*) (also referred to as covariates or regressor).

The regressors, which form the columns of the design matrix (and have one value of *x* for each time point *j*), are created for each explanatory variable manipulated in the

experiment (the experimental conditions) by placing delta functions at the time points corresponding to the events of interest and convolving this vector with the haemodynamic response function. The HRF is modelled in SPM with a multivariate Taylor expansion of a mixture of gamma functions (Friston et al., 1998).

Movement parameters, calculated during realignment, can be including in the model as additional regressors to account for movement artefacts which are not corrected by realignment itself. Temporal confounds must also be eliminated from the data. Prior to fitting the model a high pass filter is applied to the data to eliminate drifts in the magnetic field and the effects of movement. A low pass filter is applied to eliminate the effects of biorhythms such as respiration or heart rate. The cut off of this filter is typically 128 seconds. Due to the serial acquisition of the fMRI data time-series successive time points will be correlated. To account for this temporal auto-correlation an autoregressive model of order 1 + white noise is fitted to the data. The β parameters (often referred to simply as 'betas') for each voxel are then estimated by multiple linear regression so that the sum of the squared differences between the observed data and the values predicted by the model is minimised.

2.3.2.3 t and F-statistics

Inferences about the relative contribution of each explanatory variable (*x*), each represented by one column in the design matrix, can be made by conducting T or F-tests on the parameter estimates. The null hypothesis that the parameter estimates are zero is tested by an F-statistic, resulting in an SPM(F). To compare the relative contribution of one explanatory variable compared to another one can contrast or subtract the parameter estimates from one another, and test whether the result is zero using a *t*-statistic, resulting in an SPM(*t*). The *t*-statistic is calculated by dividing the contrast of the parameter estimates by the standard error of that contrast. To make inferences about regionally specific effects the SPM(*t*) or SPM(F) is thresholded using height and spatial extent thresholds specified by the user.

2.4 Retinotopic Mapping

The response properties of neurons in primary visual cortex are often significantly different to those of neurons in V2 or V3. This holds for basic properties; such as receptive field size (Smith et al., 2001) and more complex properties; such as the modulation of responses by directed attention (Kastner et al., 2004). This means that precise delineation of the borders of early visual areas is of crucial importance to the success of fMRI studies of human vision. In addition, it is often necessary to localize activations in the occipital cortex to specific early visual areas. However, there is wide inter-subject anatomical variability of early visual areas which precludes the assignment of visual area borders based on stereotactically normalised coordinates (Dougherty et al., 2003). Thus, unless a more accurate method is used, voxels representing adjacent visual areas (with very different neuronal response properties) will often be incorporated into a single 'visual' region of interest or visual activations will be mislocalized. Fortunately, early visual cortical areas are retinotopically organised, that is, their neurons respond to stimulation of limited receptive fields whose centres are organized to form a continuous mapping between the cortical surface and the contralateral visual field. This consistent organisation can be utilised to accurately determine the boundaries between early visual cortical areas using fMRI (Engel et al., 1994;Sereno et al., 1995).

In order to appreciate the basis of retinotopic mapping, it is necessary to review the anatomy of the occipital lobe. Within each hemisphere, human area V1 occupies a roughly 4- by 8-cm area located at the posterior pole of the brain in the occipital lobe. A large fraction of area V1 falls in the calcarine sulcus. The relationship between locations in retinotopic space and those of the cortical surface of V1 are shown in Figure 2.1. From posterior to anterior cortex, the visual field representation shifts from the centre (fovea) to the periphery. The midline of V1 represents the horizontal meridian, while the boundary of V1 and V2 represents the vertical meridian (both dorsally and ventrally). The local representation of the visual field on the cortical surface changes its orientation at the boundaries between V1 and V2 (and V2 and V3). Therefore, the spatial extent of

activations elicited by visual stimuli representing the horizontal and vertical meridians can be used to functionally define these borders (Figure 2.2). This technique is called meridian mapping, and is a rapid method of retinotopic mapping. However, it provides poor information about eccentricity encoding within visual areas, and is not able to accurately define V4. To overcome these limitations usually requires the use of phase encoded retinotopic mapping methods (using a rotating wedge and expanding ring stimulus to generate a spatiotemporal pattern of stimulation of the visual field). In this thesis meridian mapping was used in all studies as the relevant experimental questions did not require accurate eccentricity information and were limited to V1-3.

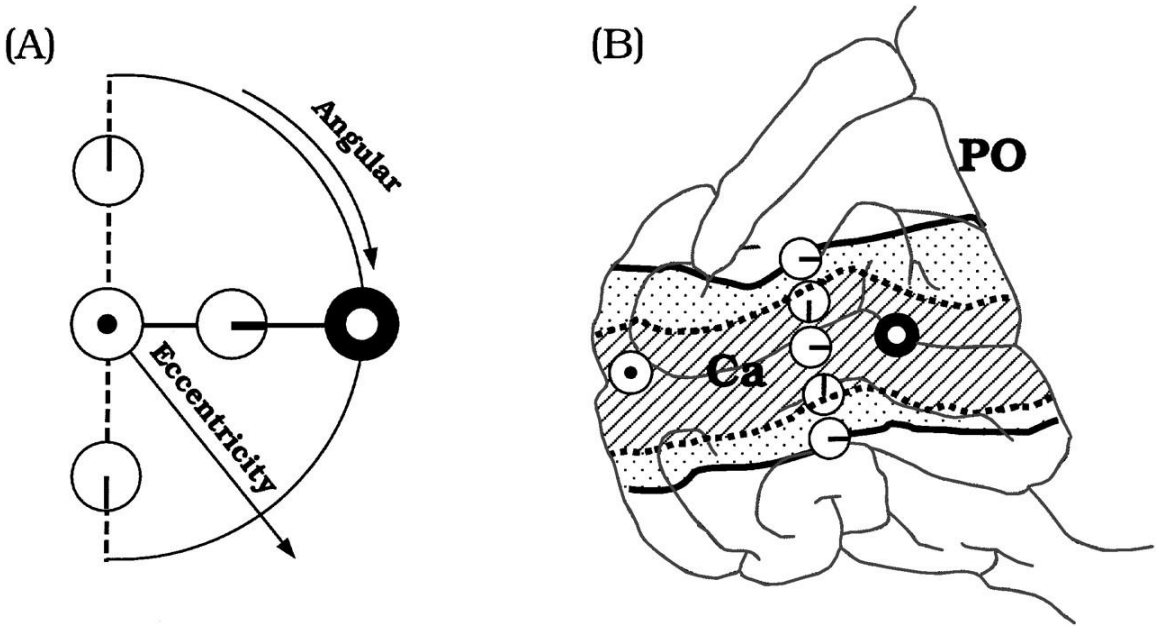

Figure 2.1. Retinotopic organization of visual areas in the left hemisphere.
(*A*) Icons indicating the visual field positions of the central fixation and periphery (*black dot, white surround*; *white dot, black surround*) and the horizontal and vertical meridian (*dashed lines*) are shown. (*B*) The approximate positions of areas V1 (*hatch marks*) and V2 (*dotted area*) on the medial surface of the left occipital lobe are shown. The visual field icons are superimposed on the sketch to indicate the retinotopic organization within areas V1 and V2. The positions of the calcarine sulcus (Ca) and parieto-occipital sulcus (PO) are also shown (adapted from Wandell, 1999).

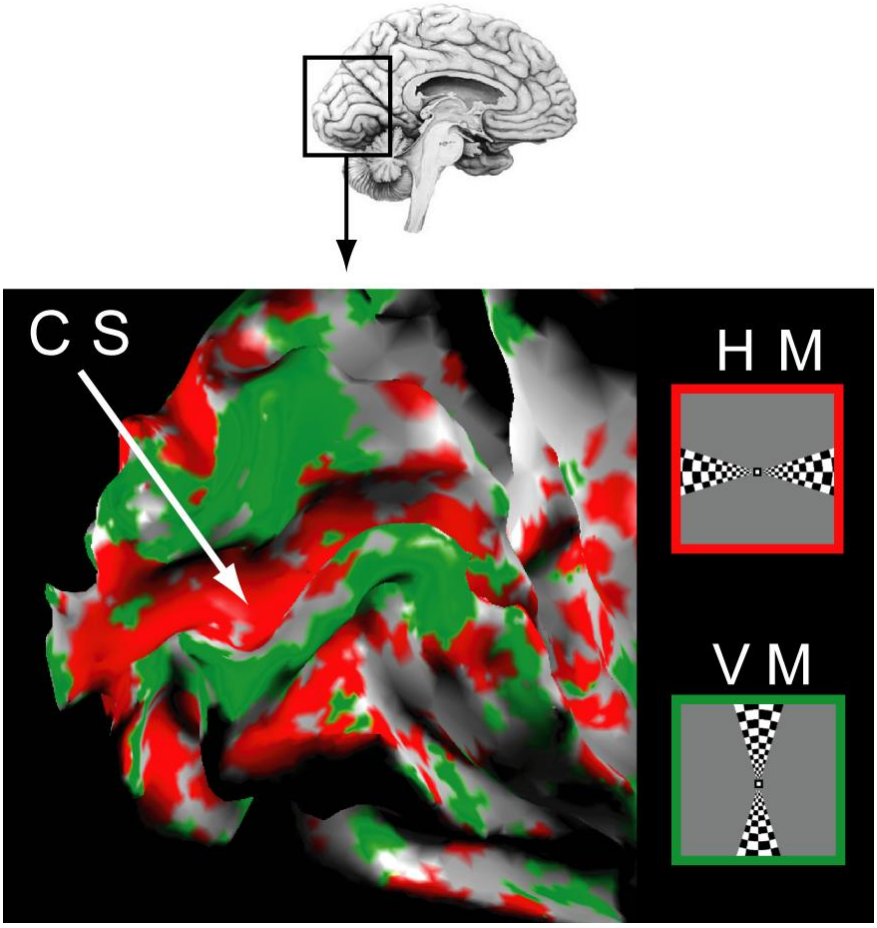

Figure 2.2. Meridian mapping to identify cortical visual areas in human occipital cortex
The patterns of activation elicited by horizontal (HM – shown in red) and vertical (VM – shown in green) meridian stimuli in a single subject are overlayed onto a 3D reconstruction of that subject's occipital lobe. The horizontal stimulus activates the midpoint of the calcarine sulcus (CS) and the vertical stimulus the gyri on either side of the CS. This alternating pattern of activation by horizontal and vertical meridian stimulation can be used to map the boundaries of early visual areas.

2.4.1 Meridian mapping procedure

The aim of retinotopic mapping is to accurately define the boundaries of early cortical visual areas. Initially a high resolution T1 structural scan and functional retinotopic mapping data (in response to stimuli comprising the horizontal and vertical meridians) is collected from each subject. This procedure is described in detail in the Methods section of each experimental chapter of the thesis. The variation in BOLD response to these

meridian stimuli is encoded in 3D Cartesian space that can be projected onto the 3D reconstruction of the anatomical image. However, the retinotopic map is best described in terms of two-dimensional coordinates on the cortical surface, an idealized, two-dimensional representation of the cortical sheet (rather than in three dimensional Cartesian coordinates). There are two main reasons for this. First, for a given point on the cortical surface, receptive fields of neurons from different cortical layers are centered on the same point in the visual field. And second, adjacent points on the cortical surface represent adjacent points in the visual field. Therefore, retinotopic mapping requires first requires flattening of the cortical surface. This thesis uses MrGray software developed at Stanford (Teo et al., 1997;Wandell et al., 2000) and requires a number of stages:

1) The white and grey matter in the T1 structural scan is segmented manually (see figure 2.3).

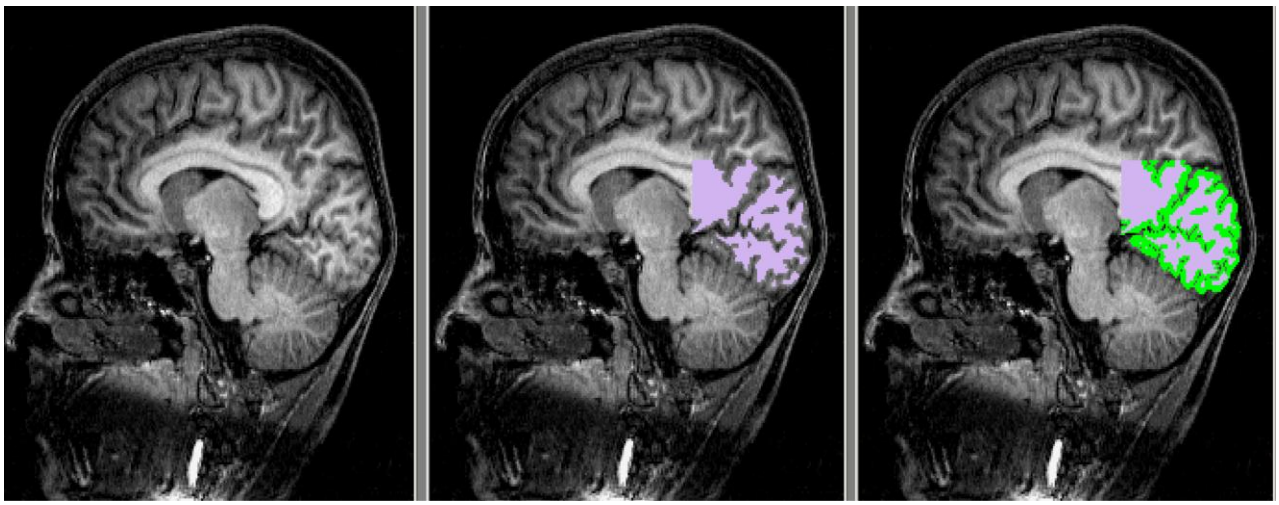

Figure 2.3. Segmenting white and grey matter in MrGray.
All panels show the same high resolution T1 saggital image from a single subject.
The middle panel has the white matter (shown in purple) in the occipital lobe segmented from the grey matter. The right panel has 4 layers of grey matter (shown in green) 'grown' onto the white matter surface.

2) The white/grey matter interface that is generated during segmentation is then used to reconstruct the surface anatomy of the occipital lobe which can be rendered into 3D (figure 2.4). It can also be represented as a mesh that nodes of grey matter

can be mapped onto. This can then be used to make a flattened representation of the segmented cortical surface.

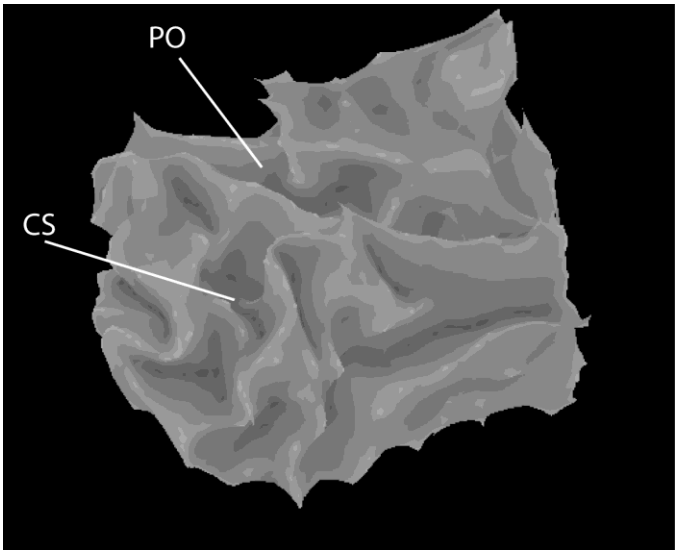

Figure 2.4. 3D rendering of the cortical surface of the right occipital lobe of a single subject
The calcarine sulcus (CS) and the parieto-occipital sulcus (PO) are labelled.

3) The 3D mesh is unfolded by flattening the mesh but maintaining the distance between adjacent grey matter nodes to create a flatmap (this is represented by a greyscale system – where black represents sulci and white gyri on the cortical surface). This is illustrated in Figue 2.5 below.

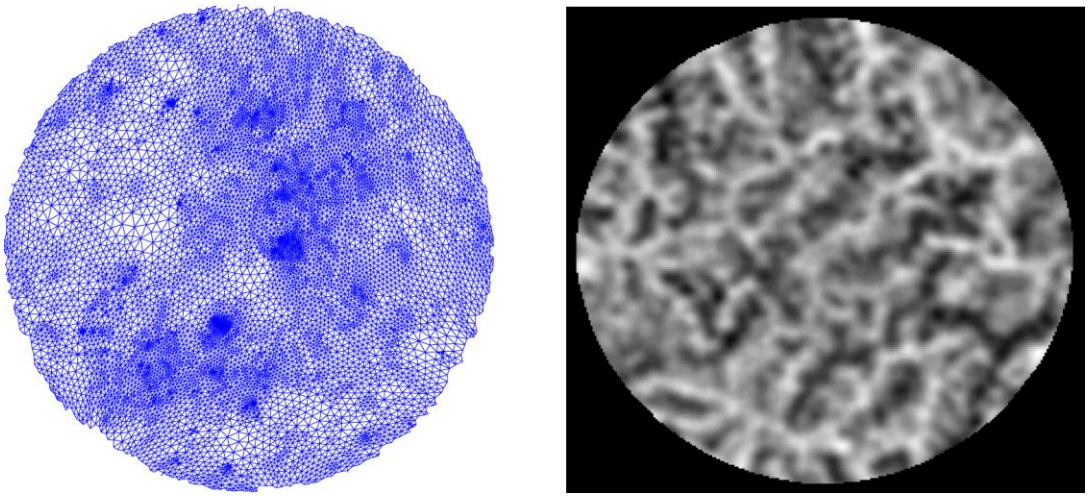

Figure 2.5. Unfolded occipital lobe represented as a mesh (left panel) and a flatmap (right panel).

4) The functional activations elicited by horizontal – vertical and vertical – horizontal meridian stimulation (as estimated using a GLM in SPM) are then superimposed onto the flattened representation of the occipital cortex using local software code. As the local representation of the visual field on the cortical surface changes its orientation at the boundary between visual areas, the boundaries can easily be localised (Figure 2.6) and the voxels contained within each visual area exported as a mask image (to be used in later retinotopically specific analyses).

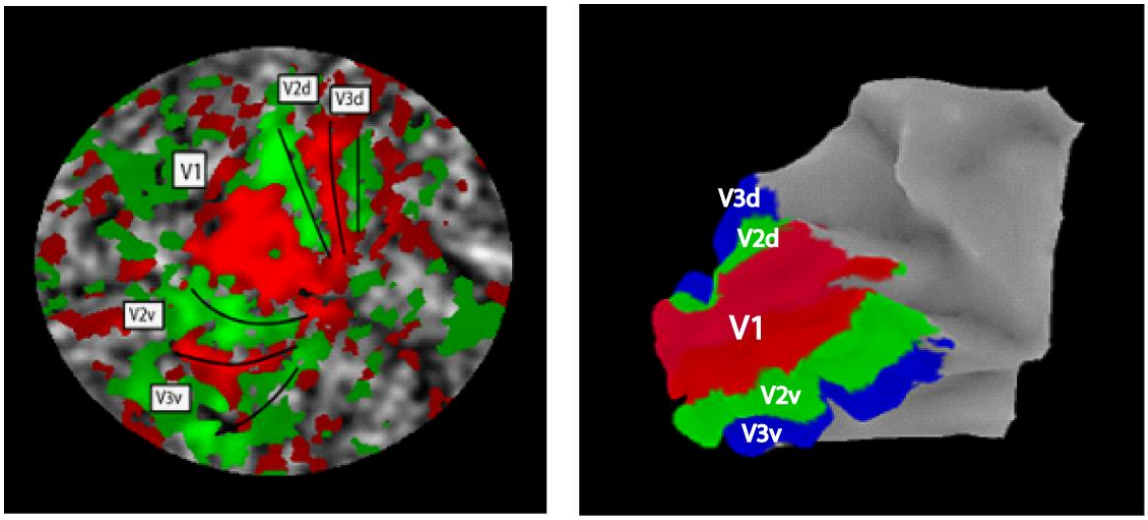

Figure 2.6. Functional data from meridian mapping projected onto a flatmap of a single subject's left occipital lobe

The left panel shows functional data from meridian mapping projected onto a flatmap of a single subject's left occipital lobe with boundaries between visual areas added (red represents horizontal – vertical, green represents vertical – horizontal). The right panel shows a 3D reconstruction of the same subject's left occipital lobe with the masks defined in the right panel projected onto its surface.

2.5 Conclusion

This chapter has described fMRI and retinotopic mapping, the methods that were used in all of the experiments presented in this thesis. I have presented a summary of the physics

and physiology underlying fMRI and the statistical basis of SPM which was used to analyse fMRI data. In addition, I have discussed the physiological basis of retinotopic mapping and how this technique was practically implemented. However, for practical reasons the precise use of these methods varied across experiments and each experiment utilised additional methods. Therefore each experimental chapter in this thesis has a methods section describing these points in more detail.

CHAPTER 3: SACCADIC INFLUENCES ON HUMAN LGN AND V1

3.1 Introduction

Saccades are rapid, ballistic, stereotyped rotational eye movements that occur three or four times each second. The need for saccades arises from the lack of uniformity in the spatial and chromatic sensitivity of the retina. Maximal visual sensitivity occurs only at the fovea which reduces the volume of information that flows from retina to brain. Although this has computational advantages, it means that for any part of the visual field to be processed with the greatest available resolving power, it must be brought onto the fovea. This requires a precise, efficient and most of all rapid mechanism for moving the eyes to foveate specific locations in the visual field. Saccades provide such a mechanism; they are incredibly accurate, carried out with minimal cost to other cognitive functions and can reach speeds of up to 800 degrees per second. The study of oculomotor mechanisms underlying saccade generation has provided important insights into neural processes of motor and cognitive control. However, this chapter is concerned with how the visual system deals with the disruptive perceptual consequences of frequent, high velocity eye movements.

During a saccade the visual image moves across the retina at high velocity, yet our perception of the visual world is stable and no blurring or motion of the visual scene is perceived. Several groups have studied this phenomenon using purely psychophysical methods (Bridgeman et al., 1975;Deubel et al., 1998;Honda, 1993;Honda, 1995;Morrone et al., 1997;Ross et al., 1997). In contrast, this chapter addresses the underlying neural mechanisms that lead to the lack of perception of motion that occurs during saccades.

3.1.1 Saccadic Suppression of Vision – Active or Passive Process?

One possible reason for lack of motion perception during saccades is that the image moves too fast to be perceived (Dodge, 1905). However, with static eyes, object motion is perceived at velocities greater than 1000° s^{-1} (Burr and Ross, 1982), a figure higher

than the maximum velocity of saccades. Another suggestion (Holt, 1901) is that saccades lead to a 'momentary central visual anaesthesia', implying a total suspension of vision through modulation of brain processes during saccades. Indeed, many groups have found significant perisaccadic decreases in human visual sensitivity (Burr et al., 1982;Riggs et al., 1974;Volkmann et al., 1980;Zuber and Stark, 1966). However, certain stimuli are only seen *during* saccades (Castet and Masson, 2000), suggesting that suppression of vision is not total and saccadic modulation of visual perception may solely reflect visual masking by presaccadic and postsaccadic perception (rather than any central mechanism, see Garcia-Perez and Peli, 2001). This view has difficulty explaining the findings that suppression of visual sensitivity only occurs for real but not simulated saccades (Diamond et al., 2000), occurs prior to saccade initiation (Burr et al., 1994) and is limited to stimuli processed by the magnocellular system (Burr et al., 1994). Thus, current evidence is consistent with a modification of Dodge's theory; perceptual continuity during saccades is maintained by central mechanisms that influence some but not all stages of visual processing.

3.1.2 The Site and Nature of Saccadic Suppression

The precise nature and location of active saccadic influences on the human visual system are not clear. Indirect evidence suggests that the earliest stages of human visual processing are suppressed peri-saccadically. Psychophysically, saccadic suppression occurs beyond the retina (Diamond et al., 2000) but prior to the site of contrast masking (Burr et al., 1994) and precedes visual motion analysis (Burr et al., 1982). Visual phosphenes generated by TMS stimulation of human occipital cortex are perceived during saccades, whereas those produced by electrical stimulation of the eye are suppressed (Thilo et al., 2004). This suggests that saccades modulate visual processing at or before primary visual cortex (V1). Consistent with this, single cell responses in monkey V1 and LGN show substantial changes in activity during saccades (Duffy and Burchfiel, 1975;Ramcharan et al., 2001;Reppas et al., 2002). In humans, although saccadic suppression has been observed in higher visual areas (Kleiser et al., 2004), and regions of occipital visual cortex show modulation of responses during saccades (Bodis-

Wollner et al., 1997;Bodis-Wollner et al., 1999;Paus et al., 1995;Wenzel et al., 2000), there has been no direct examination of activity in either retinotopically defined V1 or LGN during saccades.

In addition to uncertainty over the loci involved in saccadic suppression, empirical findings have not produced a consistent view of the nature of the modulatory influence of saccades on visual processing. In monkeys, saccades cause both *enhancement* and *suppression* of single neuron responses in LGN, V1, MT and MST compared to fixation (Duffy and Burchfiel, 1975;Ramcharan et al., 2001;Reppas et al., 2002;Thiele et al., 2002). In humans both positive (Paus et al., 1995;Wenzel et al., 2000) and negative (Bodis-Wollner et al., 1997;Bodis-Wollner et al., 1999) saccade-related signals have been observed in occipital cortex. One possible reason for these discrepant findings could be that the effect of saccades on visual cortex may depend on the precise conditions of visual stimulation. For example, for saccadic suppression to be observed visually responsive neurons might need to exhibit a minimum level of tonic activity.

These questions were addressed empirically by measuring activity in LGN and V1 using fMRI while subjects made saccades under different visual conditions. The presence (versus absence) of saccades, the presence (versus absence) of full-field flickering visual stimulation and the nature of the visual flicker (isoluminant or achromatic) were independently manipulated. Participants wore diffuser goggles to ensure that eye movements did not alter the spatiotemporal structure of the retinal image. Two analyses of the fMRI data were performed; a whole brain analysis to confirm activation of cortical oculomotor control regions, and individual retinotopic analyses to examine any modulatory effects of saccades on early visual areas.

3.2 Methods

3.2.1 Participants

Ten healthy subjects gave informed written consent to participate in the study (approved by the local ethics committee). Following scanning, three subjects were rejected on the

basis of excessive head movement (>5mm). Seven subjects (all male, mean age 30 years) were included in the analyses reported here.

3.2.2 Stimuli and Apparatus

Subjects lay supine in the scanner, wearing customised spherical goggles made of semi-opaque plastic that created near-Ganzfeld conditions (Figure 3.1).

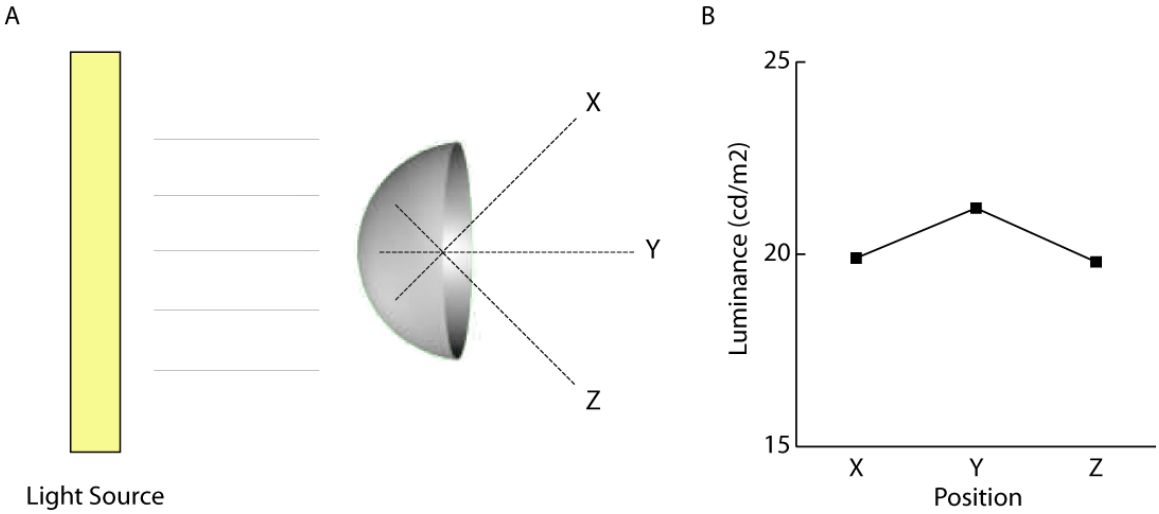

Figure 3.1 Quantification of Ganzfeld conditions.

Fig 3.1A. To quantify luminance changes as the eyes moved within the goggles, we compared the luminance (measured with a Minolta CS-100a photometer) evoked by an external light source at an angle orthogonal to the surface of the goggles at central (0 deg) and peripheral positions (+/- 45 deg) in the goggles (under conditions mimicking those in the scanner).

Fig 3.1B. The luminance at each of the points X,Y and Z are plotted. We found that there was a small luminance drop-off from centre to periphery of around 7% (central luminance 21.2Cd/m^2, peripheral luminance 19.8Cd/m^2). Note that saccade amplitude, estimated from two subjects under simulated experimental conditions was 35° (±5°) either side of central fixation. We found that there was a small luminance drop-off from centre to periphery of around 5-7%. Any overall modulation of luminance was therefore extremely small and at a very low spatial frequency so unlikely to affect our findings.

While wearing the goggles, subjects reported seeing uniform black in the dark condition. During visual stimulation, subjects could identify whether the stimulus was chromatic or achromatic, but perceived the visual stimulus as uniform throughout the visual field. This provided a featureless visual stimulus that lacked distinctive saccadic targets, and was free from perceived contours that might move across the retina during saccades.

Visual stimuli were projected from an LCD projector (NEC LT158, refresh rate 60 Hz) onto the surface of the goggles via a mirror positioned within the head coil. All stimuli were presented using MATLAB (Mathworks Inc.) and COGENT 2000 toolbox (www.vislab.ucl.ac.uk/ cogent/index.html). Visual stimuli consisted of full field flicker of either achromatic (black/white) or chromatic (isoluminant red/green) stimuli (time-averaged luminance - 9.5 Cd/m^2) at a rate of 7.5 Hz (8 screen refresh cycles) presented for 30s. We created isoluminant red/green stimuli by measuring subjective isoluminance in the scanner for each subject using an alternating red/green checkerboard (2 degree checksize) reversing colour polarity at 20 Hz. The luminance of the red checks was fixed and subjects adjusted the luminance of the green stimulus to minimise perceived flicker (three repetitions). This flicker photometry was performed without the goggles to avoid blur of the checkerboard grid. Isoluminance was not influenced by the goggles, because the average luminance attenuation by the goggles was very similar for red and green channels (red: 37%, green: 34%; confirmed by measurement of the spectral absorption of the goggles using a PR-650 SpectraScan colorimeter). This was confirmed in four subjects under experimental conditions. The mean luminance of green flicker subjectively required to minimise perceived flicker was similar with and without the goggles (4% less with the goggles).

The average pooled cone contrast of the *retinal* stimuli (taking into account the absorption by the goggles) was calculated using the following equation (Brainard, 1996):

$$C = \frac{\sqrt{CL^2 + CM^2 + CS^2}}{\sqrt{3}}$$

The cone contrast was 0.57 for the red/green flickering stimuli and 0.98 for the black/white flickering stimuli (measured relative to the spectral mean of the two flickering stimuli under each condition). Thus, the cone contrast of the achromatic stimuli was greater than that of the chromatic stimuli. This is of little practical importance in this study as any comparisons are made between responses to chromatic and achromatic stimuli, but between responses to chromatic **or** achromatic visual stimuli in the presence or absence of saccades (see below).

3.2.3 Experimental Paradigm

In the main experiment, two factors were manipulated independently in a 2x3 factorial blocked design. The factors were saccades (present or absent) and visual stimulation (chromatic flicker, achromatic flicker or no flicker), giving a total of six conditions. During scanning, conditions were presented pseudo-randomly in blocks of 30s with a 20s rest period between blocks (rest periods were not modelled subsequently). Each block was preceded by an auditory command presented through pneumatic headphones that instructed subjects to either move their eyes or keep their eyes still. A sequence of pacing tones at 1.5 Hz was presented auditorily throughout each block. In 'saccade' blocks, subjects were instructed to make a large horizontal saccade with their eyes open in response to each tone. In 'no saccade' blocks, subjects were instructed to fixate centrally with their eyes open. Thus during each 30s block about 45 saccades were made. As saccadic suppression only occurs perisaccadically and saccades only last approximately 40-60ms (Carpenter, 1988), modulation of activity by saccades would only occur for <10% of the total block time. Therefore even with a blocked design to maximise the power to detect saccadic suppression, such a signal may be difficult to detect.

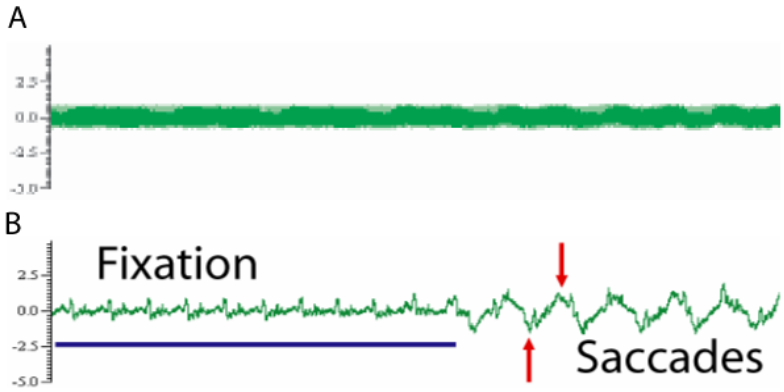

Figure 3.2 EOG monitoring of saccadic eye movements during fMRI study.

Fig 3.2A. The raw EOG signal prior to removal of scanner artefact from a single subject. Electromagnetic noise related to scanning masks any signal from saccades.

Fig 3.2B. The same EOG tracing following post-processing removal of components of the signal related to scanning interference. Subjects task performance (e.g. fixation during fixation blocks and horizontal saccades during saccade blocks) could be accurately assessed.

Electrooculographic (EOG) recording (see figure 3.2) in three participants confirmed that they were able to reliably make paced horizontal saccades at 1.5Hz during each 'saccade' block and made no more than one saccade in total in each 'no saccade' block. Saccade amplitude for two subjects under simulated experimental conditions was 35° either side of central fixation (SD±5°), and was not significantly different across visual stimulation conditions.

3.2.4 Imaging and Preprocessing

A 3T Siemens Allegra system was used to acquire BOLD contrast image volumes. Volumes were acquired continuously every 2.6s, each comprising 40 contiguous 3-mm-thick slices, giving whole brain coverage with an in-plane resolution of 3x3 mm. Six scanning runs of 110 image volumes were then acquired (one subject completed only four runs).

Imaging data were analysed using SPM2 (www.fil.ion.ucl.ac.uk/spm). After discarding the first five image volumes from each run to allow for T1 equilibration effects, image volumes were realigned, coregistered to each subject's structural scan and smoothed with an isotropic 6mm Gaussian kernel (Turner et al., 1998). Activated voxels in each experimental condition were identified using a statistical model containing boxcar waveforms representing each of the six experimental conditions, convolved with a canonical haemodynamic response function and mean-corrected. Motion parameters defined by the realignment procedure were added to the model as six separate regressors of no interest. Multiple linear regression was then used to generate parameter estimates for each regressor at every voxel. Data were scaled to the global mean of the time series, and high-pass filtered (cut-off - 0.0083 Hz) to remove low-frequency signal drifts.

3.2.5 Visual Area Localisation

Retinotopic mapping is crucial for accurate delineation of V1, as wide inter-subject anatomical variability of early visual areas precludes assignment of activations to visual areas based on stereotactically normalised coordinates (Dougherty et al., 2003). To identify the boundaries of primary visual cortex (V1) and extra-striate retinotopic cortex, standard retinotopic mapping procedures were used (Sereno et al., 1995). Checkerboard patterns covering either the horizontal or vertical meridian were alternated with rest periods for 16 epochs of 26s over a scanning run lasting 165 volumes. Mask volumes for each region of interest (left and right V1, V2d, V2v, V3 and V3v) were obtained by delineating the borders between visual areas using activation patterns from the meridian localisers. We followed standard definitions of V1 together with segmentation and cortical flattening in MrGray (Dougherty et al., 2003;Teo et al., 1997). To identify V5/MT a standard motion localiser was used consisting of randomly moving low contrast dots (moving at 4°/s) alternating with static dots for 14 epochs of 13s over a scanning run lasting 73 volumes (Dumoulin et al., 2000).

The location of the LGN in each subject was first identified using an anatomical and radiological brain atlas (Duvernoy, 1999) to identify anatomical landmarks close to LGN on each subjects high resolution structural scan using. Next, functional data co-registered to the structural scan was used to locate visually responsive voxels within the previously defined anatomical boundaries, using the statistical contrast of visual stimulation with eyes still versus darkness with eyes still. Voxels identified in this way were all located in sub-cortical regions and were thus unlikely to represent activity in nearby temporal cortex (which responds weakly to visual stimuli). In a further two subjects, we confirmed that these voxels were highly likely to represent LGN activity by using alternating left/right hemifield checkerboard stimuli to functionally localise LGN (Kastner et al., 2004; O'Connor et al., 2002). In each case, all voxels previously identified as representing LGN in the main experiment, were within clusters activated by this new LGN localiser. Finally, we confirmed that the stereotactic locations identified in this way closely matched (in all subjects) previous reported studies (Kastner et al., 2004; O'Connor et al., 2002). LGN activation by contralateral visual field stimulation is shown for a representative subject (figure 3.3).

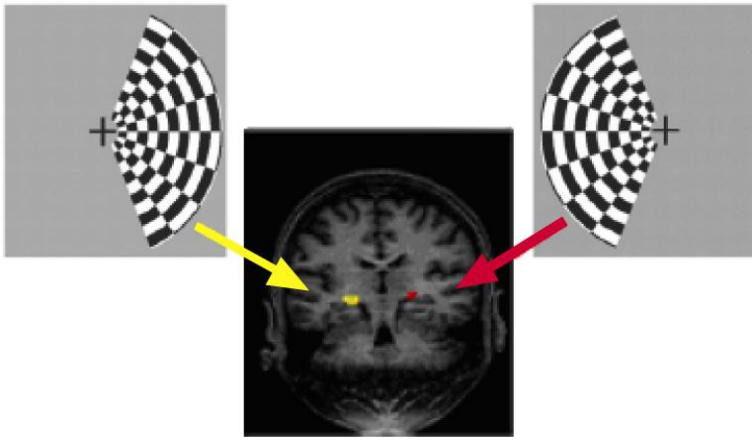

Figure 3.3. LGN localisation in one representative subject.
Hemifield checkerboards were used to identify visually responsive voxels. Voxels that were activated by right field stimulation are in yellow, while those activated by left field stimulation are in red ($p<0.05$, FDR corrected for multiple comparisons). Note that bilateral subcortical structures are activated corresponding to bilateral LGN.

To extract activity from retinotopic visual cortex we created mask volumes for each region of interest (left and right: LGN, V1, V2d, V2v, V3d, V3v, V5/MT. Regression parameters resulting from analysis of the experimental imaging time series were extracted for the maximally activated voxel (comparing visual stimulation with darkness in 'no saccade' conditions) in each region of interest, yielding a plot of percent signal change for each experimental condition in LGN, V1, V2, V3 and V5/MT averaged across subjects. Averaging across all voxels in each area produced virtually identical results confirming that the pattern of responses was consistent over each region.

To compare the effects of saccades across different brain areas, we took the mean regression parameter estimates (β) of activity in each visual condition and computed a modulation index $(\beta_{\text{no saccade}} - \beta_{\text{saccade}}) / (\beta_{\text{no saccade}} + \beta_{\text{saccade}})$ for each subject. Modulation index values were then averaged across subjects.

3.3 Results

3.3.1 Oculomotor structures: normalised analysis

Before carrying out retinotopic analyses on individual subjects, we conducted an initial fixed effects group analysis to confirm that oculomotor structures were activated during task performance. Pre-processing and statistical analysis were the same as for the retinotopic analyses (see Methods), however functional data was stereotactically normalised to a standard EPI template volume based on the MNI reference brain to enable group analysis. Areas activated by the comparison of conditions where saccades occurred (versus no saccades) were then identified using an appropriately weighted linear contrast and determined using the t-statistic on a voxel-by-voxel basis. A restricted set of cortical areas (see Table 3.1) were significantly ($P<0.0001$, corrected) activated, corresponding to the previously described location of the human frontal eye fields, supplementary eye fields and parietal eye fields (Grosbras et al., 2005) (Figure 3.4). In addition, significant bilateral activation of the cerebellum was found. These findings replicate previous neuroimaging studies that have identified cortical loci responsible for the generation and execution of horizontal saccades (Anderson et al., 1994;Berman et al., 1999;Darby et al., 1996;Luna et al., 1998).

	LEFT				RIGHT			
	X	Y	Z	T	X	Y	Z	t
SEF	-6	0	57	14.85	6	0	57	15.96
FEF	-39	-3	60	24.83	45	3	57	23.5
PEF	-36	-48	57	18.12	45	-48	60	14.65
CER	-27	-66	-24	20.13	30	-69	-24	16.99

Table 3.1 Location and t values of peak activations during saccades.

MNI coordinates and t values for loci activated during saccade conditions compared to no saccade conditions from a group analysis of seven subjects (see Experimental Procedures). These areas reached significance at $p<0.0001$ corrected for multiple comparisons (SEF=supplementary eye field; FEF=frontal eye field; PEF=parietal eye field; CER=cerebellum).

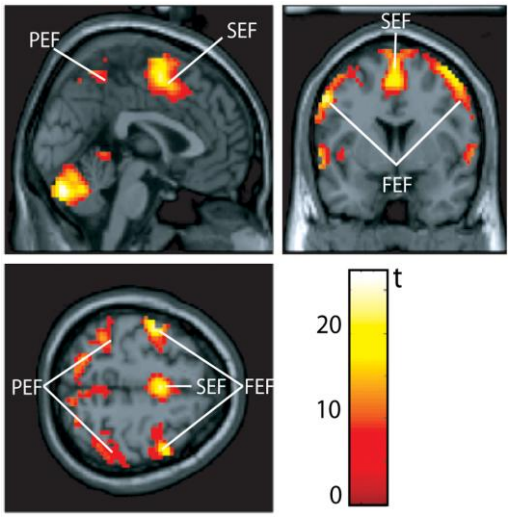

Figure 3.4 Oculomotor structures associated with saccade generation and execution

Loci activated by the comparison of 'saccade' and 'no-saccade' conditions, irrespective of the presence of visual input, overlaid on three slices of a T1-weighted anatomical template brain in MNI space. Loci reflect a normalised group analysis (n=7); see Experimental Procedures for full details. Areas shown reached a significance level of P<0.0001, corrected for multiple comparisons across the whole brain volume. The supplementary eye fields (SEF), frontal eye fields (FEF), parietal eye fields (PEF) and the cerebellum are activated. The colour bar shows the t values of the functional data.

3.3.2 Retinotopic analysis

3.3.2.1 Primary visual cortex and LGN

Activity in V1 and LGN was altered by saccades in a similar fashion in both areas. Saccades strongly affected Blood Oxygenation Level-Dependent (BOLD) responses both in the presence and absence of visual stimulation but in opposite directions (Figure 3.5 A/B). In darkness there was a significant *increase* in activity during saccades compared to the no saccade condition in V1 and LGN (LGN ($t(6)= 4.3$, $p=0.005$ and V1 ($t(6)=5.32$, $p=0.002$). During visual stimulation there was a significant *decrease* in activity for chromatic and achromatic visual stimuli during saccades compared to the no saccade condition in both V1 and LGN (LGN chromatic: $t(6)= -2.6$, $p=0.047$, achromatic: $t(6)= -3.3$, $p=0.017$; and V1 chromatic: $t(6) = -3.2$, $p=0.019$, achromatic: $t(6) = -4.9$, $p=0.003$), with no significant interaction between eye movements and type of visual stimulus (chromatic/achromatic) in V1 ($F(1,6)= 3.006$, $p=0.134$) or LGN ($F(1,6)=1.54$, $p=0.26$). Formal quantification of the degree of saccadic suppression during visual stimulation

revealed greater suppression in LGN compared to V1 (t(6)=-4.02, p=0.007) (figure 3.5 C). Individual subjects followed the trend that was shown in the group analysis (figure 3.6).

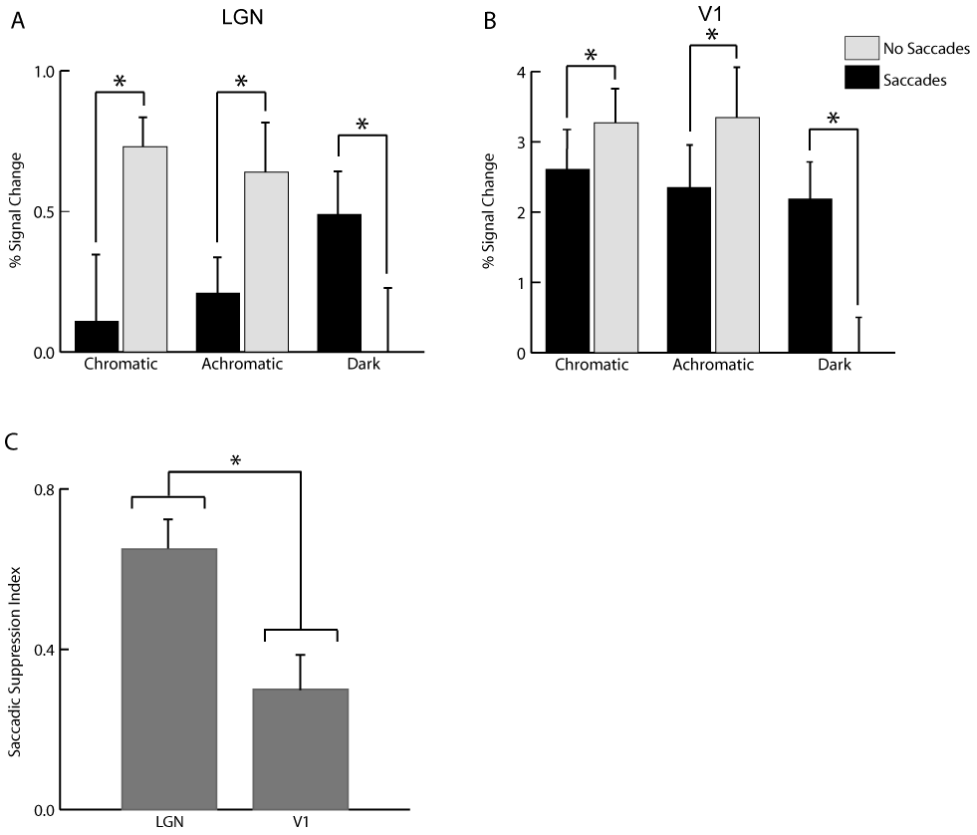

Figure 3.5 Modulation of responses in human LGN and V1 by saccades

Fig 3.5 A/B. BOLD contrast responses in human LGN (Fig. 3A) and V1 (Fig. 3B) during saccade and no saccade conditions in darkness, and in the presence of chromatic or achromatic visual stimulation. Data are taken from individual subject retinotopic analyses (see methods). The percent signal change is plotted as a function of condition, averaged across seven subjects (error bars ± 1 SE). Saccade conditions are plotted in black and no-saccade conditions in light gray. Both LGN and V1 show significantly increased BOLD signal during saccades in darkness compared to no saccades in darkness, but significantly decreased signal for chromatic and achromatic stimuli during saccades compared to the same stimuli during no saccade conditions.

Fig. 3.5C. Saccadic effects were quantified and normalised to give an index of modulation of responses to visual stimulation in LGN and V1. Index values were computed for each subject based on the mean responses obtained in the saccade and no saccade conditions for each type of visual stimulus. Averaged index values are presented for seven subjects (error bars ± 1 SE). Larger values represent greater suppression of responses during saccadic eye movements. Suppression effects were greater for LGN than V1. The '*' symbol denotes statistical significance ($p<0.05$, two-tailed).

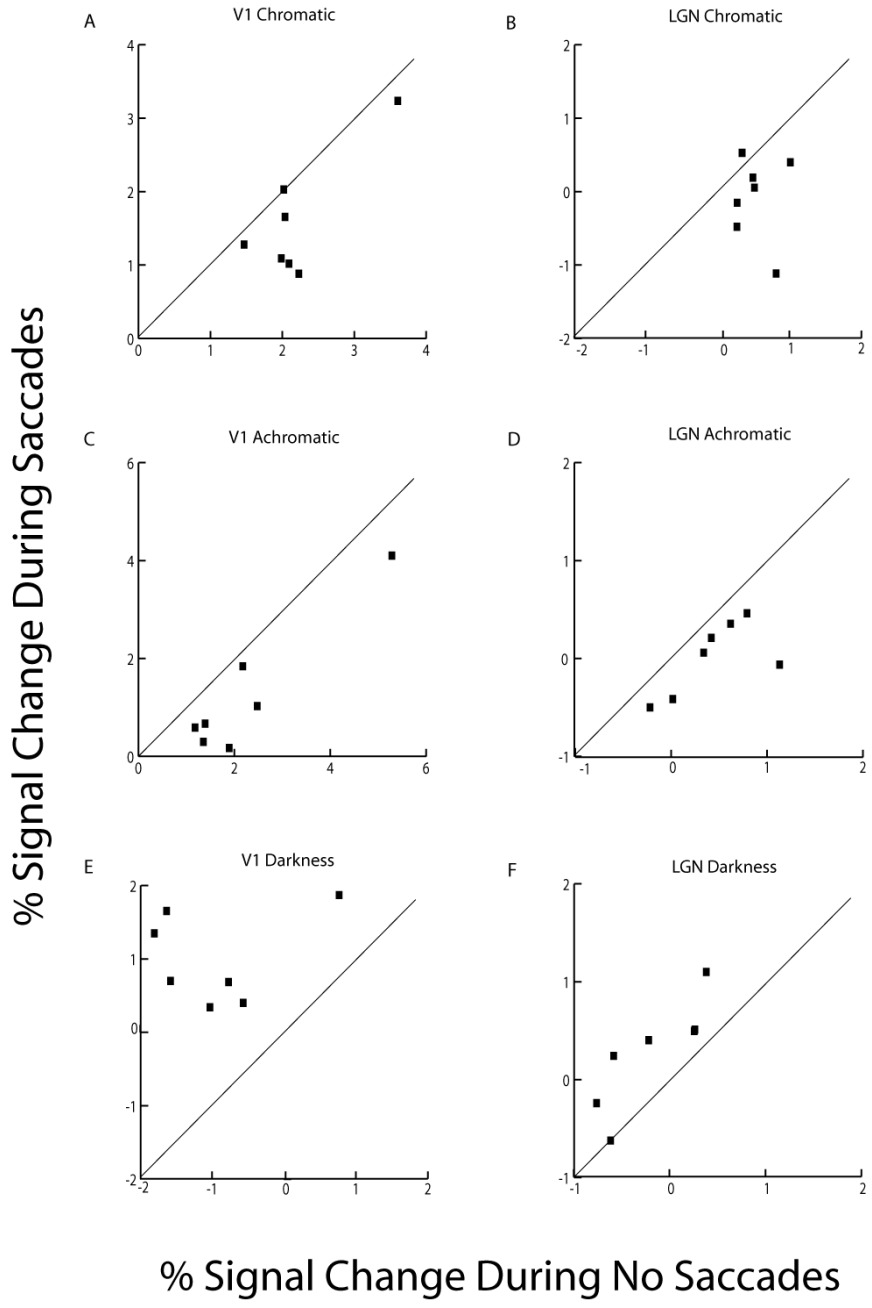

Figure 3.6 Individual subject data for LGN and V1

Figures 3A-F. Scatter plots showing data from each of the seven subjects in the study. % signal change for no-saccades is plotted against % signal change for saccades for each subject in each visual condition: chromatic (A/B), achromatic (C/D) and darkness (E/F), for V1 (A/C/E) and LGN (B/D/F). Plots that fall below unity indicate reduced Reponses during saccades. Plots that are above unity indicate increased Reponses during saccades. For both V1 and LGN at least 6/7 subjects show suppression of responses during saccades in the presence of visual stimulation and enhancement of responses during saccades in darkness.

3.3.2.2 Higher visual areas

Higher visual areas V2, V3 and V5/MT showed a qualitatively similar pattern of modulation to LGN/V1, but responses were weaker overall (Figure 3.7). Saccades in darkness resulted in significant increases in activity in V2 darkness ($t(6)= 2.52$, $p=0.045$), and a trend towards significance in V3 ($t(6)= 2.3$, $p=0.061$). Responses of V5/MT were not affected by saccades in darkness ($t(6)=0.19$, $p=0.85$), but responses overall were weak suggesting that the visual stimuli used were not optimal for activating V5/MT. During visual stimulation saccades evoked small reductions in activity that did not reach significance in V2 (chromatic: $t(6)= -1.99$, $p=0.09$, achromatic: $t(6)= -1.44$, $p=0.2$), V3 (chromatic: $t(6)= -2.2$, $p=0.07$, achromatic: $t(6)= -1.59$, $p=0.16$) and V5/MT (chromatic: $t(6)= -0.9$, $p=0.39$, achromatic: $t(6)= -1.5$, $p=0.17$). There was no significant interaction between eye movements and visual stimulus type (V2: $F(1,6)=0.85$, $p=0.39$, V3: $F(1,6)=1.38$, $p=0.29$, V5/MT: $F(1,6)=0.09$, $p<0.7$). This pattern of results did not differ between dorsal and ventral portions of V2/V3.

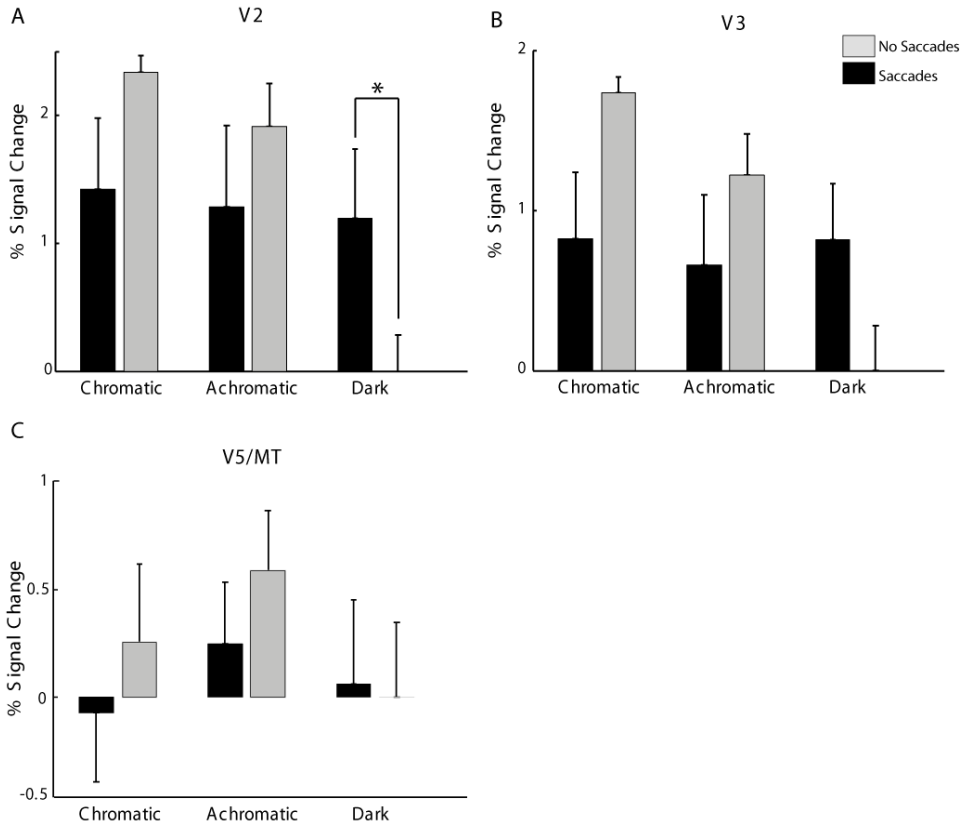

Figure 3.7 Modulation of responses in human V2, V3 and V5/MT by saccades

BOLD contrast responses in human V2 (Fig. 3.7A), V3 (Fig. 3.7B) and V5/MT (Fig. 3.7C) during saccade and no saccade conditions in darkness and in the presence of chromatic or achromatic visual stimulation. Data are taken from individual subject retinotopic analyses (see Methods). The percent signal change is plotted as a function of condition, averaged across seven subjects (error bars ± 1 SE). Saccade conditions are plotted in black and no-saccade conditions in light gray. Both V2 (A) and V3 (B) show increased BOLD signal during saccades in darkness compared to no saccades in darkness. V5/MT (C) shows no modulation of responses during saccades in darkness. Responses to chromatic and achromatic stimuli during saccades compared to the same stimuli during no saccade conditions were reduced, but not significantly in V2, V3 and V5/MT. The '*' symbol denotes statistical significance ($p<0.05$, two-tailed).

3.4 Discussion

The major finding in this study was that saccades altered activity in LGN and retinotopic visual cortex in two distinct ways. First, the presence (versus absence) of saccades was

associated with significant modulation of activity in both the LGN and V1. Second, this modulation differed depending on whether saccades were made in the presence or absence of visual stimulation.

3.4.1 LGN and V1 activity is modulated during saccades

A recent TMS study suggested that saccadic suppression occurs at or before V1 (Thilo et al., 2004). However this study could neither unequivocally identify V1 as the site of modulation, nor examine the influence of saccades on subcortical structures. In contrast, the findings presented above represent the first unambiguous evidence for saccadic modulation of activity in retinotopically-defined V1, and confirm that modulatory signals associated with saccades can also be seen in the human LGN. In monkey LGN, both facilitation or weak suppression followed by stronger facilitation of visual responses are seen in single trials, with suppression of burst firing over longer time intervals (Ramcharan et al., 2001;Reppas et al., 2002). The precise relationship between these multiphasic responses and BOLD contrast fMRI signals remains to be determined (Logothetis et al., 2001), but these observations show that the overall fMRI signal in human LGN to visual stimulation is suppressed during saccades. These results are all the more striking given that the actual time subjects spent making saccades during the experiment was very small compared to the time spent in the absence of saccades. Therefore it may be expected that any effects of saccadic suppression would be difficult to detect but that was clearly not the case.

Functional MRI is sensitive to both feed-forward and feedback signals (Logothetis et al., 2001). Our findings, of LGN modulation by saccades, are therefore consistent either with a direct effect of oculomotor signals on the LGN or an indirect effect of feedback signals from V1. However, the relative degree of saccadic suppression of responses to visual stimulation was greater for LGN than for V1 (Figure 3.5C). One possibility is that this may relate to methodological differences in recording fMRI signals from cortical and

subcortical structures. However, fMRI measurement of LGN and V1 contrast response functions reveal similar monotonic increases in BOLD activation with increasing stimulus contrast (Kastner et al., 2004). This finding could also reflect the pattern of connectivity between V1 and LGN. Feedback from V1 to LGN may arise from a subset of V1 neurons but provide a numerically extensive input to LGN leading to a situation where small changes in average V1 activity could lead to larger changes in LGN activity. An alternate possibility is that feedback from V1 is not the only source of the LGN modulation that we observed. The LGN is well placed to receive direct modulatory influences from the oculomotor system due to its connections with the superior colliculus, a crucial structure in the saccade generation (Sparks, 2002). Intriguingly, greater modulation of LGN (versus V1) responses is also seen during voluntary shifts of spatial attention (O'Connor et al., 2002). It has been proposed that this arises from direct top-down influences of attentional signals on LGN rather than feedback from V1 (O'Connor et al., 2002). Our findings suggest that LGN activity can be influenced not only by attentional, but also by extra-retinal oculomotor signals.

It is not entirely clear how saccadic suppression is mediated on a cellular level in the LGN, but one intriguing possibility is via the influence of the parabrachial region. This cholinergic area is involved with sleep and arousal and projects to the dLGN where postsynaptic cholinergic receptors act to modify visual gain in LGN neurons (Fjeld et al., 2002). Retinogeniculate transmission is also modified by activity in the perigeniculate nucleus which shows mirror responses to dLGN and could also mediate saccadic suppression (Funke and Eysel, 1998). These issues will be explored in greater detail in chapter 4, where data concerning changes in effective connectivity between V1 and LGN during saccades will be presented.

3.4.2 Saccadic suppression depends on visual stimulation

Saccadic effects on LGN and retinotopic visual cortex differed in the presence and absence of visual stimulation. In darkness, saccades evoked a positive BOLD signal in LGN, V1 (Figure 3.5) and to a lesser degree higher retinotopic areas (Figure 3.6). However, during visual stimulation, saccades reduced the signal in both LGN and V1. This differential modulation of activity cannot be accounted for by changes in saccade rate, which was the same in all conditions. Instead, the saccadic modulation of activity in LGN and V1 that we observed, may reflect the superposition of a positive signal (corollary discharge) that is independent of visual stimulation and a negative signal (saccadic suppression) that is dependent on the presence of visual stimulation. This is consistent with a proposed theoretical model of saccadic suppression based on psychophysical data (Diamond et al., 2000). The existence of two distinct modulatory effects of saccades on early visual areas may go some way in explaining the previously disparate neuroimaging findings regarding saccadic suppression, which took place under different conditions of visual stimulation. For example, Kleiser and colleagues (Kleiser et al., 2004) found suppression under conditions of visual stimulation, while Bodis-Wollner and colleagues (Bodis-Wollner et al., 1997;Bodis-Wollner et al., 1999) found enhancement in darkness, consistent with the present findings (though see Wenzel et al., 2000). To examine this issue further, an experiment was conducted where the degree of visual stimulation under which saccades take place was systematically varied in order separate the influence of corollary discharge and saccadic suppression (see Chapter 5).

Psychophysical measurements of perceptual suppression during saccades were not performed, so any connection between perception and brain activity must be tentative. Of note a recently published event-related fMRI study found suppression of visually evoked human V1 responses that closely match the time course of psychophysical measures of saccadic suppression (Vallines and Greenlee, 2006). This provides further evidence for neural correlates of saccadic suppression at least as early as V1. Psychophysically, perception of achromatic visual stimuli is suppressed more strongly than for chromatic stimuli (Burr et al., 1994) even for uniform full-field stimuli used in the current study (Sato and Uchikawa, 1999). However, no evidence for *selective* suppression of achromatic stimuli during saccades in LGN and early visual cortex was found. Rather,

the finding that saccades significantly modulated the processing of *both* achromatic and chromatic stimuli in these areas was demonstrated. Although the achromatic stimulus we used had a higher cone contrast than the achromatic stimulus (see methods), observations of saccadic suppression presented here do not derive from any direct comparison of chromatic and achromatic stimuli. Thus although the achromatic and chromatic stimuli were not matched in terms of cone contrast, this cannot explain the finding that responses to *both* types of stimuli are significantly reduced in V1 and LGN during saccades. The difference in cone contrast between the chromatic and achromatic stimuli may account for the approximately equal brain responses that were measured under both conditions, as V1 responds significantly stronger to chromatic than achromatic stimuli of identical cone contrast (Engel et al., 1997). Some caveats in interpreting saccadic suppression of chromatic and achromatic stimuli do require mention. It is possible that the "low" spatial frequency of the full-field flicker stimulus did not optimally drive the parvocellular system in early visual cortex. It should also be noted that equiluminance is very difficult to achieve over large fields as it varies with eccentricity, so the stimuli used may not be perfectly isoluminant over their full spatial extent. Despite these caveats, these findings are consistent with recent observations that selective suppression of magnocellular processing during saccades can be observed in higher visual areas such as V5/MT rather than in early visual cortex (Kleiser et al., 2004).

3.5 Conclusion

Taken together, these findings may argue against the notion of saccadic suppression as a unitary process resulting from modulation of activity at a single cortical location. Instead, it may manifest itself in different ways depending on the nature of the visual stimulus, consistent with the idea that the perceptual phenomenon of saccadic suppression results from an interaction of oculomotor and visual signals (Diamond et al., 2000). The mechanism underlying this interaction will be explored in the next chapter, which examines how saccades modulate the effective connectivity between oculomotor and visual brain areas.

CHAPTER 4: MODELING SACCADIC EFFECTS ON EFFECTIVE CONNECTIVITY IN VISUAL AND OCULOMOTOR NETWORKS

4.1 Introduction

The data presented in the previous chapter demonstrate that BOLD responses in human early visual areas are strongly modulated by saccadic eye movements (Sylvester et al., 2005) and that the direction of this modulation is dependent on the presence or absence of visual stimulation. Specifically, responses in LGN and V1 are reduced during saccades in the presence of visual stimulation, but increased during saccades made in total darkness (figure 3.5). However, the functional role of this differential modulation and the mechanisms by which it arises are not clear. One possible explanation for this differential modulation is that saccades have two separable influences on activity in visual areas. First, a reduction in visually evoked activity that represents a neural correlate of saccadic suppression; and second, an increase in activity in darkness representing an extraretinal occulomotor signal. Evidence for this explanation is presented in Chapter 5. The current chapter will examine the mechanisms underlying saccadic modulation of early visual areas in greater detail.

Three main issues arise concerning the mechanisms underlying saccadic modulation of visual areas. First, where do saccadic influences on the visual system originate? Second, which structures are directly modulated by saccades and which structures are influenced indirectly? Finally, how does differential modulation of visual areas during saccades in light and dark arise? One way to investigate these mechanisms in more detail is to examine the effect of saccades and visual context on the pattern of connectivity between structures in the visual and oculomotor systems. This may provide more information than that gained from solely examining changes in activity in individual brain areas. This is particularly true when a network of brain areas is likely to subserve the effects under consideration (as is the case with saccadic modulation of visual processing).

4.1.1 Modeling Effective Connectivity

A number of methods can be utilized to model the pattern of connectivity in a neuronal system. Methods that measure *functional connectivity*, such as psychophysiological interactions (Friston et al., 1997), are purely correlative – examining the temporal correlation between spatially remote neurophysiological events. Establishing the causal influences that elements of a neuronal system exert over each other requires measures of *effective connectivity*. One recently developed computational approach for modeling effective connectivity using fMRI time series data is Dynamic Causal Modeling (DCM) (Friston et al., 2003b)[1]. DCM uses a hemodynamic model of fMRI measurements to estimate the underlying neuronal activity from the observed hemodynamic response. This hemodynamic model is combined with a bilinear model of neural population dynamics allowing statistical inferences to be made about BOLD responses in terms of the connectivity at the underlying neural level. DCM makes use of the temporal information contained in fMRI time series to assess the causal relationships between activity changes in different brain regions (Friston et al., 2003b;Stephan et al., 2004b). Thus one can

[1]DCM is based on a bilinear model of neural population dynamics that is combined with a hemodynamic model describing the transformation of neural activity into predicted BOLD responses. The neural dynamics are modeled by the following bilinear differential equation

$$\frac{dz}{dt} = Az + \sum_{j=1}^{m} u_j B^{(j)} z + Cu \qquad (1)$$

where z is the state vector (with one state variable per region), t is continuous time, and u_j is the j-th input to the modelled system (i.e. some experimentally controlled manipulation). This state equation represents the strength of connections between the modeled regions (the A matrix – intrinsic connections), the modulation of these connections as a function of experimental manipulations (e.g. changes in task; the $B^{(1)}...B^{(m)}$ matrices) and the strengths of direct inputs to the modeled system (e.g. sensory stimuli; the C matrix). These parameters correspond to the rate constants of the modeled neurophysiological processes. A Bayesian estimation scheme is used to determine the posterior density of the model parameters. Overall, the parameters of the neural and hemodynamic models are fitted such that the modeled BOLD signals are as similar as possible to the observed BOLD responses.

separately model and make inferences about feed-forward and feedback connectivity, which is particularly relevant in the context of saccadic modulation of visual areas.

4.1.2 Evidence informing the design of a model of saccadic effects on visual activity

While the hemodynamic model used by DCM has been biophysically validated (Friston et al., 2000;Stephan et al., 2004a), the design of specific neural models depends on the framework of a particular experiment and the scientific hypotheses posed. Assumptions therefore have to be made with respect to the brain regions included in the neural model, the anatomical connectivity between them, and the modulation of regions and connections by experimental context (Penny et al., 2004). Therefore to a large extent, the biological validity of any conclusions based on DCM analysis is dependent on using anatomical and physiological evidence to inform model design. In this case, evidence concerning the origin, site of action and mechanisms of saccadic influences on the visual system needs to be considered.

In relation to the origin of saccadic effects in visual areas, existing evidence implicates the frontal eye fields. Activity in this structure is consistently associated with saccade planning and execution (Grosbras et al., 2005;Tehovnik et al., 2000a). Simultaneous microstimulation of monkey FEF while recording from V4 neurons shows that FEF modulates activity in primate visual cortex (Moore and Fallah, 2004). An analogous finding has recently been reported using concurrent TMS-fMRI in humans. Ruff et al (Ruff et al., 2006) showed remote modulation of visual cortex (V1-V4) BOLD responses by TMS applied to the FEF. Although these findings do not require the existence of direct anatomical connections between FEF and visual cortex, as TMS could have remote effects through indirect pathways, they do provide physiological plausibility to the idea that modulation of visual areas activity seen during saccades may originate from the FEF. It is also therefore possible that differential effects on visual processing seen in the presence and absence of visual stimulation (Sylvester et al., 2005), may reflect changes in the influence that FEF has on visual areas under these conditions.

There is less evidence concerning the locations within the visual system that are directly influenced by saccades. Multiple locations in the human visual system including LGN, V1-3 (Sylvester et al., 2005), V4, V7 and hMT+ (Kleiser et al., 2004), are influenced by saccades. Whether one of these sites represents a critical modulatory site has not been established. For example, saccades could act in a 'top-down' manner, influencing higher visual areas directly and earlier visual areas through alterations in the strength of feedback connections, or in a 'bottom-up' manner, influencing sub-cortical areas directly and higher visual areas through feedforward connections. These two possibilities can be examined in the light of the earlier findings (presented in Chapter 3) that saccades modulate the earliest stages of visual processing in the LGN and V1. In the 'top-down' model, saccades might first modulate V1 (or higher visual areas) and effects on LGN would then occur via the feedback connection between V1 and LGN. In the 'bottom-up' model saccades might first modulate LGN and effects in V1 (and later visual areas) are then mediated through the feedforward connection between LGN and V1. A third possibility is that saccades might modulate both LGN and V1 directly and their effects could be mediated by both feedforward and feedback connections. Feedforward and feedback connections between V1 and LGN are well established anatomically and changes in the pattern of connectivity between these structures can profoundly alter the flow of visual information to higher visual areas (Sherman and Guillery, 2002;Sillito and Jones, 2002). The LGN is also well placed to receive direct modulatory influences from the oculomotor system due to its connections with the SC (Sparks, 2002) and both behavioral (Burr et al., 1999) and TMS (Thilo et al., 2004) evidence suggest that the critical locus of saccadic suppression of vision is subcortical. Of note, the data presented in Chapter 3 showed that saccades caused a significantly greater degree of modulation in LGN than V1 (figure 3.5C) indirectly supporting a 'bottom-up' rather than 'top-down' model of saccadic influences within the visual system. However, this may merely reflect methodological differences in recording fMRI signals from cortical and subcortical structures rather than any differences caused by the action of saccades.

4.1.3 Model to be Tested Using DCM

With the above evidence in mind, a model of saccadic influences on FEF, V1 and LGN was designed that could be tested using DCM (figure 4.1). DCM permits three components of a connected network of brain areas to be modeled. First, the external inputs to areas (e.g. sensory inputs - which are the primary focus of conventional regionally specific analyses), second, the intrinsic connectivity between areas and finally, the contextual influences that modulate the strength of connections between areas. The intrinsic connectivity between brain areas represents the degree to which activity in one area is causally related to activity seen in the second area (or vice versa – as the connections are directionally specific), in the absence of driving inputs and contextual modulations. Note that modeling intrinsic connectivity between areas in this way does not imply that these areas must be directly connected by a monosynaptic anatomical pathway. The influence of one area on another could also be mediated by a third area (or through a network of areas).

In the model shown in figure 1, feedforward and feedback connections between FEF and V1 and between V1 and LGN can be tested. In the model the external inputs are light (which drives LGN activity) and saccades (which drives FEF activity). Two contextual modulations are also included in the model, the effect of saccades on the connections between LGN and V1 and the effect of visual stimulation on the feedforward and feedback connections between FEF and V1. Contextual modulations reflect the extent to which an experimental manipulation modulates how activity in one area might be causally related to activity in a second area. This can be positive or negative depending on whether the experimental manipulation under consideration causes an increase or decrease in the effective connectivity between two areas.

In summary the DCM model shown in figure 1 allows two different hypotheses generated from the results presented in Chapter 3 to be empirically tested:

1) Saccades primarily modulate visually evoked brain activity by directly acting on LGN. Therefore, V1 modulation during saccades is mediated through changes in

the effective connectivity between LGN and V1 (the model can also test the competing hypotheses that saccades act primarily on later visual areas or both LGN and later visual areas).

2) Differential modulation of LGN and V1 during saccades made in darkness and light arises from differential modulation of effective connectivity between FEF and LGN/V1 in the presence compared to the absence of visual stimulation.

This model cannot test where saccadic influences on visual areas originate or the location of direct anatomical connections between the oculomotor and visual system.

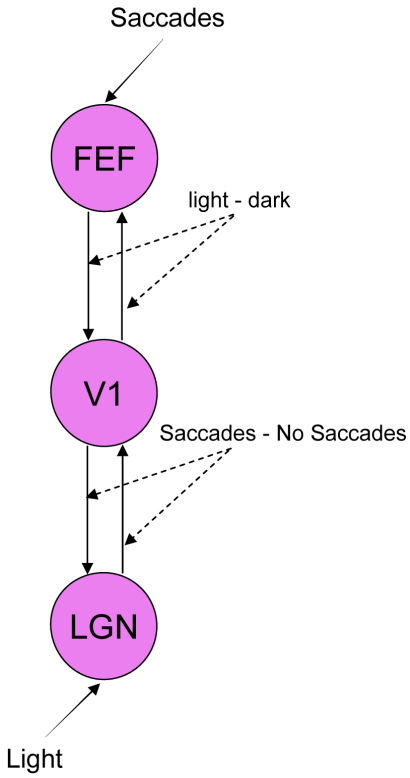

Figure 4.1. Model of Saccadic Influences on Early Visual Areas used in DCM analysis

The model uses three brain areas FEF, V1 and LGN. Feedforward and feedback connectivity are explicitly modeled by connections between V1 and FEF and V1 and LGN. Light – dark drives LGN and saccades – no saccades drive FEF. Visual context can modulate connections between FEF and V1 while oculomotor context can modulate connections between LGN and V1.

4.2 Methods - DCM Analysis

The data generated from the study of saccadic influences on early visual areas was used as the basis for this new DCM analysis (see Chapter 3). In that study seven normal

subjects were scanned using a 3T fMRI scanner and two factors were manipulated independently in a block design: saccades (present or absent) and visual stimulation (chromatic flicker, achromatic flicker or no flicker), giving a total of six conditions. For the purposes of the DCM analysis chromatic and achromatic flicker conditions were considered together as visual stimulation. This was justified as there was no difference between the activity evoked in V1 and LGN, and its modulation by saccades, when these conditions were analysed separately (figure 3.6). Pre-processing and visual area localisation are described in the methods section of Chapter 3. The maximally active voxels in left and right LGN, V1 and FEF were identified using a t-contrast of light – dark for LGN and V1 and a t-contrast of saccade – no saccade for FEF. Time series for these voxels were extracted using SPM2. DCM analysis was carried out separately for each hemisphere of each subject and the results were then averaged across hemispheres in each subject. The coupling parameters from the DCM of each of the seven subjects were then averaged. To test whether these effects were statistically significant, the coupling parameters from each subject were used in paired sample t-tests (in the case of contrasts, such as the modulatory influence of saccades – no saccades) or one sampled t-tests (in the case of intrinsic connections).

4.3 Results

The results of the initial DCM analysis are outlined in figure 4.2. The results are presented as an average coupling parameter derived from all subjects and a measure of statistical significance using two-tailed paired t-tests (or one sample t-tests in the case of intrinsic connections) across subjects. The value of any coupling parameter represents a measure of the strength of direction-specific coupling between one area and another.

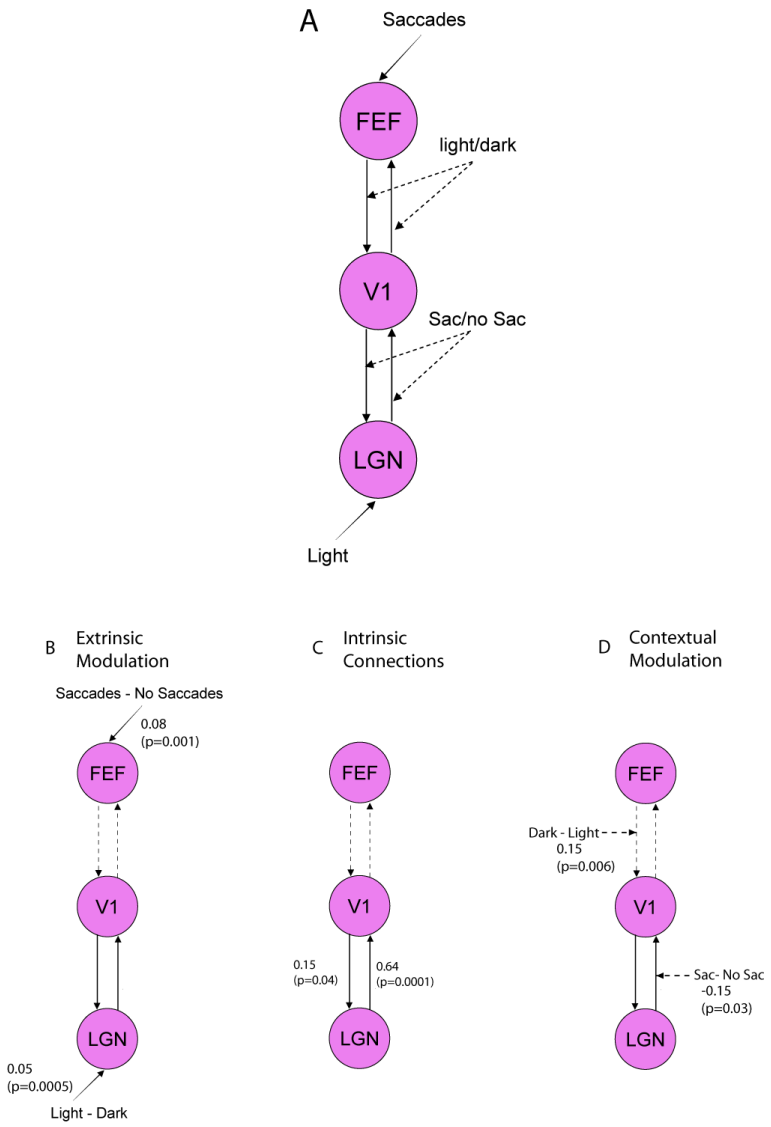

Figure 4.2. Results of DCM analysis

The overall model analysed using DCM is shown for reference in figure 2A. The components of the model that reached significance when averaged across all seven subjects are shown below the model. These are the external modulatory factors (2B), the intrinsic connections (2C) and the contextual modulatory factors (2D). The average coupling parameter and significance level (two-tailed) are shown on each of the figures. Both extrinsic modulatory factors were significant. Saccades significantly increase activity in FEF and visual stimulation significantly increases activity in LGN as expected (2C). The significant intrinsic connections in the model were the feedforward connection from LGN to V1 and the much weaker feedback connection from V1 to LGN (2B). The significant contextual modulatory factors were saccades decreasing the positive feedforward connection between LGN and V1 (reducing activity in V1) and darkness increasing the connection between FEF and V1 (increasing activity in V1).

4.3.1 External Inputs

External inputs to a region (figure 4.2B) represent the extent to which an experimental manipulation (such as sensory stimulation) drives regionally specific activity. In this model light – dark significantly drives LGN (c=0.05, t(6)=6.7, p=0.0005) and saccades – no saccades drives FEF (c=0.08, t(6)=5.9, p=0.001). These results are expected both on a conceptual level (LGN responds to visual stimulation and FEF activity is correlated to saccades) and on a practical level (voxels were selected on the basis of their response to these contrasts in a standard SPM).

4.3.2 Intrinsic Connections

Intrinsic connections (figure 4.2C) represent the impact that one region has over another in the absence of experimental perturbations. In this model, both the feedforward and feedback connections between V1 and LGN were significantly greater than zero (LGN – V1: c=0.64, t(6)=9.17, p=0.00001. V1-LGN: c=0.15, t(6)=2.6, p=0.04). Note that the feedforward connection from LGN to V1 is much stronger (and significant) than the feedback connection. Both the connection between FEF and V1 and the connection between V1 and FEF were not significantly different to zero across subjects (FEF – V1: c= -0.03, t(6)= -0.4, p=0.69. V1 – FEF: c= -0.13, t(6)= -1.24, p=0.26).

4.3.3 Contextual Modulations

Contextual modulations (figure 4.2D) represent the effects that experimental perturbations have on the connectivity between areas. In this model the contextual modulatory factors tested were the effect of saccades on connections between V1 and LGN and the effect of visual context on connections between V1 and FEF. The effect of saccades (derived from saccades – no saccades) significantly decreased the strength of the feedforward connection between LGN and V1 (c= -0.15, t(6)= 2.7, p=0.035) but had no significant effect on feedback from V1 to LGN (c= -0.07, t(6)= 1.25, p=0.26). The strength of the connection between FEF and V1 (which was not significantly different to

zero in the absence of experimental inputs) was significantly enhanced in darkness (derived from dark – light) ($c=0.15$, $t(6)=4.11$, $p=0.006$) but there was no significant effect on the V1 to FEF connection ($c= -0.03$, $t(6)= 0.5$, $p=0.59$).

4.3.4 Model Comparison

These results suggest that differential modulation of V1 during saccades can be accounted for by two independent contextual modulations. The decrease in visually evoked activity during saccades was associated with a decrease in the excitatory feedforward connection from LGN to V1. In contrast, increased V1 activity during saccades in darkness was related to an increase in the excitatory connection from FEF to V1. This account assumes that both the contextual modulatory effects make a similar contribution to how well the DCM model fits the fMRI data. However, there is no a priori reason why these two contextual factors should contribute equally to the DCM. Therefore, in order to validate the results of the DCM one must empirically assess the relative contribution of each modualtory factor to the DCM. One method for doing this is to remove specific components of the model and then quantify the resulting effects on model fit. To this end, two new reduced models were designed and their coupling parameters estimated using DCM (figure 4.3). The first model was the same as the original DCM but the modulatory influence of visual stimulation on connections between FEF and V1 was removed. The second model was the same as the original DCM but the modulatory influence of saccades on connections between LGN and V1 was removed.

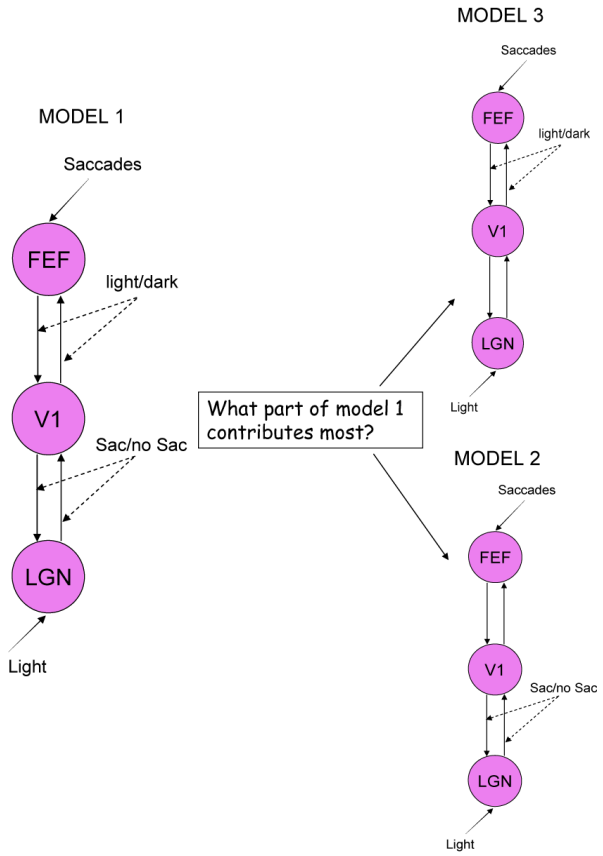

Figure 4.3. Splitting the DCM model into two reduced versions to allow assessment of the relative contributions of each of the contextual modulatory factors affecting FEF-V1 and LGN-V1.

These reduced models were then compared in terms of their ability to explain the observed fMRI data. If the original DCM model is a plausible explanation of differential modulation of LGN and V1 during saccades in light and darkness, these two new models should fit the fMRI data to an equal extent.

Models derived from DCM analysis can be compared on the basis of measures of model fit and complexity using Bayesian model selection[2]. Given some data this method allows

[2] Given some observed data, which of several alternative models is the optimal one? Any decision requires consideration of the relative fit and complexity of the competing models. Model complexity is important because there is a trade-off between model fit and generalizability. As model complexity is increased, model fit increases monotonically whereas beyond a certain point model generalizability decreases. This is due to "overfitting", where an increasingly complex model starts to fit noise that is specific to one data set and thus become less generalizable across multiple realizations of the same underlying generative process.

selection of the optimal model from several alternatives. This can be expressed statistically in terms of a Bayes Factor, where a value is assigned to the hypothesis that one model fits the data more than another. The Bayes Factor was calculated for the comparison between model 2 (modulation of LGN-V1 by saccades) and model 3 (modulation of FEF-V1 by visual context) in each of the individual subjects, and was less than 3 in all subjects. When trying to find the optimal model for a group of individuals using BMS, it is likely that the optimal model will vary, at least to some degree, across subjects. An overall decision for n subjects can be made by computing an average Bayes Factor which corresponds to the *n*-th root of the product of the in dividual Bayes Factors In this case, the average Bayes Factor was 1.091 suggesting that both models are equally

---

Therefore, the question "What is the optimal model?" can be reformulated as "What is the model that represents the best balance between fit and complexity?" In a Bayesian context, the latter question can be addressed by comparing the evidence, $p(y \mid m)$, of different models. Unfortunately, this cannot be solved analytically, therefore an approximation to the model evidence is needed. Suitable approximations, which do not depend on the prior density, are the Bayesian Information Criterion (BIC) and Akaike Information Criterion (AIC), respectively. In the context of fMRI data, BIC will be biased towards simpler models whereas AIC will be biased towards complex models. Therefore the convention that, for any pairs of models to be compared, if AIC and BIC decisions do not concur; the decision is then based on that approximation which gives the smaller *Bayes factor* has been adopted. This approach to Bayesian model selection (BMS) provides a robust procedure to decide between competing hypotheses represented by different DCMs. When trying to find the optimal model for a group of individuals by BMS, it is likely that the optimal model will vary, at least to some degree, across subjects. An overall decision for *n* subjects can be made by computing an average Bayes factor which corresponds to the *n*-th root of the product of the individual Bayes factors.

good at explaining the observed data[3]. This means that a model incorporating both contextual modulatory factors was optimal for this dataset and the results of the DCM are valid.

.

4.4 Discussion

Regionally specific responses (in LGN and V1), measured with fMRI, are strongly modulated during saccadic eye movements. The direction of this modulation depends on the presence (or absence) of visual stimulation (Sylvester et al., 2005). However, the mechanisms underlying this pattern of modulation are not clear. To understand these mechanisms, an empirically derived model of a network of oculomotor and visual structures and their effective connectivity was designed and tested with DCM (using the fMRI data presented in Chapter 3. This analysis allowed testing of two hypotheses. First, whether saccades primarily influence LGN, with later visual areas being only indirectly influenced through changes in effective (feedforward) connectivity. Second, whether differential modulation of early visual areas in darkness and light is due to differential effects on the effective connectivity between FEF and V1 under these two conditions. The results of the DCM will be summarized below and then discussed in relation to these hypotheses.

---

[3] **Table 4.1 Interpretation of Bayes factors**

B_{ij}	$p(m = I \mid y)$ (%)	Evidence in favor of model i
1–3	50–75	Weak
3–20	75–95	Positive
20–150	95–99	Strong
≥150	≥99	Very strong

Bayes factors can be interpreted as follows. Given candidate hypotheses *i* and *j*, a Bayes factor of 20 corresponds to a belief of 95% in the statement 'hypothesis *i* is true'. This corresponds to strong evidence in favor of *i* (taken from (Penny et al., 2004)).

4.4.1 Summary of DCM results

1) A model incorporating both saccades and visual context is required to optimally fit the observed fMRI data (from Chapter 3).
2) Visual stimulation strongly influences LGN and saccades strongly influence FEF.
3) Activity in LGN strongly influences V1 activity but saccades reduce the strength of this effect (leading to reduced V1 activity). Saccades significantly decrease connectivity between LGN and V1.
4) Activity in FEF does not strongly influence activity in V1 unless visual stimulation is absent (FEF activity leads to increased V1 activity in darkness).

These results are consistent with the following mechanism of differential modulation of visual areas during saccades made in the presence and absence of visual stimulation. Passively viewing visual stimuli directly increases LGN activity which increases V1 activity through feedforward connections (positive feedback from V1 to LGN also occurs). Saccades modulate this connection by specifically reducing the strength of feedforward connectivity between LGN and V1 leading to a reduction in visually evoked activation in LGN and V1 during saccades. Saccades also directly increase FEF activity. As FEF is not intrinsically connected to V1, under normal circumstances this increased activity has no direct effect on V1 activity. However darkness increases the strength of connectivity between FEF and V1, so that when saccades are made in darkness, increased activity in FEF results in increased V1 activity (increased LGN activity could occur through V1-LGN feedback or directly, but the current model cannot test between these alternatives). Thus the interaction between saccades and visual context found LGN and V1 responses can be explained by changes in effective connectivity between LGN, V1 and FEF due to modulatory influences of saccades and background visual conditions.

4.4.2 The primary site of saccadic modulation of visual activity

DCM analyses suggests that suppression of visually evoked activity in V1 during saccades (as measured using fMRI) can be best explained by reduced effective

feedforward connectivity between LGN and V1 but not by alterations in effective feedback connectivity from V1 to LGN. These results support LGN, rather than later visual areas, as the primary site at which saccades modulate visual processing. This is consistent with the fMRI data presented in Chapter 3, which showed that the degree of saccadic suppression of visually evoked responses was significantly greater in LGN than for V1. Three separate lines of evidence are consistent with LGN as a critical site for saccadic influences on vision. First, psychophysically saccadic suppression occurs very early in the visual processing stream prior to the sites of contrast masking (Burr et al., 1994) and visual motion analysis (Burr et al., 1999). Second, visual phosphenes generated by TMS stimulation of human occipital cortex are perceived during saccades, whereas those produced by electrical stimulation of the eye are suppressed (Thilo et al., 2004). Finally, monkey LGN neuronal responses are strongly modulated during saccades (Bartlett et al., 1976;Ramcharan et al., 2001;Reppas et al., 2002) and similar modulation in cat LGN is seen (Felisberti and Derrington, 1999) and can be modulated by inactivation of the pretectum (Fischer et al., 1998), consistent with saccadic influences in LGN arising from brainstem occulomotor circuits. However, saccades also lead to complex effects on receptive field properties in later monkey visual areas, such as V5/MT (e.g. reversal of their preferred direction of motion) (Thiele et al., 2002), which are very difficult to explain through reduction in LGN output alone. Such findings suggest that later visual areas may also be directly modulated by cortical oculomotor structures (such as FEF – see below). In the model tested using DCM, this would appear as reduced feedback from V1 to LGN during saccades. Although the DCM analysis did not provide evidence for saccadic modulation of cortico-geniculate feedback, there are a number of reasons why reduced feedback from V1 to LGN remains an attractive mechanism for saccadic suppression. Firstly, abolishing cortico-geniculate feedback has similar effects functional effects to directly inhibiting LGN (Przybyszewski et al., 2000). Furthermore, awareness of visual stimuli has been linked to intact recurrent processing (Lamme and Roelfsema, 2000). Disruption of cortico-geniculate feedback might also therefore explain the *lack* of awareness during saccades.

DCM is useful for testing hypotheses involving effective connectivity using fMRI data. However, direct testing of predictions based on DCM findings is important to establish their validity. For example, one could test whether cortico-geniculate feedback is necessary for saccadic modulatory effects in LGN, by repeating the experiment outlined in Chapter 3 using subjects with unilateral optic radiation (or V1) lesions and hemianopia. These subjects have no intact cortico-geniculate pathways in the damaged hemisphere (but functioning pathways in the intact hemisphere). Therefore the presence of modulation of LGN in the damaged hemisphere during saccades would prove that cortico-geniculate feedback is not necessary for saccadic modulation of LGN (the intact hemisphere would act as a within subject control). Lack of LGN modulation would suggest that cortico-geniculate pathways are required for the saccadic effects seen in LGN.

4.4.3 Differential modulation of V1/LGN by saccades in darkness and light

The DCM findings suggest that reduced visual responses in LGN and V1 during saccades can be explained by a reduction in LGN activity and its effective connectivity to V1. However, this cannot explain why saccades made in darkness lead to an increase in V1 and LGN activity. The DCM suggests that this is due the influence of a second modulatory factor, visual stimulation, and effective connectivity between FEF (which is significantly activated during saccades) and V1 is increased in darkness compared to light. This increase in effective connectivity leads to increased V1 activity seen during saccades in darkness. The concurrent increase in LGN activity could occur through V1-LGN feedback from oculomotor input (FEF or SC), but the current model cannot test between these alternatives.

The DCM result suggests that the FEF has a key role in saccadic modulation of visual areas. Although it is worth mentioning that in a preliminary analysis of the data presented here replacing FEF with either PEF and SEF gave similar results (suggesting that these areas may also be involved in saccadic modulation of V1/LGN). FEF is known to be critically involved in saccade planning and execution (Grosbras et al., 2005;Tehovnik et

al., 2000b) and covert shifts of attention (Wardak et al., 2006). But microstimulation of sites in FEF leads to enhanced visual responses of retinotopically corresponding monkey V4 neurons (Moore and Fallah, 2004), suggesting that FEF activity also modulates early visual cortical activity. In humans, TMS to FEF has been shown to modulate early VEPs (Taylor et al., 2006) and V1-V4 BOLD responses (Ruff et al., 2006). In particular TMS applied to FEF led to suppression of V1-V4 BOLD responses in retinotopic representations of the central visual field and increased activation of representations of the peripheral visual field. Ruff and colleagues report that this pattern was identical in darkness and during visual stimulation, suggesting that any influence of FEF on visual cortex is not altered by visual conditions (see above). However, the TMS pulses applied to the FEF did not elicit saccades, whereas subjects in the current study made large horizontal saccades. It is possible that effective connectivity between FEF and V1 is only increased when FEF activity is above the threshold required to elicit saccades. If this is the case then evidence of the saccade related signal seen in LGN and V1 in darkness should be present when a saccade is made in light. This possibility will be explored in Chapter 5.

4.5 Conclusion

The results presented in Chapter 3 showed that saccades differentially modulate BOLD responses in early visual areas depending on visual context. In this chapter the effect of saccades and visual context on the effective connectivity between visual and oculomotor areas was investigated using DCM. The results of this analysis demonstrate that saccadic modulation of visual brain areas can be explained by changes in the effective connectivity between LGN, V1 and FEF. Specifically, saccades modulate LGN activity rather than later visual areas (which are modulated through decreased feedforward effective connectivity). Second, differential modulation of visual areas during saccades in darkness and light can be explained by changes in the effective connectivity between FEF and V1. As DCM is primarily a computational modeling method, further empirical research based on hypotheses derived from the DCM results are required in order to validate these findings.

CHAPTER 5: EXTRARETINAL SACCADIC SIGNALS IN HUMAN LGN AND EARLY RETINOTOPIC CORTEX

5.1 Introduction

The data presented in chapter 3 demonstrated that activity in human early visual areas is strongly modulated by saccadic eye movements (Sylvester et al., 2005) and that the direction of this modulation is dependent on the presence or absence of visual stimulation. The previous chapter used DCM to show that this pattern of modulation could be explained by changes in the effective connectivity between visual and oculomotor areas. This chapter presents data that examines the nature of the modulation of visual areas by saccades in greater detail.

One possible explanation for the finding that saccades lead to differential modulation of visual areas in the presence and absence of visual stimulation, is that the positive and negative modulation represent separate saccadic influences on visual areas. A reduction in visually evoked activity could represent the neural correlate of saccadic suppression (perisaccadic reduction in visual sensitivity), while increased activity seen during saccades in darkness could represent an extraretinal signal related to oculomotor activity. Support for this view comes from the recent finding that the time course of suppression of visual responses in human V1 by saccades closely matches the time course of the reduction in observed behaviorally (Vallines and Greenlee, 2006). Additionally, reduced visually evoked activity during saccades is consistent with some monkey LGN and V1 single cell studies (Duffy and Burchfiel, 1975;Ramcharan et al., 2001), although the most definitive study suggests a more complex biphasic response in LGN (Reppas et al, 2002).

Although a reduction in visual activity during saccades seems likely to represent neural correlate of saccadic suppression, the hypothesis that increased activity in visual areas

represents an oculomotor signal is problematic. Results from other imaging studies have been inconsistent, with both increases (Bodis-Wollner et al., 1997) and decreases (Paus et al., 1995;Wenzel et al., 2000) in occipital cortex found when saccades are made in total darkness. Additionally, saccadic enhancement of visually responsive brain areas in total darkness must reflect an extraretinal signal (as in this situation retinal activation is minimal[4]), However, it is not clear what the basis of such a signal might be. There are two mutually exclusive possibilities concerning the nature of this extraretinal signal. First, an extraretinal signal might be present in visual cortex only in total darkness. Darkness may be a special 'resting state' for the visual system (Raichle et al., 2001), in which visual areas respond to extraretinal information that does not elicit activity in the presence of visual stimulation. Alternatively, differential saccadic modulation of LGN and V1 activity in the presence and absence of visual stimulation might reflect the superposition of a positive extraretinal signal (independent of visual stimulation) and a negative signal (saccadic suppression - dependent on the presence of visual stimulation). The positive extraretinal signal represents a copy of the efferent motor command (corollary discharge) that is present whenever the eyes are moved. Such an oculomotor corollary discharge in early visual areas could be used to aid compensation for the visual consequences of eye movements. Interestingly, single unit recording data in non-human primates suggest that V1 neurons may encode corollary discharge, in the form of precise spatial information about upcoming saccades (Super et al., 2004). Furthermore, eyeblinks, another disruptive oculomotor action leading to suppression of visual perception (Volkmann et al., 1980), have similar effects to saccades on responses in early visual areas (Bristow et al., 2005).

Significant saccadic suppression of *visual sensitivity* still occurs with weak visual stimuli (Diamond et al., 2000). However, the two possibilities above make different predictions about how saccades might modulate *visual responses* to weak visual stimuli. If an extraretinal signal is only present in total darkness, suppression of visually evoked

[4] If large saccades are performed in total darkness, one has the impression of very faint peripheral visual phosphenes, presumably due to mechanical stimulation of the retina (secondary to torsion of the eye muscles). This phenomenon was originally described by Helmholtz and is analogous to the perception one gets when applying light pressure to the eyeball when the eye is closed. Therefore it is not strictly true to say that there is no retinal stimulation during saccades, although any stimulation that does occur is minimal.

responses during saccades should be observable over a range of visual stimulus strengths. However, if an extraretinal signal is present whenever saccades are executed, it should instead mask suppression of visually evoked activity during saccades at lower visual stimulus strengths, leading to an underestimate of the extent of saccadic suppression. The graded reduction (or absence) of a neural signature of saccadic suppression at intermediate visual stimulation levels could then be interpreted as evidence in favor of an additive explanation, where measured BOLD activity in visual areas during saccades results from the sum of retinally and extraretinally evoked signals. In contrast, saccadic suppression of visually evoked responses over the whole range of visual stimulation strengths, would be more consistent with the extraretinal signal only occurring in darkness.

To test these hypotheses, the effect of systematically manipulating the strength of visual stimulation on saccadic modulation of LGN and V1 responses was examined. In order to replicate previous findings and to explore the role of other visual areas (V2 and V3), a paradigm related to the study presented in Chapter 3 was used. Specifically, activity in LGN and V1/V2/V3 (identified using retinotopic mapping in individual participants) was measured using high field fMRI while participants made saccades under different visual conditions. The presence (versus absence) of saccades, the presence (versus absence) of full-field achromatic flickering visual stimulation and the mean luminance of the visual flicker driving visual responses (0%, 15%, 45% and 90%; see Methods) was independently manipulated. The effect of saccades on luminance-evoked signals was studied, as these can strongly modulate BOLD signals in human early visual cortex (Haynes et al., 2004). Participants wore diffuser goggles to ensure that eye movements did not alter the spatiotemporal structure of the retinal image, and eye movements were monitored using electro-oculography. Individual retinotopic analyses of each participant were performed so that modulatory effects of saccades on early visual areas over the range of different visual stimulation conditions could be examined.

5.2 Methods

5.2.1 Participants

Seven healthy volunteers gave written informed consent to participate in the study, which was approved by the local ethics committee. Following scanning, one participant was rejected on the basis of excessive head movement (>5mm). Six participants (four male, mean age 27.8 years) were included in the analyses reported here.

5.2.2 Stimuli and Apparatus

Stimuli and apparatus used were very similar to those used for the experiment outlined in Chapter 3. Participants lay supine in the scanner, wearing customised spherical goggles made of semi-opaque plastic that created near-Ganzfeld conditions (Figure 3.1). The goggles minimized the effect of eye movements on the pattern of retinal stimulation. Visual stimuli were presented with an LCD projector (NEC LT158, refresh rate 60 Hz) and projected onto the surface of the goggles via a mirror positioned within the head coil. All stimuli were presented using MATLAB (Mathworks Inc.) and COGENT 2000 toolbox (www.vislab.ucl.ac.uk/ cogent/index.html). Visual stimuli consisted of full field flicker of achromatic (black/white) stimuli at a rate of 7.5 Hz (8 screen refresh cycles) presented for 16s, with the white aspect of the stimuli set to 15%, 45% or 90% of the maximal output of the projector in the scanning environment (10cd/m^2). Thus mean luminance of the visual stimulus was varied while keeping the Michelson contrast constant. Using electro-oculography, eye movements were recorded during scanning in four of the six participants whose scanning data were analyzed.

In the main experiment, two factors were manipulated independently in a 2x4 factorial blocked design. The factors were saccades (present or absent) and the mean luminance of visual stimulation (0%, 15%, 45% or 90% of maximum mean luminance), giving a total of eight conditions. During scanning, conditions were presented pseudo-randomly in blocks of 16s with a short 20s rest period between blocks (rest periods were not modelled in the subsequent analysis). Each block was preceded by an auditory command presented through pneumatic headphones that instructed subjects to either move their eyes or keep

their eyes still in the subsequent block. During the block, a sequence of pacing tones at 1.5 Hz was presented binaurally for 16s. In 'saccade' blocks, subjects were instructed to make a large horizontal saccade with their eyes open in response to each tone. In 'no saccade' blocks, subjects were instructed to fixate centrally with their eyes open. Note that pacing tones were always present in all blocks, regardless of whether eye movements were required, and that the eyes were always open throughout the experiment.

5.2.3 Imaging and Analysis

A 3T Siemens Allegra MRI system was used to acquire Blood Oxygenation Level-Dependent (BOLD) contrast image volumes. Volumes were acquired continuously every 1.56s, each comprising 24 contiguous 3-mm-thick slices to give coverage of early visual brain areas with an in-plane resolution of 3x3 mm. Six scanning runs were then acquired, each comprising 180 image volumes for each subject.

Imaging data were analysed using SPM2 (www.fil.ion.ucl.ac.uk/spm). After discarding the first five image volumes from each run to allow for T1 equilibration effects, image volumes were realigned, coregistered to each subject's structural scan and smoothed with an isotropic 6mm Gaussian kernel (Turner et al., 1998). Voxels that were activated in each experimental condition were identified using a statistical model containing boxcar waveforms representing each of the eight experimental conditions, convolved with a canonical haemodynamic response function and mean-corrected. Motion parameters defined by the realignment procedure were added to the model as six separate regressors of no interest. Multiple linear regression was then used in order to generate parameter estimates for each regressor at every voxel. Data were scaled to the global mean of the time series, and high-pass filtered (cut-off frequency 0.0083 Hz) to remove low-frequency signal drifts.

5.2.4 Visual Area Localisation

To identify the boundaries of primary visual cortex (V1) and extra-striate retinotopic cortex, standard retinotopic mapping procedures were used (Sereno et al., 1995). Checkerboard patterns covering either the horizontal or vertical meridian were alternated with rest periods for 5 epochs of 20s over a scanning run lasting 155 volumes. Mask volumes for each region of interest (left and right V1, V2d, V2v, V3d, V3v) were obtained by delineating the borders between visual areas using activation patterns from the meridian localisers. Standard definitions of V1 together with segmentation and cortical flattening in MrGray were followed (Wandell et al., 2000). LGN was localised in each subject by using 10 alternating 20s epochs of left/right hemifield checkerboard stimuli over a scanning run lasting 155 volumes (O'Connor et al., 2002). These data were pre-processed and co-registered to each subjects structural scan as in the main experiment. LGN activations generated from a contrast of left greater than right hemifield stimulation (for right LGN) or right greater than left hemifield stimulation (for left LGN) in each subject were identified using an anatomical and radiological brain atlas (Duvernoy, 1999) to locate anatomical landmarks close to LGN on the high resolution structural scan of each subject. In two subjects LGN was only reliably localised unilaterally; therefore for these two subjects, data from unilateral LGN was used in the main analysis (one subject right side only, the other subject left side only).

To extract activity from early retinotopic visual mask volumes for each region of interest were created (left and right – LGN, V1, V2d, V2v, V3d and V3v). Regression parameters (estimates of evoked brain activity) resulting from analysis of the experimental imaging time series were extracted for the maximally activated voxel (comparing visual stimulation with darkness in ‘no saccade’ conditions) in each of these regions of interest to yield a plot of percent signal change for each experimental condition in LGN, V1, V2 and V3 averaged across subjects. To ensure that responses were consistent across each region, we performed an identical analysis but averaging across all voxels in each area, which produced virtually identical results.

To compare the effects of saccades across different brain areas, a saccadic modulation index for visual areas that showed significant saccadic suppression of visual responses was calculated. This was done by taking the mean regression parameter estimates (β) of activity in each condition and computing the modulation index ($\beta_{\text{no saccade}} - \beta_{\text{saccade}}$) / ($\beta_{\text{no saccade}} + \beta_{\text{saccade}}$) for visual stimulation conditions in every subject. Modulation index values were then averaged across subjects.

5.3 Results

5.3.1 Eye Movement Data

Electro-oculographic recording in four participants confirmed that they were able to reliably make paced horizontal saccades at 1.5Hz during each 'saccade' block and made no more than one saccade in total in each 'no saccade' block. There was no difference in the number of saccades made under the various visual stimulation conditions. Saccade amplitude for two participants under simulated experimental conditions was 35° either side of central fixation (SD±5°), and was not significantly different across visual stimulation conditions.

5.3.2 FMRI Data

In the absence of saccades, BOLD responses in each visual area (LGN, V1, V2 and V3) averaged across participants, increased as a function of increasing mean luminance of the visual stimulus (Figure 5.1). Responses were weakest in darkness and were greatest for the 90% visual stimulation condition. Response magnitudes were greatest in V1 and became consecutively smaller in V2, V3 and LGN.

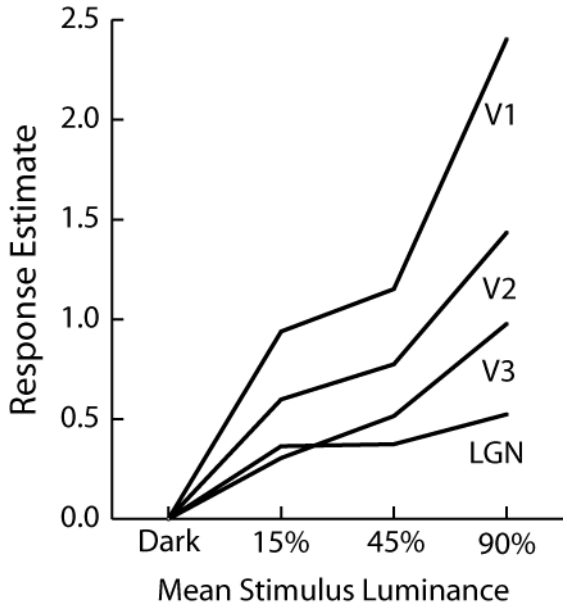

Figure 5.1. LGN and V1-V3 responses to increasing illumination in the absence of saccades.
BOLD contrast responses for LGN, V1, V2 and V3 in darkness and across three different levels (15%, 45% and 90%) of mean stimulus luminance. Data are taken from individual participant retinotopic analyses (see Methods). The modelled estimate of fMRI activity is plotted for each visual area at each illumination level, averaged across six participants. Responses were weakest in darkness and were greatest for the 90% visual stimulation condition in each visual area. Response magnitudes were greatest in V1 and became consecutively smaller in V2, V3 and LGN.

Saccades modulated activity in early visual areas in a highly consistent fashion (Figure 5.2). In darkness, there was a significant *increase* in activity during saccades compared to the no saccade condition in LGN, V2 and V3 (LGN: $t(5)=2.89$, $p=0.015$, V2: $t(5)=2.52$, $p=0.025$ and V3: $t(5)=2.09$, $p=0.045$ paired t-test, one-tailed). V1 showed the same direction of effect although this narrowly missed statistical significance ($t(5)=1.79$, $p=0.066$). During visual stimulation with the highest level of visual stimulation (90%), there was a significant *decrease* in activity during saccades compared to the no saccade condition in LGN, V1 and V3 (LGN: $t(5)= -3.23$, $p=0.015$, V1: $t(5)= -2.44$, $p=0.03$ and V3: $t(5) = -3.23$, $p=0.01$). V2 showed the same direction of effect which narrowly missed significance ($t(5)= -1.62$, $p=0.068$). At intermediate levels of visual stimulation (15% and 45%), there was no significant modulation of activity during saccades

compared to the no saccade conditions in any of the visual areas examined ($t(5)<-1.5$, $p>0.2$, paired t-test, two-tailed).

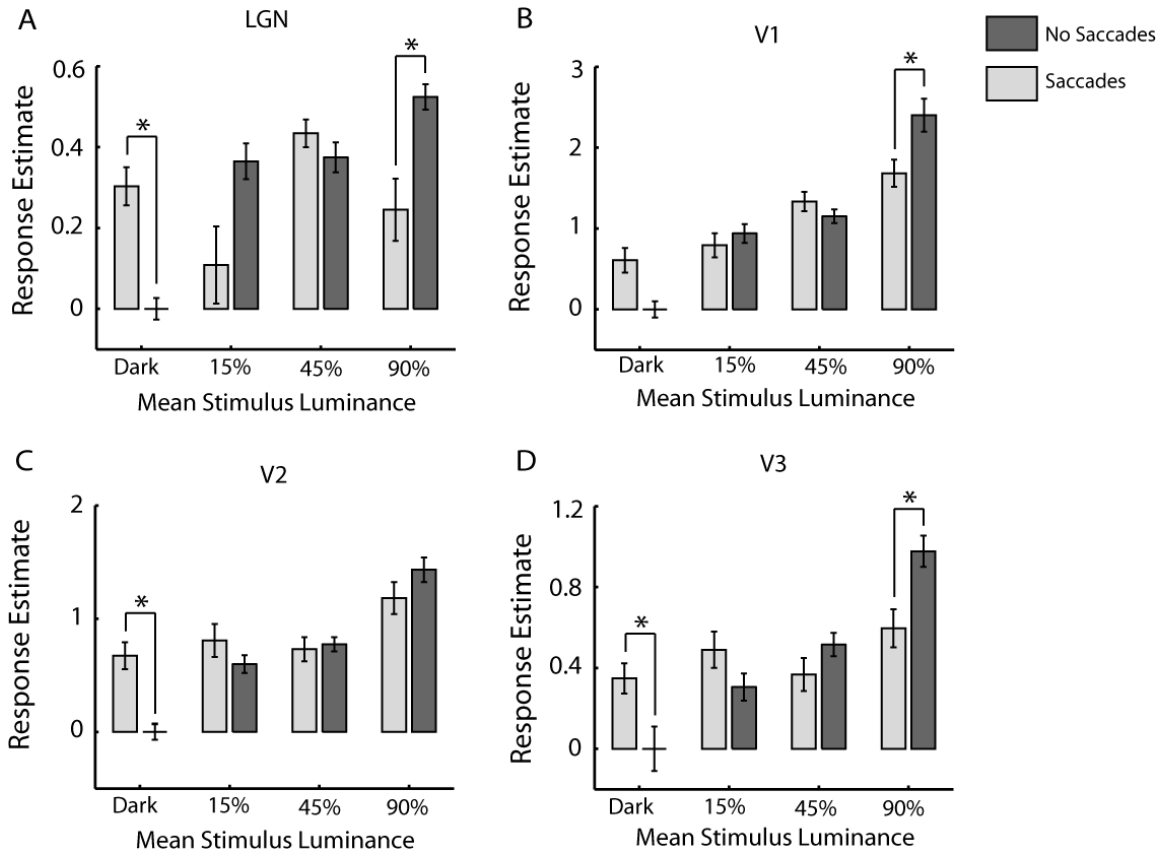

Figure 5.2. Modulation of responses in human LGN and V1-V3 by saccades

Fig 5.2 A/B/C/D. BOLD contrast responses in human LGN (A), V1 (B), V2 (C) and V3 (D) during saccade and no saccade conditions in darkness, and in the presence of three levels of mean stimulus luminance (15%, 45% and 90%). Data are taken from individual participant retinotopic analyses. The modelled estimates of fMRI activity are plotted as a function of condition, averaged across six participants (error bars ± 1 SE). Saccade conditions are plotted in light grey and no-saccade conditions in dark gray. All areas show a similar pattern of results. LGN and V2 and V3 show significantly increased BOLD signal during saccades in darkness compared in darkness. V1 showed the same direction of effect but did not reach significance ($p=0.066$). LGN, V1 and V3 show significantly decreased BOLD signal during saccades in strong visual stimulation (90%) compared to the same stimuli during the no saccade condition. V2 showed the same direction of effect but did not reach significance ($p=0.068$). There was no significant change in the BOLD signal during saccades in weaker visual stimulation (15% and 45%) compared to the same stimuli during the no saccade condition (all $p>0.2$). The '*' symbol denotes statistical significance ($p<0.05$, one-tailed).

Formal quantification of a saccadic modulation index for each visual area revealed no significant difference between visual areas in the degree of enhancement of activity during saccades in darkness (Figure 5.3A). However, the degree of suppression of activity during visual stimulation was significantly greater in LGN than in V1 ($t(5)= 3.17$, $p=0.02$) and V2 ($t(5)= 2.97$, $p=0.03$) (Figure 5.3B).

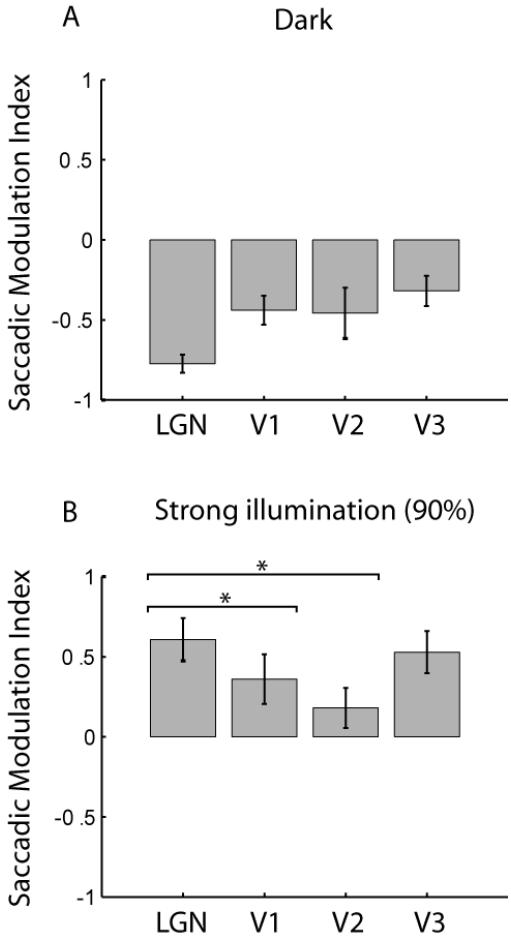

Figure 5.3 Saccadic Modulation Indices for LGN, V1-V3 in darkness and strong visual stimulation.
Fig. 5.3A/B Saccadic effects were quantified and normalised to give an index of saccadic modulation of responses in the presence and absence of visual stimulation in LGN, V1, V2 and V3. Index values were computed for each participant based on the mean responses obtained in the saccade and no saccade conditions in darkness and during strong visual stimulation. Averaged index values are presented for six participants (error bars ± 1 SE). Positive values represent suppression of responses during saccadic eye movements. Negative values represent enhancement of responses during saccadic eye movements. The degree of modulation is represented by the magnitude of the modulation index. There were no significant differences in the degree on saccadic enhancement seen in darkness (Fig. 5.3A). Suppression effects were significantly greater for LGN than V1 and V2 but there were no other significant differences between areas Fig. 5.3B). The '*' symbol denotes statistical significance ($p<0.05$, two-tailed).

5.4 Discussion

Using a comparable paradigm in a different group of participants, previous findings that saccades alter activity in human LGN, V1 and V2 were replicated (Sylvester et al., 2005). In that earlier study, the effects of saccades on activity in V3 did not reach conventional levels of statistical significance. However, in the present study we were able to confirm that saccades significantly modulate activity in V3. Taken together, the present and previous studies provide consistent evidence that in total darkness, the presence (versus absence) of saccades is associated with increased activity in human LGN, V1, V2 and V3. In contrast, saccades decrease activity in these areas during strong visual stimulation (Fig. 5.2). Consistent with the previous fMRI and DCM analysis, the degree of suppression was significantly greater in LGN compared to V1.

To investigate the mechanisms underlying these differential saccadic effects in greater detail, the intensity of visual stimulation (by varying the mean luminance of full field flicker) during saccade and no-saccade conditions was manipulated. Responses in early visual cortex are strongly modulated by the mean luminance of full field achromatic visual stimuli (Haynes et al., 2004) and consistent with this, response amplitude was modulated by changes in the mean luminance of our flickering stimuli in retinotopic areas V1-V3, plus LGN (Figure 5.1). The effect of saccades on these stimulus-evoked responses varied according to stimulus luminance. At intermediate levels of visual stimulation, the presence (versus absence) of saccades did not lead to significant modulation of activity in LGN, V1, V2 or V3. These findings suggest that the positive extraretinal signal seen during saccades in darkness may exert an influence during visual stimulation (by masking the suppressive effect of saccades on visually evoked responses at lower visual stimulus strengths), and is consistent with retinal and extraretinal signals combining in an additive manner during saccades. These findings are less consistent with extraretinal signals only occurring in visual areas in the absence of visual stimulation. Before discussing how this finding relates to the neural mechanisms of saccadic suppression, other possible explanations require discussion.

5.4.1 Saccadic suppression at low stimulus intensity

The loss in visual sensitivity accompanying saccades is reduced at low luminance. Reducing stimulus luminance from 17 to 0.17 cd/m^2 decreases the loss of visual sensitivity (measured as contrast sensitivity in normal participants) during saccades by about 50% (Diamond et al., 2000). A more recent study examining the effect of stimulus contrast on saccadic suppression (measured by detection of a bar stimulus peri-saccadically) found that decreasing stimulus contrast led to decreased perception of stimuli peri-saccadically (a greater loss of visual sensitivity) (Michels and Lappe, 2004). Thus it seems that visual stimuli with low luminance or contrast are seen less easily during saccades than when the eyes are still.

In the current study the 15% and 45% visual stimuli were of reduced mean luminance compared to the 90% stimulus. Psychophysical evidence suggests that visual sensitivity for low luminance stimuli is reduced during saccades, but this reduction is less than that seen at higher stimulus luminance. If the decrease in visually evoked responses during saccades (versus no saccades) represents a neural signature of saccadic suppression (an assumption, given that perceptual suppression during saccades was not measured), then decreasing the luminance of visual stimulation would lead to a lesser degree of suppression of visual responses. However, no consistent effect of saccades on retinotopic visual areas at low levels of visual stimulus luminance was found (even at non-significant levels, Figure 5.2). This suggests that a reduced sensitivity in detecting (weaker) saccadic suppression at low visual stimulation strengths is not a likely explanation for the results.

5.4.2 The relationship between extraretinal signals and saccadic suppression

This study, together with the data presented in Chapter 3, provides consistent evidence that saccades alter activity in early human retinotopic visual areas. In the present study, whether saccades modulated signals evoked by changes in mean luminance of achromatic full-field flicker was specifically examined. In future research it would be interesting to examine whether similar effects of saccades can also be observed on BOLD signals in

retinotopic cortex evoked by different types of stimulus-driven manipulation (e.g. contrast or color; see Kleiser et al 2004).

The precise source of these saccadic modulatory influences and exactly how they lead to suppression of visual perception remains poorly understood. Saccadic effects on visual processing could logically derive from two extraretinal sources; efferent motor commands (corollary discharge from oculomotor control areas) or afferent signals (produced by ocular muscle proprioceptors as the eyes move). There is now considerable evidence that ocular muscle proprioceptors are functionally significant (see Weir et al., 2000) for review). However, proprioceptive feedback cannot account for the loss of visual sensitivity that occurs prior to saccade initiation (Diamond et al., 2000) and any influence of proprioception during saccades is likely to be small compared to corollary discharge (Bridgeman and Stark, 1991). The precise anatomical pathway through which corollary discharge from oculomotor structures might influence early visual cortical areas is not addressed by the present study. In monkey, stimulation of the frontal eye fields (FEF) can alter activity in retinotopic area V4 thus providing evidence for a causally efficacious connection between the two (Moore and Armstrong, 2003b). Similarly, there is evidence that transcranial magnetic stimulation of human FEF can modulate VEPs (Taylor et al., 2006) and BOLD signals in early retinotopic cortex including V1 (Ruff et al 2006). Although the DCM analysis presented in Chapter 4 is consistent with a role for FEF in corollary discharge, it remains an intriguing question for future research to understand the anatomical pathways underlying any such causal relationship between oculomotor activity and visual signals.

These results are consistent with early retinotopic visual areas containing both information relating to efferent oculomotor commands and compensatory mechanisms to null the visual consequences of eye movements. This raises the issue of whether saccadic suppression arises through the modulatory influence of corollary discharge on the responsiveness of early visual areas. Intriguingly, a model of saccadic suppression based on psychophysical data proposes exactly this (Diamond et al., 2000). The model takes the contrast change resulting from the presentation of a test stimulus and the image motion of

that stimulus during a saccade and combines it with a corollary discharge signal. The addition of corollary discharge (present only during saccades) acts to transiently reduce the sensitivity of the visual system to the test stimulus, effectively reducing the contrast response function of observers during saccades.

Corollary discharge may also play a role in other changes in visual perception around the time of oculomotor activity. Peri-saccadic spatial compression, in which targets flashed around the time of saccades are seen as displaced in external space towards the saccade target (Ross et al., 1997), has a similar time course (Diamond et al., 2000) and contrast dependency (Michels and Lappe, 2004) as saccadic suppression, suggesting common underlying neural mechanisms. Recently, it has been shown that blinking in total darkness also leads to increased activity in early retinotopic areas (Bristow et al., 2005). This may suggest that motor signals relating to other self-induced disruptions to visual continuity are also expressed in early retinotopic visual cortex. Indeed, the notion of shared mechanisms for the visual effects of blinks and saccades is consistent with the known effects of blinks on the kinematics of saccadic oculomotor programming (Rambold et al., 2004).

5.5 Conclusion

Taken together, these results suggest that the motor component of saccades alone can lead to increased activity in retinotopic visual areas. This can be measured directly in darkness using fMRI, but only inferred during visual stimulation (by the absence of suppression of visual activity at low levels of visual stimulation). The source of this extraretinal signal is not clear, nor whether it is involved in suppression of visually evoked responses seen during strong visual stimulation and whether different oculomotor behaviors (such as blinks and saccades) lead to specific neural signatures in early visual areas. However, oculomotor signals in visual brain areas have the potential to explain many of the interesting perceptual phenomena that occur around the time of eye movements.

CHAPTER 6: THE EFFECT OF GAZE DIRECTION ON EARLY VISUAL PROCESSING

6.1 Introduction

So far this thesis has been concerned with the effects that saccadic eye movements have on activity in human early visual areas (Chapter 3,4,5). I have presented evidence demonstrating that saccades strongly modulate responses in the LGN and early cortical visual areas. In many respects this finding is not surprising, given that during saccades the pattern of light that falls on the retina profoundly changes without any disruption to the continuity of our conscious visual experience. Indeed, it seems likely that modulation of early visual activity has a crucial role in maintaining perceptual continuity during saccades (an assertion supported by the demonstration of similar modulation of visual activity during eyeblinks - another visually disruptive oculomotor behaviour, see Bristow et al., 2005). However, whether other oculomotor behaviors modulate early visual processing also needs to be considered. This chapter will examine the effect of altering the location of the eyes in relation to the head (static eye position) on human early visual cortex responses.

When an identical visual stimulus is foveated from two different gaze positions, the pattern of light that falls on the retina is closely matched in both conditions. Therefore, altering gaze direction leads to minimal disruption of perceptual continuity. Thus one might expect that altering gaze direction, while foveating identical visual stimuli, would not lead to modulation of activity in early visual areas. However, oculomotor influences on visual processing may have roles in addition to minimizing disruptions to visual continuity. For instance, successful visually guided action requires that visual signals encoded in retinal co-ordinates be combined with information about the position of the eyes in the head. The neural hallmark of such a sensorimotor transformation is modulation of visually evoked activity by static eye position. If early visual areas are involved in this transformation, one could expect their visually evoked activity to be modulated by changes in static eye position.

Traditional accounts have emphasised a critical role for parietal cortex in the transformation from retinal to head centred co-ordinates (Andersen et al., 1985;Baker et al., 1999;Brotchie et al., 1995;DeSouza et al., 2000). Single cell recordings in monkey show that parietal neurons jointly encode direction of gaze and the position of visual stimulation on the retina (Andersen and Mountcastle, 1983;Brotchie et al., 1995). However, visual responses of neurons in many earlier visual areas, including primary visual cortex, also show modulation by gaze direction (Rosenbluth and Allman, 2002;Trotter and Celebrini, 1999;Weyand and Malpeli, 1993). These findings suggest that this sensorimotor transformation may occur in early visual areas in addition to parietal cortex. In humans, the sites where direction of gaze interacts with visual processing are not well defined. There is strong evidence that parietal cortical responses are influenced by eye position. For example, parietal BOLD responses to finger movements (Baker et al., 1999) and memory guided reaching (DeSouza et al., 2000) are modulated by gaze direction. However, there is no evidence that gaze direction directly modulates visual responses in the parietal cortex as is the case in non-human primates. The role of earlier sites in the human visual stream is also poorly understood. Human V4 and V5/MT show gaze modulation of baseline BOLD responses but not visually evoked responses (DeSouza et al., 2002). In addition, gaze direction modulates short latency visual evoked potentials (Andersson et al., 2004) and the strength of the perceptual tilt aftereffect (Nishida et al., 2003) which are both thought to arise from activity in early retinotopic cortex. Furthermore, occipital BOLD responses are greater in the hemisphere that is contralateral to direction of lateral gaze (Deutschlander et al., 2005), although whether this solely reflects gaze modulation of visually evoked responses is unclear (this study used a single small LED as a visual stimulus but found that gaze led to spatially extensive activity changes throughout the occipital lobe). In summary, responses in many monkey visual areas are modulated by eye position and there is some evidence for similar influences in humans. However, there has been no direct examination of whether direction of gaze modulates visual responses in early retinotopic cortex in humans.

In order to directly examine the effects of direction of gaze on human early visual cortex, I measured visual responses while subjects passively viewed closely matched visual

stimuli and manipulated the direction of horizontal gaze (to the left or right of the subjects' midline). The effect of gaze on activity in retinotopic early visual cortex (V1-3 – identified in each subject using standard retinotopic mapping techniques) was then analysed. If gaze direction modulated visually evoked responses in early visual cortex, I hypothesised that there would be a difference in retinotopic cortical activity evoked from viewing identical visual stimuli under different directions of gaze.

6.2 Methods

6.2.1 Experimental Paradigm

Six healthy subjects (4 male, mean age 28.4 years) gave written informed consent to participate in the study, which was approved by the local ethics committee. Subjects lay supine in the scanner and viewed visual stimuli that were projected from an LCD projector (NEC LT158, refresh rate 60 Hz) onto a screen viewed via a mirror positioned within the MR head coil. Stimuli were presented using MATLAB (Mathworks Inc.) and COGENT 2000 (www.vislab.ucl.ac.uk/Cogent/index.html). In addition to a small central fixation spot, the visual stimuli comprised a ring shaped annulus with a radius between 3° and 5°, made up of alternating black/white checks reversing contrast at 8Hz (see Fig 6.1). Complete darkness was achieved in the scanning environment by manually masking the fMRI projection screen, head coil and internal bore with matt black card. This eliminated discernable non-retinotopic luminance cues, ensuring that the only source of visual stimulation during experimental runs was the experimental stimulus.

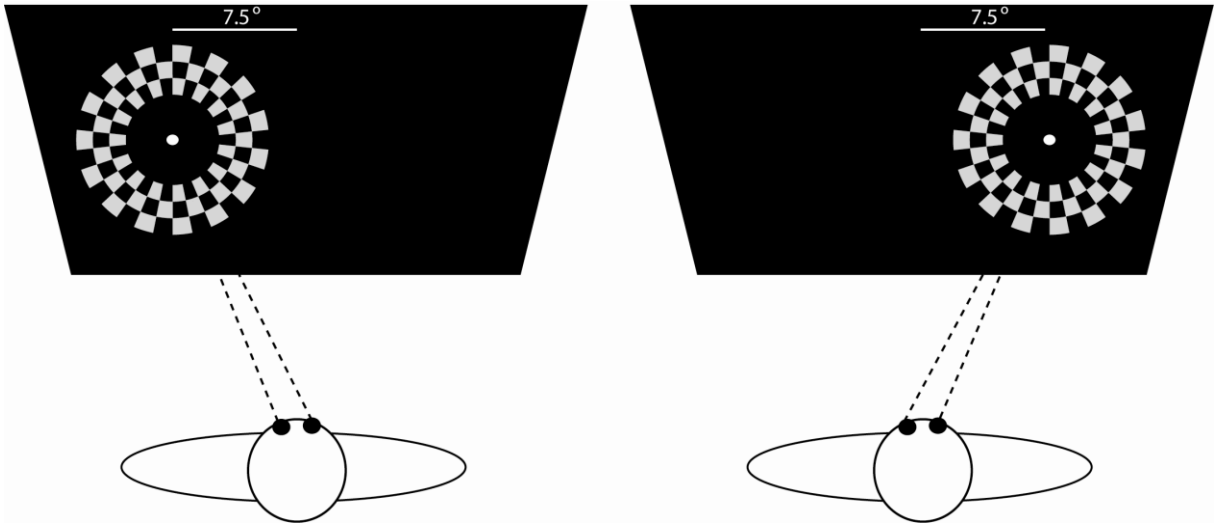

Figure 6.1 Experimental Stimulus

Each participant fixated either 7.5° to the left or to the right of midline in separate sessions, while passively viewing a flickering annulus presented in the near periphery around fixation. All discernable non-retinotopic luminance cues in the scanning environment were manually masked using matt black card, ensuring that the only source of visual stimulation during experimental runs was the experimental stimulus.

All subjects were scanned for a total of 10 runs, alternating the site of visual stimulation 7.5° to the left or right of the subject's midline on each successive run, in a manner that was counterbalanced across subjects. Each run lasted 104s and started with the appearance of the central fixation spot for 8s, followed by the flickering annulus surrounding the fixation point for the rest of the run (figure 6.1). Subjects were instructed to fixate on the fixation spot for the duration of the run. Between each run the part of the screen that was not being stimulated in the next run was manually masked to prevent scattered light from the projector illuminating it. Fixation accuracy was ensured by separate offline measurement in two subjects with high-speed eye tracking; during scanning it was precluded as the infrared illuminant from commercially available eye trackers produces visible light causing a non-retinotopic illumination that would thus systematically vary across gaze directions. These methodological considerations ensured that retinotopically very closely matched visual stimulation was presented in two different directions of lateral gaze.

6.2.2 Imaging Parameters

A 3T Siemens Allegra system acquired T2*-weighted Blood Oygenation Level Dependent (BOLD) contrast image volumes using a descending sequence every 1.3s. Each volume comprised 30 3-mm-thick slices, positioned on a per subject basis to give coverage of the occipital lobe with an in-plane resolution of 3x3 mm. To maximize signal to noise in early visual cortex an occipital head coil was used. In total, 10 scanning runs of 80 image volumes were acquired per subject.

6.2.3 Visual Area Localisation

To identify the boundaries of primary visual cortex (V1) and extra-striate retinotopic cortical areas V2 and V3, standard retinotopic mapping procedures were used (Sereno et al., 1995). Checkerboard patterns covering either the horizontal or vertical meridian were alternated with rest periods for 16 epochs of 26s over two scanning runs each lasting 165 volumes. Mask volumes for each region of interest (left and right V1, V2d, V2v, V3d, V3v) were obtained by delineating the borders between visual areas using activation patterns from the meridian localisers. Standard definitions of V1 were followed together with segmentation and cortical flattening in MrGray (Teo et al., 1997;Wandell et al., 2000).

6.2.4 Imaging data analysis

Data were preprocessed using Statistical Parametric Mapping software (SPM2, www.fil.ion.ucl.ac.uk/spm). After discarding the first five image volumes from each run to allow for T1 equilibration effects, functional image volumes were realigned to the first of the remaining volumes and co-registered to the individual participants' structural scans. Data were not spatially smoothed.

6.2.5 Univariate analysis

Activated voxels in each experimental condition were identified using a statistical model containing boxcar waveforms representing the two experimental conditions convolved with a canonical haemodynamic response function. Multiple linear regression was then used to generate parameter estimates for each regressor at every voxel. Data were scaled to the global mean of the time series, high-pass filtered (cut-off - 0.0083 Hz) to remove low-frequency signal drifts and autocorrelations removed. Regression parameters resulting from analysis of the experimental imaging time series were extracted for voxels activated by visual stimulation regardless of gaze direction at a statistical threshold of $p<0.001$ (uncorrected) in each region of interest (Figure 6.2), yielding a plot of response estimate for identical visual stimulation when gaze was left or right of midline in V1, V2 and V3 averaged across subjects (figure 6.3).

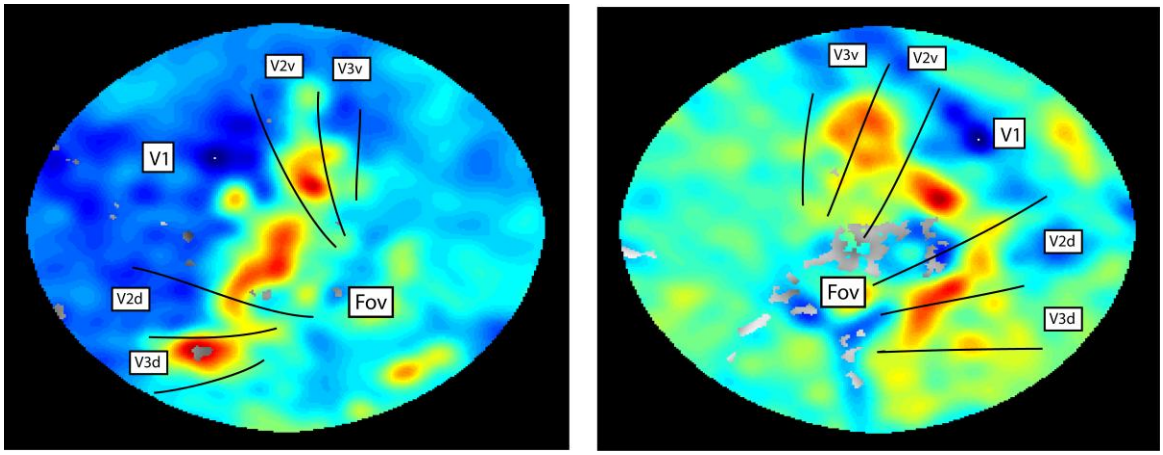

Figure 6.2. Activation evoked by the experimental stimulus in visual cortex

Voxels activated by the presence of the flickering annulus stimulus regardless of gaze direction at a statistical threshold of $p<0.001$ (uncorrected) are projected onto a flattened representation of the left (left panel) and right (right panel) occipital cortex of a representative subject. The boundaries of visual areas V1-3 are also overlaid onto this representation. The pattern of activation is as expected for an annulus presented in the near periphery. These voxels were then used in further analyses to compare activity evoked under different gaze directions (Fov = Fovea).

6.4 Univariate results

The responses of voxels that were significantly activated by the experimental visual stimulus regardless of gaze direction ($p<0.001$, uncorrected – see Figure 6.3) were compared under left and right gaze conditions. An ANOVA showed a significant main effect of visual area ($F(2,10) = 17.7$, $p=0.001$), but no main effect of gaze direction ($F(2,10) = 0.17$, $p=0.91$) or interaction between visual area and gaze ($F(2,10) = 1.05$, $p=0.38$). All areas show no significant difference in visually evoked BOLD signal during fixation to the left compared to the right ($t(5)<0.5$, $p>0.6$, two-tailed).

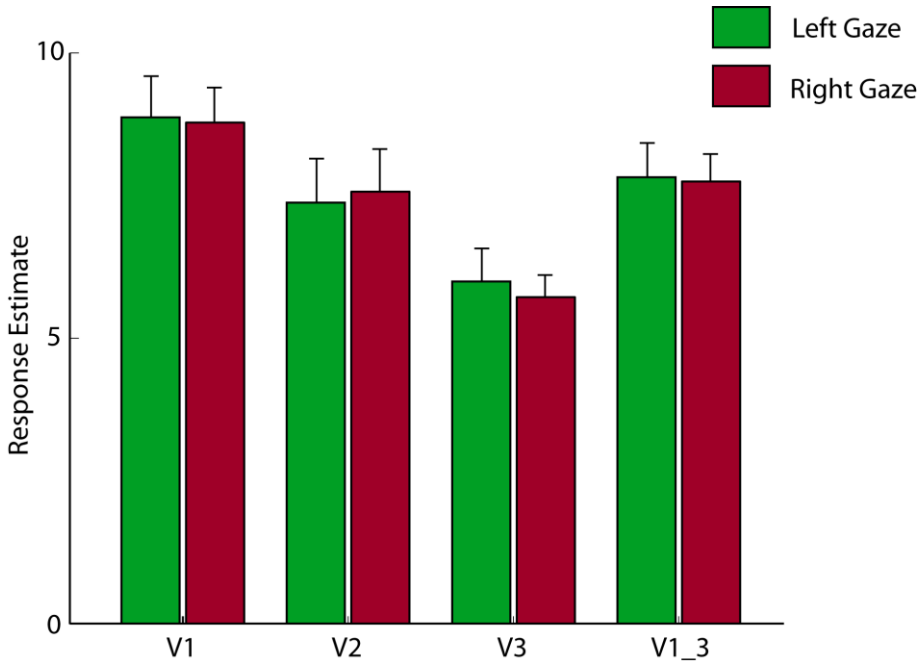

Figure 6.3. Modulation of mean visually evoked activity by gaze direction in visual areas V1-3.

BOLD contrast responses in human V1, V2, V3 and V1-3 during identical visual stimulation viewed by subjects while fixating to the left (green bars) and right (red bars) of midline. Data are taken from individual participant retinotopic analyses and based on the mean of all voxels activated by visual stimulation (regardless of gaze direction) at a threshold of $p<0.001$, uncorrected. The modelled estimates of fMRI activity are plotted as a function of condition, averaged across six participants (error bars ± 1 SE). All areas show no significant difference in visually evoked BOLD signal during fixation to the left compared to the right ($t(5)<0.5$, $p>0.6$, two-tailed).

6.4.2 Discussion of univariate results

The data presented in Figure 6.3 suggest that there is no effect of lateral gaze direction on visual responses evoked by carefully matched visual stimuli in human early retinotopic visual cortex when averaged across the ROI. This is in direct contrast to findings in non-human primates, where single cell recording has consistently shown that gaze direction modulates visual responses in these areas. It is conceivable that this is an example of interspecies difference, and human visual cortical responses are not modulated by gaze. However, there is evidence that activity in human early visual cortex is modulated by static eye position which makes such an assertion unlikely. For example, gaze direction modulates short latency visual evoked potentials (Andersson et al., 2004) and the tilt aftereffect (Nishida et al., 2003) which are both thought to arise from activity in early retinotopic cortex. It is possible that gaze does indeed modulate human early visual cortex, but that averaging the activity across each visual area (as was done in the analysis above) cancels out any modulatory effects of gaze. To illustrate this point, consider the effects of left and right gaze on a population of neurons in a visual area such as V1. If some neurons are weakly modulated by left gaze and a similar proportion are weakly modulated by right gaze – when responses are averaged across the whole population, no modulation by gaze would be seen. When all directions of gaze are taken into account, the visual activity of many neurons could be weakly modulated by a certain direction of gaze. This pattern of weak biases would mean that gaze direction could be encoded as a spatially distributed pattern within each cortical visual area. However, the analysis presented in Figure 6.3 averages the responses over all voxels activated by the visual stimulus meaning that the information avaliable at each voxel (in the form of weak biases) is lost. Therefore this type of analysis may not be ideally suited to distinguishing stimulus properties that are encoded in the brain as spatially distributed patterns of weak biases. Analysis of such patterns of brain activity can be achieved using multivariate anaylysis of fMRI data (Cox and Savoy, 2003;Haynes and Rees, 2006). For example, physical attributes that are known to have a spatially distributed representation in the monkey visual cortex have recently been shown to be encoded in a similar fashion in

human visual areas (e.g. orientation selectivity (Haynes and Rees, 2005;Kamitani and Tong, 2005), motion direction (Kamitani and Tong, 2006), (see Figure 6.4).

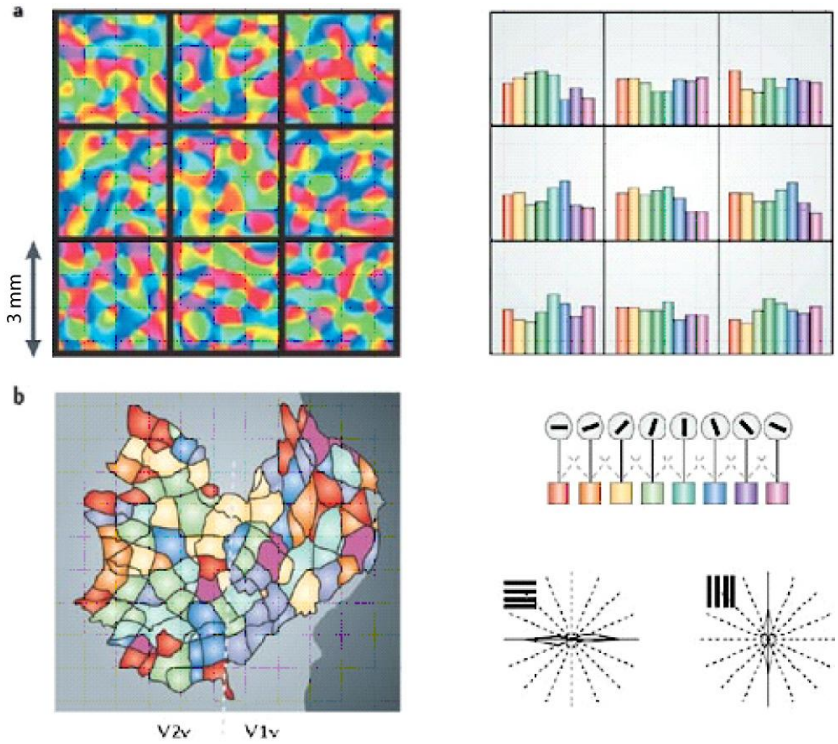

Figure 6.4 Orientation selectivity in early human visual cortex shown using multivariate analysis
A. In primate V1, neurons with different orientation preferences are systematically mapped across the cortical surface. Regions containing neurons with similar orientation tuning are separated by approximately 500μm (Obermayer and Blasdel, 1993) (left panel, different colours correspond to different orientations). The cortical representation of different orientation preferences is too closely spaced to be resolved by functional MRI at conventional resolutions of 3mm (indicated by the measurement grid in the left panel). Nonetheless, simulations (Haynes and Rees, 2005)reveal that irregularities in these maps may cause each voxel to sample a slightly different proportion of cells with different tuning properties (right panel), leading to potential biases in the orientation preference of each voxel.
B. When subjects view images consisting of bars with different orientations, each orientation causes a subtly different response pattern in the early visual cortex (Haynes and Rees, 2005;Kamitani and Tong, 2005). The map shows the spatial pattern of preferences for different orientations in V1 and V2 plotted on the flattened cortical surface (Kamitani and Tong, 2005) (v, ventral). Although each individual measured areas preference is small, perceived orientation can be decoded with high accuracy when the information in the entire spatial response pattern is taken into account. Two different orthogonal orientation stimuli can be accurately decoded when a linear support vector classifier is trained to classify the responses to different orientations (right panel) (Kamitani and Tong, 2005). This figure is adapted from (Haynes and Rees, 2006).

If direction of gaze is represented in a spatially distributed fashion in early visual areas, multivariate (rather than univariate) analysis of human fMRI data may be required to demonstrate gaze dependent modulation of visual responses in these brain areas. This could explain why the univariate analysis of the fMRI data presented earlier (figure 6.3) failed to find gaze modulation of early visual areas. To test this hypothesis, a further analysis of the data was performed using multivariate methods. This enabled assessment of whether lateral gaze direction is encoded as a spatially distributed pattern of responses in retinotpic areas V1-V3.

6.5 Overview of multivariate analysis in fMRI

Before describing the details of how multivariate analysis was implemented in this study, I will consider how multivariate analyses work in the context of fMRI data. Consider the example shown in Figure 6.5. Two visual stimuli (images 1 and 2) evoke overlapping response patterns in visual cortex. These response patterns are sampled at low spatial resolution using fMRI to give a set of voxels that show two sets of responses (one for each visual stimulus – figure 6.5a). The core of multivariate analysis methods involves testing whether the response patterns evoked by the two stimuli are the same or different. If the response patterns to the two stimuli are different then the brain area under study can be said to encode the stimulus feature that varies between the two stimuli, whereas if the converse is true, this cannot be said to be the case. In univariate analyses each voxel is considered separately, therefore if differential neuronal responses to image 1 and 2 are distributed over a wide area, the difference in the response to each image at each voxel will be small. The advantage of multivariate analyses is that information is accumulated from all voxels enabling maximisation of any differences in activity evoked by image 1 and 2. Multivariate analysis therefore allows assesment of whether the pattern of activity evoked by each stimulus can be accurately differentiated.

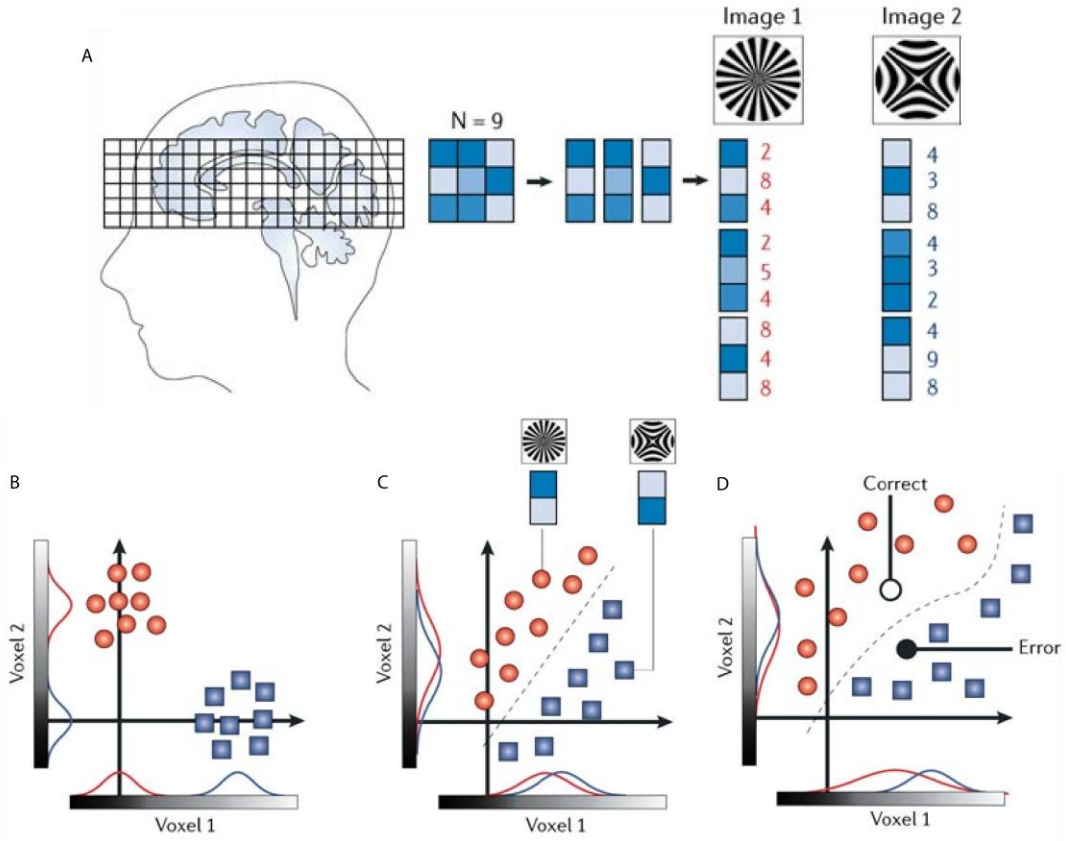

Figure 6.5 Analysis of spatial patterns using a multivariate pattern recognition approach.

A. FMRI measures brain activity repeatedly every few seconds in a large number of voxels (left). The joint activity in a subset (N) of these voxels (shown here as a 3x3 grid) constitutes a spatial pattern that can be expressed as a pattern vector (right). Different pattern vectors reflect different mental states; for example, those associated with different images viewed by the subject.

B-D. Each pattern vector can be interpreted as a point in an N-dimensional space (shown here in panels b–d for only the first two dimensions, red and blue indicate the two conditions). Each measurement of brain activity corresponds to a single point. A successful classifier will learn to distinguish between pattern vectors measured under different mental states. In panel b, the classifier can operate on single voxels because the response distributions (red and blue Gaussians) are separable within individual voxels. In panel c, the two categories cannot be separated in individual voxels because the distributions are largely overlapping. However, the response distributions can be separated by taking into account the combination of responses in both voxels. A linear decision boundary can be used to separate these two-dimensional response distributions. In panel d, to test the predictive power of a classifier, data are separated into training and test data sets. Training data (red and blue symbols) are used to train a classifier, which is then applied to a new and independent test data set. The proportion of these independent data that are classified either correctly (open circle, 'correct') or incorrectly (filled circle, 'error') gives a measure of classification performance. This figure is adapted from (Haynes and Rees, 2006).

Practically this is achieved by training a pattern classification algorithm with the pattern of activity evoked by each image type. The classifier then attempts to blindly classify subsequently acquired test measurements to the category that evoked the most similar response pattern during the training phase (figure 6.5c). Accuracy is assessed by the comparing the classifier output with known labels (figure 6.5d). There are many methods that can be used to define the similarity between such distributed response patterns but machine learning methods such as linear discriminant analyses or support vector machines are effective and simple to implement. The steps required in this type of multivariate analysis are schematically represented in figure 6.6.

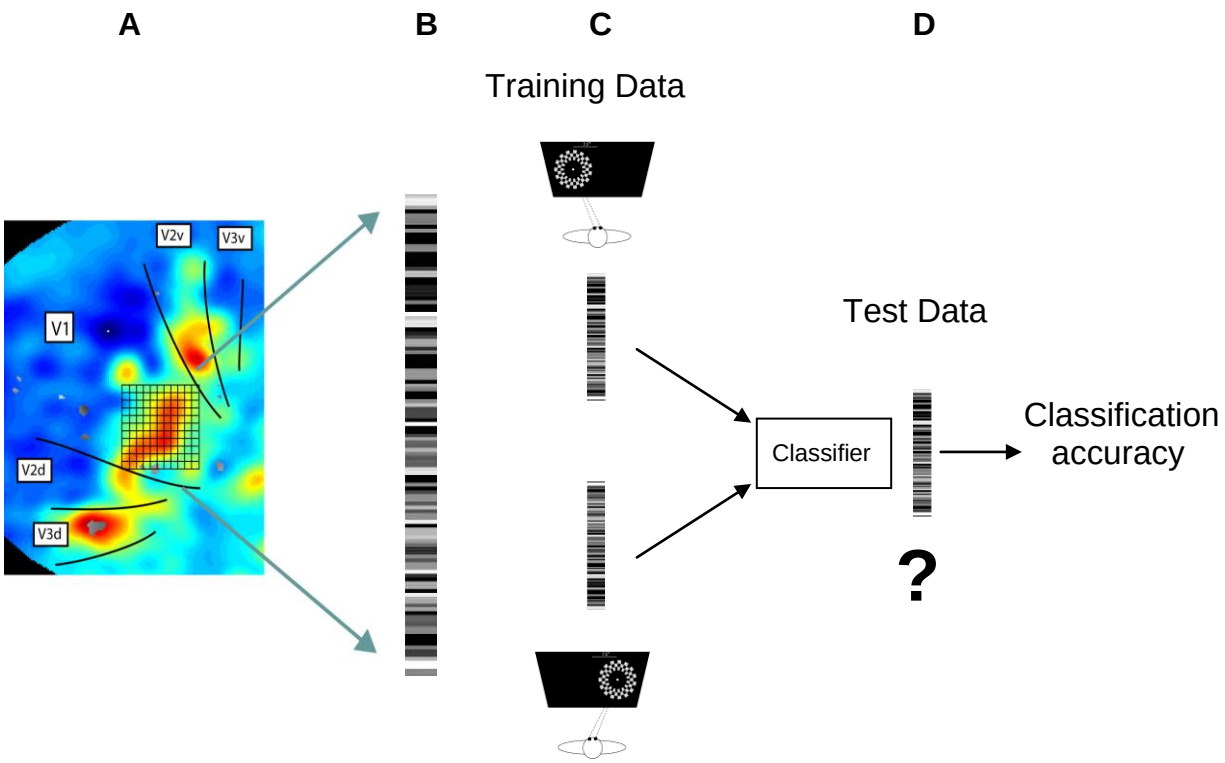

Figure 6.6 Schematic representation of the steps in multivariate analysis

A) All voxels activated by the visual stimulus (irrespective of gaze position are identified (see methods and figure 6.2 for details).

B) The raw fMRI signal over the whole experiment is extracted from each voxel in the stimulus representation (in this case in V1) to create a pattern vector of n voxels and their timecourses. This is represented vertical bar, where each voxel's activity is represented by a grayscale horizontal bar (in the pattern vector derived from experimental data each voxel will have x measures of activity – where x = the total number of volumes acquired during the experiment)

C) The pattern vectors are split into two subsets, one for responses during left gaze and the other for right gaze. These vectors are then used as training sets for a pattern classification algorithm.

D) The classifier then attmpts to classify test measurements to the category that evoked the most similar response pattern during the training phase. The accuracy of this allocation of test measurements gives a measure of whether the pattern of activity evoked by each experimental condition can be accurately differentiated.

6.6 Multivariate pattern classification methods

The BOLD signal across each visual stimulation block of each condition (see main methods) was extracted for n voxels within each ROI – V1, V2 and V3 (same voxels as used for univariate analyses – see Figure 6.2), forming a set of pattern vectors **a,** which can be considered as points in an n-dimensional Euclidean space. Pattern classification was performed using linear support vector machines (SVM) (Christianini, 2000) in the Gunn implementation (http://www.isis.ecs.soton.ac.uk/). A linear classifier finds a hyperplane

$$\mathbf{w}^T\mathbf{x} + b = 0$$

defined by weight vector **w** and offset b separating the training points **x** with two different given labels. The principle of SVM is to find the optimally separating hyperplane that maximises the margin (given by $2/\|\mathbf{w}\|$) with respect to both training classes (see (Christianini, 2000;Vapnik, 1995) for detailed algorithm). Under the presence of noise (as here) the response vectors of both stimuli might not be linearly separable and a so-called "soft-margin classifier" can be used which allows for a certain proportion of misclassifications by minimising

$$\|\mathbf{w}\|/2 + C \sum \xi_i$$

subject to

$$y_i(\mathbf{w}\mathbf{x}_i + b) \geq 1 - \xi_i \qquad i = 1,2,...,N \qquad \xi \geq 0$$

where ξ_i is a slack variable representing misclassification error for the *i*th pattern $\mathbf{x}_i$ with label $y_i 0\{1,-1\}$ and C a regularisation parameter determining the trade-off between largest margin and lowest number of misclassifications.

In the analysis presented here, the optimal value for C was determined using a leave-one-out cross-validation procedure that was independent of the actual SVM classification. The data set of N pattern vectors per condition was subdivided into a training set of N-2 pattern vectors, a validation set (1 pattern vector), and a test set (1 pattern vector), with N possible assignments of independent training, validation, and test data sets. The optimal value of C was first determined for each planned pairwise comparison in each subject, i.e., the value that produced the minimum classification error. To that end, the classifier was iteratively trained on the N possible training sets and tested on the respective *validation sets* using ten exponentially increasing values for C ($C = e^i$ for $i = 0, 1, \ldots 10$). Classification errors were averaged across all different training and validation data assignments. The optimal value of C derived from the cross-validation procedure varied widely across subjects from 148 to 8103 with a median of 2981. Therefore the optimal value of C for each subject was used in the SVM classification.

For SVM classification, the classifier was again iteratively trained on the N training data sets, but this time tested on the respective *test data set*. As the test data set in each iteration was different from the validation data set, the classification of the test data was independent of the validation procedure that was used to optimize C. Classification accuracies were averaged across all different training and test data assignments (Figure 6.6). The average classification accuracies from each participant were then for each pairwise comparison subjected to two-tailed one-sample t-tests at the group level testing for significant deviation from chance level (50 %).

6.7 Results - Multivariate analysis

SVM classification was significantly better than chance at correctly classifying the direction of lateral gaze on the basis of spatially distributed patterns of activity in stimulus-responsive voxels (Figure 6.7). Prediction accuracy from V1 was on average 64% ± 0.06 (95%CI), which was significantly greater than chance (50%; $t(5)= 4.45$, $p<0.01$, two-tailed t-test). In both V2 accuracy was also significantly greater than change (60% ± 0.07; $t(5)= 3.13$, $p<0.03$, two-tailed). In V3, the classification accuracy trended towards significance in comparison to chance (55% ± 0.05; $t(5)= 2.28$, $p<0.08$, two-tailed). Using all voxels in V1, V2 and V3 accuracy was also significantly greater than chance (62% ± 0.06; $t(5)= 4.23$. $p<0.01$, two-tailed). In contrast, if information about the spatial pattern of responses was discarded and classification attempted on the basis of the mean signal alone, performance in V1-V3 was not significantly different from chance (see Figure 6.3). There was no difference in prediction accuracy between V1 and V2 ($t(5)=1.19$, $p=0.29$) but both V1 and V2 showed significantly greater accuracy than V3 (V1-V3; $t(5)= 2.55$, $p=0.051$, V2-V3; $t(5)= 2.65$, $p=0.045$).

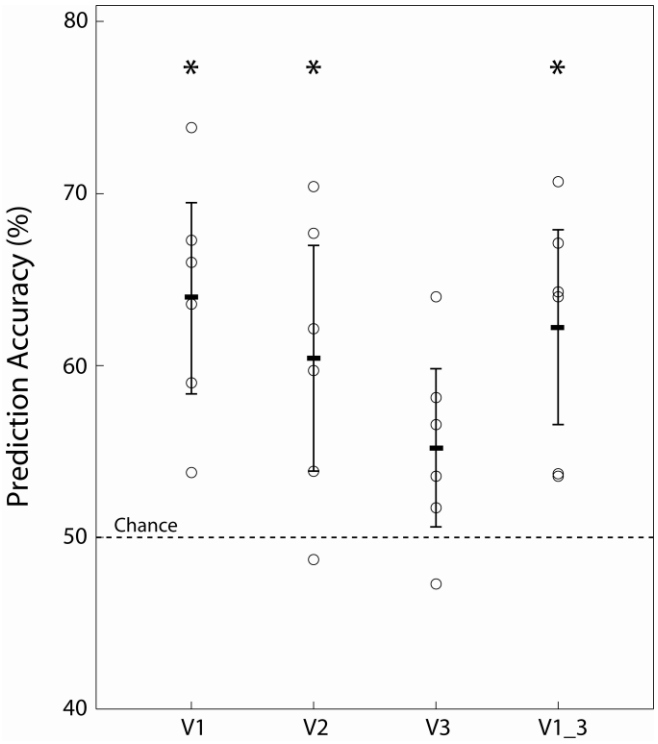

Figure 6.7. Accuracy of prediction of gaze direction from visually active voxels in V1-3.

The performance of SVM classification of gaze direction (left or right) plotted as accuracy (% correct). Data are taken from individual participant retinotopic analyses and based on SVM's using voxels activated by visual stimulation (regardless of gaze direction) at a threshold of $p<0.001$, uncorrected, in each visual area. Filled rectangles represent the accuracy averaged across six subjects (error bars = +/- 95% CI). The open circles represent accuracy of classification for each individual subject. A prediction accuracy of 50% represents chance performance. It is clear that the average accuracy in V1, V2, V3 and V1-3 is greater than 50%. This reached statistical significance in V1, V2 and V1-3, and trended towards significance in V3. The '*' symbol represents $p<0.05$, two-tailed.

6.8 Discussion

6.8.1 Human visual cortex contains sufficient information to reconstruct horizontal gaze direction

The data presented in Figure 6.7 demonstrate that the responses of retinotopically mapped stimulus-responsive voxels in human V1-V3 contained information sufficient to reconstruct horizontal gaze direction. This finding is consistent with gaze direction being

encoded in early visual areas, but there are other possible explanations that require consideration. It is possible that successful classification of gaze direction relied on neuronal responses to visual features other than the stimulus representation (for example, the edge of the display - whose retinal position varied with gaze direction). However, this is unlikely as only voxels that responded to the stimulus were used in this analysis (figure 6.2) and great care was taken to ensure that the only source of visual stimulation during experimental runs was the experimental stimulus (through manually masking all parts of the projection screen and scanning environment except the location at which the experimental stimulus appeared).

Even with these measures, activity in 'stimulus responsive voxels' could still be influenced by remote areas of the visual field, through long range horizontal interactions (Gilbert et al., 1996). Although the spatial extent of long range horizontal interactions in humans is not clear, horizontal influences in monkey V1 occur over a maximal distance of 6-8mm (in terms of cortical area), which equates to approximately 4° of the visual field (see for example Stettler et al., 2002). However, as the edge of the screen in the present experiment was greater than 4° away from all parts of the visual stimulus, remote parts of the visual field are likely to exert only minimal influence on the activity of stimulus responsive voxels.

Differences between the visual activity evoked during left and right gaze could also be explained by systematic differences in the pattern of eye movements during the two gaze conditions. For example, if during left gaze subjects' eyes drifted rightward towards the midline and during right gaze subjects' eyes drifted leftward towards the midline, the pattern of visual stimulation during left and right gaze would differ. If this were the case, however, one would expect univariate analysis methods to show a difference between left and right gaze. This was clearly not the case in this study (see Figure 6.3). In addition, although eye movements were not recorded during scanning as the recording process would necessarily confound any comparison of visual activity evoked in different gaze positions (by providing visual stimulation that varied in retinal position according to gaze direction), fixation accuracy was excellent when measured offline. Therefore the most

likely explanation for the results shown in Figure 6.7 is V1-3 contains sufficient information to allow above chance correct classification of the direction of gaze.

6.8.2 Gaze representation is spatially distributed in visual cortex

Single cell recordings in monkey have repeatedly shown that gaze modulates visual responses at many levels in the visual system. These areas include V1-3 (Rosenbluth and Allman, 2002;Trotter and Celebrini, 1999;Weyand and Malpeli, 1993) in addition to later visual and parietal regions. Although human fMRI studies have identified V5/MT (DeSouza et al., 2000) and parietal cortex (DeSouza et al., 2000) as sites modulated by gaze direction, these studies did not demonstrate gaze modulation of purely visual responses. There is stronger evidence that gaze direction modulates visual responses in earlier human visual areas. For instance both perceptual after effects (Nishida et al., 2003), short latency evoked potentials ander (Andersson et al., 2004) which are thought to arise from early visual cortical activity, are modulated by gaze position. The initial univariate analysis of the current experiment showed no effects of gaze position on visual responses in V1-3. This obviously contrasts strongly with the monkey single cell and human psychophysical and evoked potential studies described above. The results of the multivariate analysis partly resolve this apparent paradox, as they suggest that the distributed spatial pattern of activity in these areas, reflecting weak biases of individual voxels, encodes information about gaze direction (Figure 6.7). This information about gaze direction is lost when the signal across the whole of V1-V3 is averaged in a univariate analysis (Figure 6.6). This could explain why single cell recordings but not univariate fMRI studies demonstrate gaze modulation in early visual areas. However, it is not clear why evoked potentials, which reflect the activity of a larger neuronal population than that sampled using fMRI, can be modulated by gaze position. It is conceivable that EEG, which directly records neural activity, can identify gaze related signals not seen in indirect measures of neural activity (such as the BOLD response).

As the BOLD contrast fMRI signal indirectly measures activity in large populations of neurons, the source of the gaze signal cannot be precisely identified. For example, it is

possible that human V1 contains separate populations of neurons coding for retinotopic location of a stimulus and gaze position; or a single population whose activity is jointly modulated by stimulus and gaze. There is currently no evidence to suggest that gaze effects are systematically mapped across the cortical surface (as in the case of orientation preference, see Figure 6.5). Nevertheless, the successful reconstruction of horizontal gaze direction from visual cortex activity using multivariate methods suggests that there are reproducible gaze biases distributed throughout visual cortex. Further work could examine whether these biases exhibit any spatial structure over visual cortex ('gaze mapping').

Given that strong gaze effects have been reported in parietal and late visual areas, it is perhaps surprising that the ability to reconstruct gaze direction was significantly greater in V1 and V2 compared to V3 (Figure 6.7). However, there are a number of methodological considerations that could have contributed to this finding. First, delineation of the outer border of V3 can be difficult using the retinotopic mapping technique employed here. This could mean that voxels from other visual areas (that may or may not encode gaze) could be defined as V3 and reduce classification accuracy when used in a subsequent analyses. Second, the number of voxels significantly activated by the experimental stimulus was often greater in V1/2 than V3. Reducing the number of voxels entered into an SVM analysis can lead to a reduction in classification performance. Therefore, although the difference between V1/2 and V3 may represent differences in underlying physiology of these areas, the methodological points raised must also be considered.

6.9 Conclusion

In conclusion, the results presented in this chapter are consistent with a distributed representation of horizontal gaze direction being present at the earliest anatomical stages of cortical processing (V1-3). However, it is not clear whether this representation is functionally relevant and used to guide visiomotor behaviour. More generally, these findings indicate that oculomotor behaviours that do not lead to disruption of visual

continuity still modulate visual processing. This suggests that although the visual and oculomotor systems are spatially segregated in the brain, they show a high degree of integration at the neural level. This is consistent with our everyday experience of the visual world where frequent eye movements do not lead to disruption of visual continuity. Finally these data demonstrate the ability of multivariate approaches to reveal information in spatially localised patterns of activity that is not apparent in region-of-interest analyses. Future work could apply this approach more generally to different directions of gaze and head direction in order to uncover the neural substrate of sensorimotor coordinate transformations in human vision and action.

CHAPTER 7: VISUAL RESPONSES IN HUMAN SUPERIOR COLLICULUS SHOW TEMPORAL-NASAL ASYMMETRY

7.1 Introduction

The previous experiments in this thesis have demonstrated that even when visual stimulation remains constant, oculomotor behaviours, such as saccadic eye movements and alteration in static gaze direction, profoundly alter the pattern of activity in early visual areas. This modulation presumably reflects tight coupling between the oculomotor and visual systems, as under most circumstances eye movements result in altered visual context, but it also has functional significance. For example, disruptive effects of saccades on perceptual continuity are reduced by inhibition of visually evoked responses in LGN and V1 (see Chapter 3 and 5). Furthermore, population encoding of visual stimuli in gaze centred coordinates in V1, may contribute to successful visually guided action (see Chapter 6). Rather than looking at the effect of eye movements on visual structures when visual conditions remain constant, this chapter will examine the effect of altering visual conditions on oculomotor structures when the eyes remain still and fixated centrally. Specifically, it will focus on the visual responses of the superior colliculus (SC). The SC is a key structure in the interaction between the visual and oculomotor systems as it is intimately involved in the generation and execution of orienting eye (and head) movements in response to visual information. The experiment outlined in this chapter will examine whether the visual responses of the SC are consistent with biases in visual orienting found behaviorally.

Behavioral studies have utilized eye patching to reverse which visual hemifield (left or right) is temporal or nasal. With the right eye patched, the left hemifield becomes temporal and the right nasal; while the reverse holds with the left eye patched. The use of eye patching has uncovered temporal-nasal differences in several aspects of visual behavior. For instance, newborns show pronounced advantages for orienting towards visual stimuli in the temporal versus the nasal hemifield (Lewis and Maurer,

1992;Rothbart et al., 1990). While such biases are less absolute in adults, temporal hemifield advantages are still detectable with more subtle measures such as saccadic latencies (Kristjansson et al., 2004;Rafal et al., 1991) or choice saccades to bilateral stimuli (Posner and Cohen., 1984). However, more recent studies showing that this bias occurs even when S-cone stimuli, which are not thought to be processed by the SC, are used (Bompas et al., 2008).

It has frequently been proposed (Rafal et al., 1991) that such behavioral results may reflect a biased representation favoring the temporal hemifield in the retinotectal pathway from retina to superior colliculus (SC), which may lead to a preference for the contralateral hemifield of the contralateral eye in the SC (see figure 7.1). This might account for the pronounced temporal-hemifield advantages found in infants, whose retinotectal pathway is thought to mature prior to geniculostriate vision (Johnson, 1990). It might also explain why these same temporal-hemifield advantages can still occur in hemianopic adult patients (Dodds et al., 2002;Rafal et al., 1990), who retain intact retinotectal pathways despite damage to the geniculostriate system. Although it must be added that these results have not been replicated in a subsequent study (Walker et al., 2000).

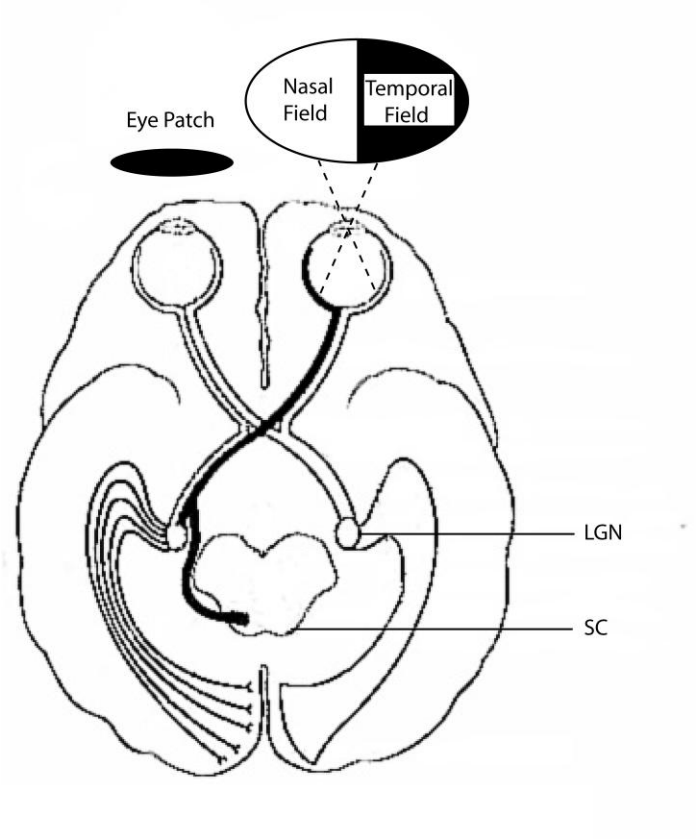

Figure 7.1. The proposed anatomical projections of the retinotectal and retinogeniculate pathways. Figure 7.1 shows a representation of the main visual pathways from the retina to early visual areas and the hypothesized difference in the source of retinal input to the SC and LGN / visual cortex. This hypothesis proposes that the SC predominantly receives input from the contralateral nasal hemiretina (which represents the contralateral temporal visual hemifield) and crosses at the optic chiasm. In contrast, the LGN and V1 are thought to receive equal input from the contralateral nasal and temporal hemiretina (representing the contralateral nasal and temporal hemifield respectively). This difference can be explored by manipulating which eye views identical hemifield visual stimuli by means of an eyepatch.

Although retinal projections from the contralateral eye that specifically represent the temporal visual field predominate in the cat retinotectal pathway (Sterling, 1973), this anatomic asymmetry may be less complete in monkeys (Hubel et al., 1975;Perry and Cowey, 1984;Pollack and Hickey, 1979;Williams et al., 1995;Wilson and Toyne, 1970). Moreover, some temporal-nasal asymmetries for the peripheral field may arise even at the retina (Stone and Johnston, 1981;Van Buren, 1963) or striate cortex in monkeys (LeVay et al., 1985) although at greater eccentricities than the behavioral effects seen in man. Thus it cannot be simply assumed that only the retinotectal pathway could show

temporal-nasal asymmetries in humans (just as one cannot assume that only the retinotectal pathway mediates visual orienting, see Sumner et al., 2002). One physiological method for examining any asymmetries in humans is to use fMRI to compare visual responses elicited by temporal and nasal visual stimulation in the SC with those of the lateral geniculate nucleus (LGN) and visual cortex.

Studies of macaque SC suggest that it is anatomically and functionally divided into superficial and deep layers. Neurons in the deep layers are weakly visually responsive but are primarily involved in orienting movements of the head and eyes in response to sensory stimuli. In contrast, neurons in the superficial layers respond to a broad range of stationary and moving visual stimuli apparently regardless of stimulus orientation, size, shape, or velocity (Cynader and Berman 1972;Goldberg and Wurtz, 1972) and contain an orderly map of the contralateral visual field (Cynader & Berman 1972). Most cells, apart from those at the posterior pole representing the far temporal periphery (Hubel et al 1975), receive binocular input (Moors and Vendrik, 1979) and many show some tuning for retinal disparity (Berman et al., 1975). Their main input is from the retinotectal pathway (Schiller and Malpeli, 1977), but their response properties may also be influenced by the geniculostriate pathway via from striate cortex (Wilson and Toyne, 1970) and extrastriate cortex (Fries, 1984). In contrast, the deep layers are primarily influenced by corticotectal feedback projections (Schiller et al., 1974). Therefore cortical influences on the deep SC are possibly better placed than retinal influences on superficial SC to cause biases in orientating behaviour.

The human SC shows BOLD contrast responses to contralateral visual field stimulation, and also some degree of retinotopy (Schneider and Kastner, 2005), If temporal-nasal differences largely reflect retinotectal pathway contributions as previously proposed (see above), then SC responses to monocular visual stimuli should presumably be greater for temporal versus nasal hemifields; but those of structures in the geniculostriate pathway should not. Accordingly, visual responses of the SC, LGN and retinotopic V1-V3 were measured using fMRI, while independently manipulating two factors; which eye viewed the stimuli, and which visual field was stimulated. Since reversing the stimulated eye

reverses whether the left or right hemifield is temporal or nasal, this design correspondingly manipulated whether visual stimulation contralateral to a particular brain hemisphere was temporal or nasal. Note that any such manipulation of temporal/nasal stimulus presentation can also be understood in terms of eye preferences in any area with responses lateralized to one visual hemifield. For instance, temporal hemifield biases could reflect a preference for contralateral stimuli presented in the contralateral eye.

The SC is small and lies close to prominent blood vessels, making it difficult to image with conventional fMRI (though see (Schneider and Kastner, 2005). Therefore high spatial resolution fMRI (3T with 1.5x1.5x1.5 mm voxels) was used, giving occipital lobe and upper brainstem coverage only. To circumvent physiological noise from cardiac-cycle influences on SC images, established algorithms were adapted to correct for cardiac induced brainstem motion (Glover et al., 2000). It was then determined whether SC and other visual structures showed any temporal/nasal biases in fMRI responses to lateralised monocular stimulation.

7.2 Methods

7.2.1 Subjects

Eight healthy right-eye-dominant subjects (mean age 30.2 years, 4 male) gave written informed consent to participate in the study, which was approved by the local ethics committee. Eye dominance was assessed using the Porta sighting test (Porta, 1593), which consists of an observer extending one arm, then with both eyes open aligning the thumb with a distant object. The observer then alternates closing of one or the other eye to determine which eye is viewing the object (i.e. the dominant eye). Subjects lay supine in the scanner and had one of their eyes covered with a patch attached to a wooden pole that could easily be moved to cover the other eye between runs. To ensure that no light leaked in through the edges of the patch, I first made sure that the patch completely blocked out light entering the eye it covered in each subject in the scanner environment. Before the start of each run in the study, it was verified that subjects were covering the

correct eye and that they could not see anything out of the patched eye. Subjects were then instructed not to move the patch until the run ended and it was verified that the patch had stayed in place before moving it over to the other eye (in preparation for the next run).

7.2.2 Stimuli

Visual stimuli were projected from an LCD projector (NEC LT158, refresh rate 60 Hz) onto a screen viewed by a mirror positioned within the MR head coil. All stimuli were presented using MATLAB (Mathworks Inc.) and the COGENT 2000 toolbox (www.vislab.ucl.ac.uk/Cogent/index.html). In addition to a 0.5° central fixation cross, the visual stimuli comprised a 13° wedge with a 3° foveal cut-out, made up of alternating black/white checks (scaled linearly with eccentricity) reversing contrast at 8Hz. This stimulation was presented either to the left or to the right of fixation, at 3° and 13° eccentricity for the innermost and outermost edge respectively (see Figure 7.2 for a diagram).

Each subject was scanned for four runs, alternating the unpatched eye on each successive run (verified by the experimenter), in a manner that was counterbalanced across subjects. In each run the wedge stimulus was presented eight times for 16s, with a 10s rest period between presentations, and with these presentations alternating between left and right hemifields. Subjects, who were all experienced psychophysical observers, were instructed to maintain fixation and this was confirmed by online monitoring of video output from a long-range infrared eyetracker (ASL 504LRO Eye Tracking System, Mass).

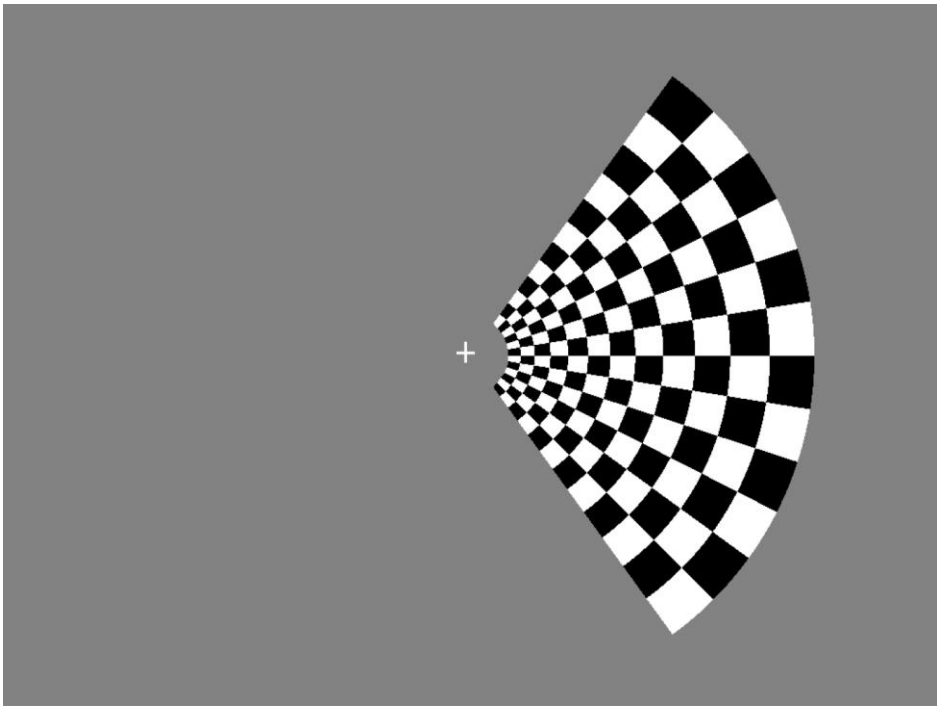

Figure 7.2. The visual stimulus used in the main study

This figure illustrates the experimental stimulus that subjects viewed during the study. In addition to a small central fixation cross, the visual stimuli comprised a 13° wedge with a 3° foveal cut-out subtending 120°, made up of alternating black/white checks (scaled linearly with eccentricity) reversing contrast at 8Hz. This stimulation was presented either to the left or to the right of fixation, at 3° and 13° eccentricity for the innermost and outermost edge respectively.

7.2.3 Imaging and Preprocessing

A 3T Siemens Allegra system acquired T2*-weighted Blood Oygenation Level Dependent (BOLD) contrast image volumes, using an interleaved sequence every 3.0s. Each volume comprised 30 contiguous 1.5-mm-thick slices, positioned on a per subject basis in parallel to the calcarine sulcus to give coverage of the occipital lobe and upper brainstem with an in-plane resolution of 1.5x1.5 mm (Haynes et al., 2005). The interleaved sequence limited signal interaction between spatially adjacent slices. In total, four scanning runs, each consisting of 125 image volumes, were acquired per subject. During scanning, pulse oximetry data were recorded continuously from the right index finger to allow analysis in relation to the cardiac cycle (see below).

Imaging data were analysed using SPM2 (www.fil.ion.ucl.ac.uk/spm). After discarding the first five image volumes from each run to allow for T1 equilibration effects, image volumes were realigned, manually coregistered to each subject's structural scan and smoothed with an isotropic 2mm Gaussian kernel (Turner et al., 1998). Automated coregistration with SPM was not employed, as it would lead to inaccuracies in registration of the EPI and anatomical images, due to limited brain-coverage and minor distortions in EPI images resulting from the high resolution sequence. Coregistration was therefore performed carefully by hand, allowing exact coregistration of the calcarine sulcus and superior colliculus on the EPI scans to each subject's structural scan.

Activated voxels in each experimental condition were identified using a statistical model containing boxcar waveforms representing each of the four experimental conditions, convolved with a canonical haemodynamic response function and mean-corrected (Turner et al., 1998). Six head motion parameters defined by the realignment procedure, plus twelve parameters related to the cardiac cycle derived from pulse oximetry data (Glover et al., 2000;Josephs et al, 1997), were added to the model as eighteen separate regressors of no interest. Multiple linear regression was then used to generate parameter estimates for each regressor at every voxel. Data were scaled to the global mean of the time series, and high-pass filtered (cut-off - 0.0083 Hz) to remove low-frequency signal drifts.

The cardiac noise correction was implemented at the level of modeling the measured signal and not at the level of image reconstruction, i.e., image data were not modified. The underlying model used assumed that cardiac effects on a voxels signal depend on the phase of the image slice acquisition within the cardiac cycle (Josephs et al, 1997). Sine and cosine series (up to 3rd order) were used to describe the phase effect on a single reference slice (passing through SC) creating six regressors. The phase for the adjacent slice (acquired 0.5 TR later) was also used to create a second set of six sine and cosine series, thus taking into account the increased temporal difference between adjacent slices

in the interleaved slice acquisition. As shown in Josephs et al (1997), the model is best adapted to the slice of reference. However, the large coherent component in the cardiac noise (due to only small variations in heart rate) can be corrected by a single set of regressors and functions well for removal of physiological noise throughout the image. This precluded the need for regressors related to the cardiac cycle to be generated for each slice (or the need for any slice timing correction). Although this method is less sensitive to incoherent noise components from throughout the image, as these will only be modelled in areas where the regressors match the cardiac activity (i.e. the reference slice), the influence of these components is minor (Josephs et al., 1997). As adjacent slices were acquired 1.5s apart, using two models (one for the slice closest to the SC and one for the slice spatially adjacent to this) captured noise related to the cardiac cycle more effectively. This approach proved to be very effective in accounting for (and thereby eliminating) variance related to the cardiac cycle, particularly in the region of the upper brainstem (see Figure 7.3 for an illustrative subject).

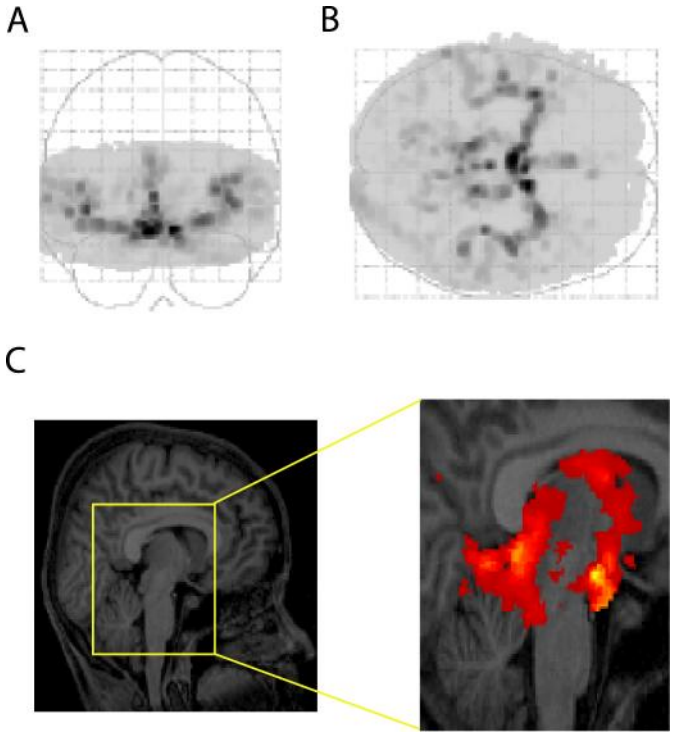

Figure 7.3. Anatomical distribution of physiological noise explained by regressors calculated from the cardiac cycle during EPI volume acquisition

(A) coronal and (B) transverse maximum intensity projections (MIP), showing voxels correlated with physiological noise related to the cardiac cycle. Regressors for these effects were derived from subjects' pulse oximetry during scanning (see Methods), and results are thresholded at $P<0.05$ uncorrected for display purposes. Dark areas denote voxels maximally correlated with the cardiac cycle. The distribution of these effects is clearly related to the anatomy of the cerebral vasculature. The greatest correlation occurs in voxels located near to the major arteries of the brain, such as the circle of Willis and the middle cerebral arteries bilaterally. These arteries can clearly be seen as the darkest parts of the MIP plots.

Fig 7.3C - (Left) A sagittal view of the T1 structural scan from the subject whose data are shown in Fig 1A/B (Right). An enlarged view of the upper brainstem, overlaid with the F-contrast for the cardiac regressors. This is displayed at a high threshold ($p<0.05$, FWE corrected) to highlight areas showing maximal correlation with the cardiac cycle. There is clearly a high correlation around the upper brainstem in the region of the SC. Correlations with this cardiac model were removed from the analysis of the experimental effects of interest, to allow increased signal detection related to the experimental factors of interest (visual stimulation) in regions where physiological noise related to the cardiac cycle was greatest (such as for the SC).

7.2.4 Cortical and Subcortical Visual Area Localisation

To identify the boundaries of primary visual cortex (V1) and extra-striate retinotopic cortical areas V2 and V3, standard retinotopic mapping procedures were used (Sereno et al., 1995). Checkerboard patterns covering either the horizontal or vertical meridian were alternated with rest periods for 16 epochs of 26s over a scanning run lasting 165 volumes (using a standard 3mm voxel sequence; note that only this localiser for determining the borders of cortical areas used a 3mm resolution and the main experimental findings in SC, LGN and V1-V3 all come from the 1.5x.1.5x1.5mm sequence described above). Mask volumes for each region of interest (left and right V1, V2d, V2v, V3d, V3v) were obtained by delineating the borders between visual areas using activation patterns from the meridian localisers. Standard definitions of V1 together with segmentation and cortical flattening in MrGray were followed (Wandell et al., 2000).

The locations of the SC and LGN in each subject were identified using an anatomical and radiological brain atlas (Duvernoy, 1999) to find anatomical landmarks on each subject's high-resolution structural scan. Next, functional data co-registered to the structural scan were used to locate visually-responsive voxels within the previously defined anatomical boundaries, using a contrast of contralateral greater than ipsilateral visual stimulation. This method of localisation has previously been used successfully to investigate human LGN responses with high resolution fMRI (Haynes et al., 2005). The LGN and superior colliculi plus their response to ipsilateral and contralateral visual field stimulation are shown for two illustrative subjects in Figures 7.4 & 7.5.

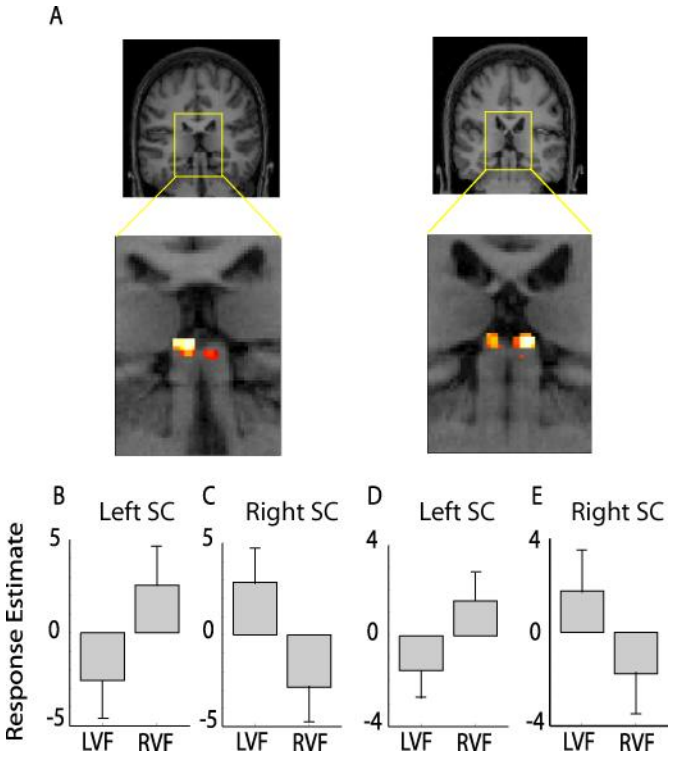

Figure 7.4. SC responses to contralateral visual field stimulation

Fig 7.4A. Coronal views of the high-resolution T1-weighted structural scan in the anatomical plane of the SC for two illustrative subjects. The yellow box indicates the anatomical area that is magnified in the lower panels to show an enlarged view of the SC. Superimposed on these enlarged views are functionally activated loci evoked by contralateral visual stimulation (from a statistical F-contrast of effects of interest thresholded at $P<0.05$, uncorrected for display purposes). The activations shown all lay inside a 3mm sphere centred on the peak voxel in the region of the SC.

Fig 7.4B-E. BOLD contrast responses of the SC to ipsilateral and contralateral hemifield visual stimulation are shown for the same representative subjects (error bars – 90% CI). Left and right SC each respond to contralateral vs ipsilateral visual stimuli. The left SC responds to right greater than left visual field stimulation as expected (Fig 7.4B,D); and right SC responds to left greater than right visual field stimulation (Fig 7.4C,E).

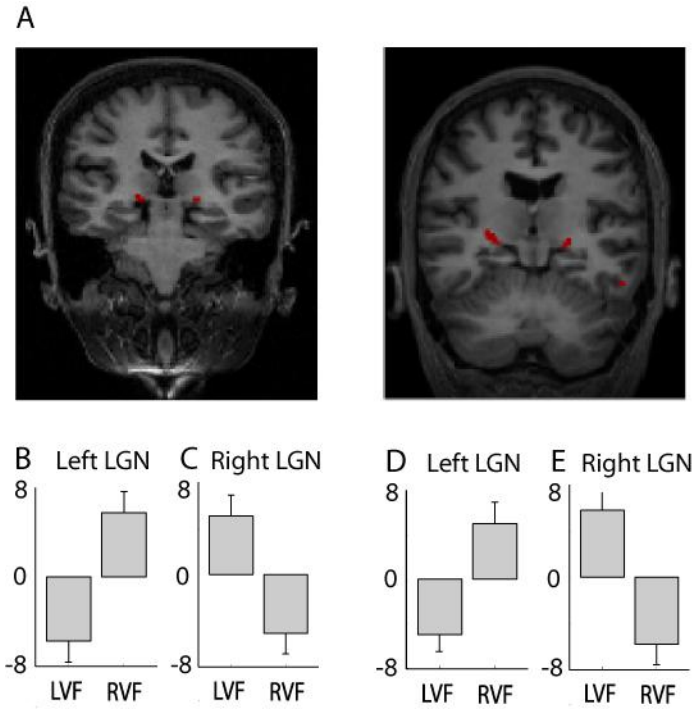

Figure 7.5. LGN responses to contralateral visual field stimulation

Fig 7.5A. Coronal views of the high-resolution T1-weighted structural scan in the anatomical plane of the LGN for two illustrative subjects. Superimposed on these views are functionally activated loci evoked by contralateral visual stimulation (from a statistical F-contrast of effects of interest thresholded at P<0.01, uncorrected).

Fig 7.5B-E. BOLD contrast responses of the LGN to ipsilateral and contralateral hemifield visual stimulation are shown for the same representative subjects (error bars – 90% CI). Left and right LGN each respond to contralateral vs ipsilateral visual stimuli. The left LGN responds to right greater than left visual field stimulation as expected (Fig 7.5B,D); and right LGN responds to left greater than right visual field stimulation (Fig 7.5C, E).

To extract activity from cortical visual structures, mask volumes were created for each region of interest (left and right V1, V2d, V2v, V3d and V3v) from the retinotopic maps. Regression parameters resulting from analysis of the imaging time series for the main experiment were then extracted for all voxels activated by visual stimulation of the contralateral hemifield in each region of interest (at a conventional statistical threshold of $p<0.001$, uncorrected). These were then averaged across subjects, yielding a plot of percent signal change in each area for each experimental condition averaged across

subjects (Figure 7.6). Responses reported for the LGN and SC are taken from the average of contiguous visually-responsive voxels within the anatomically defined boundaries. For the SC the average cluster size for contiguous visually responsive voxels in each subject was 10 voxels (SEM +/- 1) while in the LGN it was 45 voxels (SEM +/- 7).

7.3 Results

The main findings are presented in Figure 7.6. Across the group of eight subjects, all visual areas studied showed robust and statistically significant responses to contralateral visual field stimulation, as expected. The responses of subcortical structures LGN and SC to contralateral visual field stimulation were numerically lower than for retinotopic cortical areas, consistent with previous work (Kastner et al. 2004;Schneider and Kastner 2005). However, when examining responses to temporal or nasal monocular stimulation independently, a strong difference was immediately apparent when comparing SC with all other visual structures (Figure 7.6). Critically, the SC showed significantly increased responses to contralateral temporal versus nasal stimulation; but the LGN, V1, V2 and V3 did not.

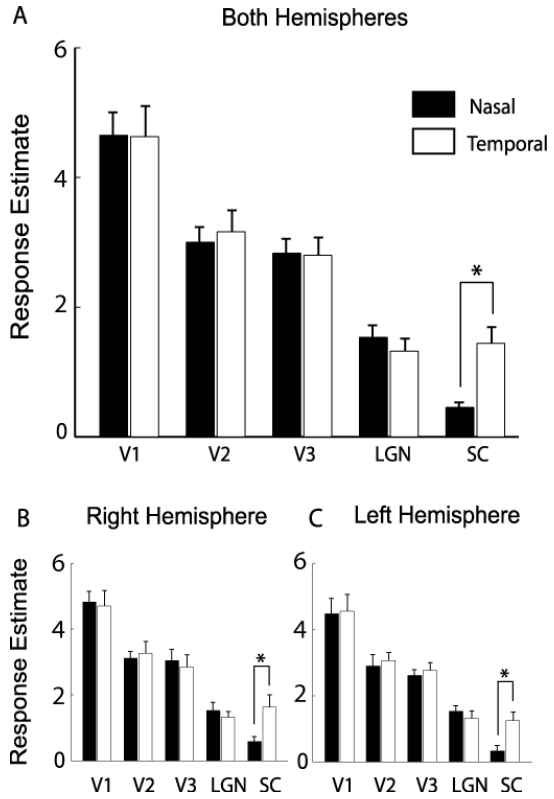

Figure 7.6. Group average responses (n=8) of human V1-V3, LGN and SC to monocular hemifield visual stimuli presented in the nasal or temporal visual field

BOLD contrast responses to identical monocular hemifield checkerboard stimuli, presented in the temporal or nasal visual field (manipulated via eye-patching), for V1-V3, LGN and SC, averaged across all subjects and both hemispheres (Fig 7.6A), or separately for the right (Fig 7.6B) or left (Fig 7.6C) hemispheres. See Methods for full details of data analysis procedure. Percent signal change averaged across eight subjects are plotted for each visual area (error bars ± 1 SE). Nasal stimulation is plotted in black and temporal stimulation in white. Only the SC showed a significantly increased response to contralateral temporal compared to nasal visual stimulation. This was the case both when averaged across subjects and hemispheres and for responses of the SC averaged across subjects within each hemisphere. There were no significant differences in the responses evoked for temporal compared to nasal stimuli in V1-V3 and LGN, neither averaged across hemispheres nor when considering either hemisphere alone, and these areas differed reliably from the SC in this respect (interaction with area – see Results). The '*' symbol denotes statistical significance ($p<0.05$, two-tailed).

This difference between SC and all other visual structures was confirmed by the presence of a highly significant interaction between visual field (temporal versus nasal) and brain region ($F(4,28)=10.163$, $p=0.001$). Significantly greater activation for temporal than for

nasal stimuli in the SC was found when pooling across colliculi for the group of eight subjects (0.3(0.05) vs 0.1(0.02) % signal change, t(7)=3.84, p=0.006, two tailed); and was also replicated for the SC when considering either hemisphere alone (left SC: 0.26(0.05) vs 0.07(0.04) % signal change, t(7)=2.58, p=0.036; right SC: 0.34(0.08) vs 0.12(0.03) % signal change, t(7)=2.45, p=0.044, both two tailed). In contrast, there were no significant differences in the responses evoked by temporal versus nasal contralateral stimulation within areas V1, V2, V3 or the LGN; neither when pooling across hemispheres (V1: 0.97(0.1) vs 0.98(0.07) % signal change, t(7)= -0.13, p =0.9, V2: 0.66(0.05) vs 0.63(0.05), t(7)= 1.05, p=0.33, V3: 0.59(0.06) vs 0.59 (0.05) % signal change, t(7)= -0.15, p=0.89, LGN: 0.32(0.04) vs 0.28(0.04) % signal change, t(7)= -1.14, p=0.14, all two tailed); nor when considering either hemisphere alone (all t(7) = <1.3, all p>0.25, all two tailed). Consistent with these results from a standard linear regression analysis, averaging the normalised raw data across subjects and brain areas revealed an identical pattern of findings (see Figure 7.7), with only SC showing a significantly greater response to temporal versus nasal stimulation.

These data show significant differences in response to temporal versus nasal stimulation for the human retinotectal pathway (SC); but not in the geniculostriate pathway (LGN, plus V1-V3; cf (Lie et al., 2004). However, it is conceivable that some local temporal-nasal differences within visual cortex might have been obscured by the procedure employed to select voxels. Voxels in each region of interest were selected on the basis of their response to contralateral visual stimulation across all runs (see Methods). This could in theory bias voxel selection towards voxels responding equally to contralateral stimulation in right and left eye, which may have excluded any voxels that showed strong eye biases. To investigate this, the analyses described above were repeated but now using independent selection of voxels responding to contralateral monocular stimulation of *either* eye (i.e. rather than selection being biased on responding to contralateral stimulation in right AND left eye, now the selection was based on right OR left eye). Reassuringly, the results were unchanged. Critically, the SC remained the only structure

showing a significantly greater response to temporal versus nasal hemifield stimulation (see Figure 7.8).

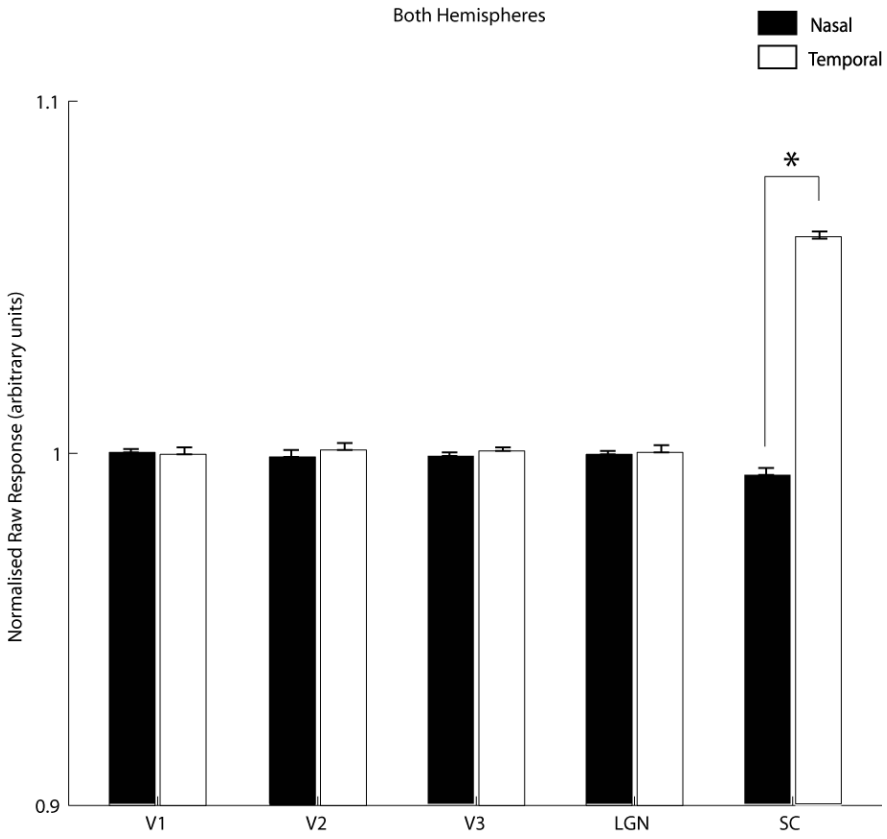

Figure 7.7. Normalised unfitted group average responses (n=8) of V1-V3, LGN and SC to monocular hemifield visual stimuli presented in the nasal or temporal visual field.

The raw responses to identical monocular hemifield checkerboard stimuli, presented in the temporal or nasal visual field (manipulated via eye-patching), for V1-V3, LGN and SC, averaged across all subjects and both hemispheres. The responses are normalised for each subject by dividing the mean response to each stimulus by the overall mean of each visual area in each subject (error bars ± 1 SE). Nasal stimulation is plotted in black and temporal stimulation in white. Only the SC showed a significantly increased response to contralateral temporal compared to nasal visual stimulation ($t(7)=2.89$, $p=0.02$, two-tailed). The '*' symbol denotes statistical significance ($p<0.05$, two-tailed).

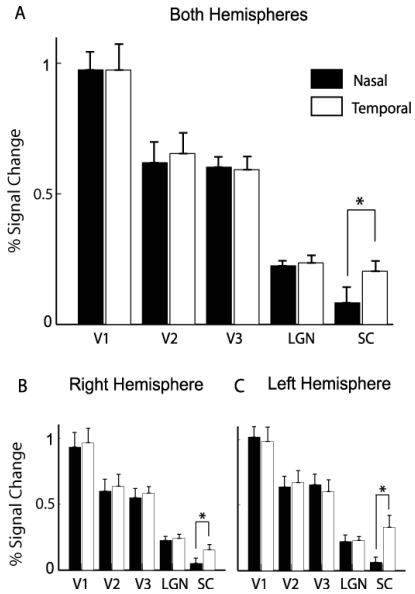

Figure 7.8. Group average responses (n=8) of V1-V3, LGN and SC to monocular hemifield visual stimuli presented in the nasal or temporal visual field using voxels selected on the basis of response to stimulation via the left OR right eye.

BOLD contrast responses to monocular hemifield stimulation, presented in the temporal or nasal visual field (manipulated via eye-patching), for V1-V3, LGN and SC, averaged across all subjects and both hemispheres, or separately for the right or left hemispheres. Percent signal change averaged across eight subjects is plotted for each visual area (error bars ± 1 SE). Nasal stimulation is plotted in black and temporal stimulation in white. Only the SC showed a significantly increased response to contralateral temporal compared to nasal visual stimulation. This was the case both when averaged across subjects and hemispheres ($t(7)=2.89$, $p=0.023$) and for responses of the SC averaged across subjects within each hemisphere (right SC: $t(6)=2.64$, $p=0.03$, left SC: $t(7)=3.09$, $p=0.02$). There were no significant differences in the responses evoked for temporal compared to nasal stimuli in V1-V3 and LGN, neither averaged across hemispheres nor when considering either hemisphere alone. The '*' symbol denotes statistical significance ($p<0.05$, two-tailed).

Another possible reason for the pattern of results presented above could be that the (standard) procedure of averaging across populations of voxels within each area, if the distribution of temporal/nasal preferences across those voxels within such areas was distributed bimodally. Indeed, monocular structures such as the LGN might at sufficiently high spatial resolution in theory show such a bimodal distribution reflecting eye preference for lateralised stimulation (although note that previous studies of LGN

with identical resolution have thus far shown a unimodal distribution of ocular preferences; see Haynes et al 2005, their Supplemental Figure S1). In order to systematically examine this possibility the responses of individual voxels in LGN and V1-V3 were further investigated. Visually responsive voxels were defined by responses to contralateral minus ipsilateral stimulation (at $p<0.001$ for V1-V3 and $p<0.01$ for LGN, both uncorrected). Parameter estimates were extracted for each voxel for contralateral hemifield stimulation when the stimulus was presented temporally or nasally. The parameter estimate for nasal hemifield stimulation was then subtracted from the parameter estimate for temporal hemifield stimulation. This gave a value that provides a measure of the extent to which each voxel shows any preference to favor stimulation of either the temporal or nasal hemifield (positive values denote a numerical temporal preference while negative values denote a nasal preference). Frequency histograms of these voxel-wise preferences confirmed that all such distributions were exclusively unimodal for all geniculostriate visual areas (i.e. LGN, V1, V2, V3) in all subjects (see Figure 7.9). Moreover, these distributions all had a peak frequency very close to zero preference, consistent with the lack of any temporal/nasal effect in Figure 6. However, a similar frequency histogram of the voxel-wise preferences in SC in all subjects showed a distribution that was systematically skewed towards temporal preference and hence a positive mean (see Figure 7.9). This is consistent with the significant temporal/nasal difference in SC responses demonstrated in Figure 7.6.

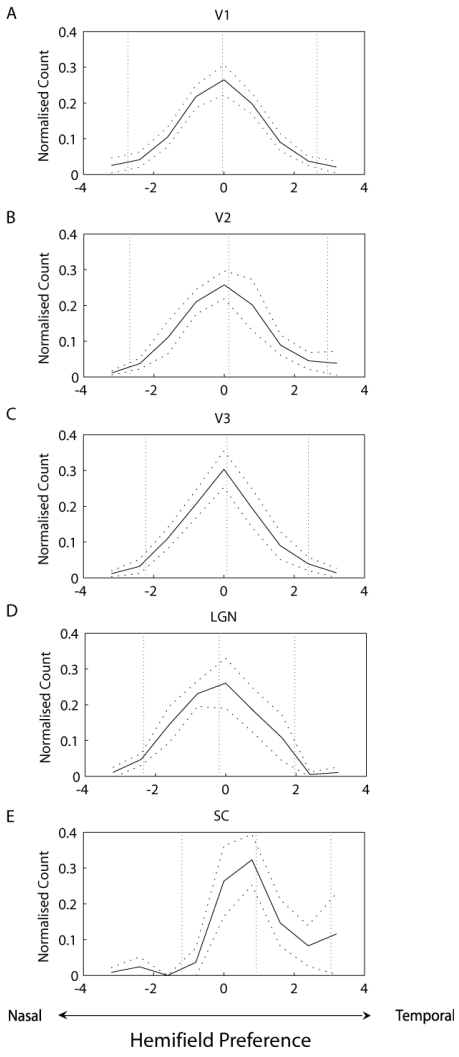

Figure 7.9. Distributions of nasal and temporal field preferences in visually responsive voxels in V1-V3, LGN and SC. (A-E). Frequency histograms across subjects plot the number of voxels in each visual area (V1-V3, LGN and SC) as a function of their numerical preference for monocular temporal versus nasal contralateral stimulation. The preference of each voxel was derived by subtracting the response estimate due to contralateral nasal stimulation from the response estimate due to contralateral temporal hemifield stimulation (see results). Positive values denote a temporal preference while negative values denote a nasal preference. For averaging across subjects, the absolute number of voxels was normalised by dividing by the total number of voxels in each visual area in each subject. Vertical dotted lines represent the mean, whilst the dashed lines represent +/- 95% CI. In areas V1-3 and LGN (A-D), it is apparent that all distributions are unimodal (rather than bimodal), suggesting that voxels in each area formed a single population with a mean response to temporal versus nasal stimulation centred on zero (see also Figure 7.6). However in the SC (E), the distribution was positively skewed and the mean was greater than zero, suggesting that the SC preferentially responded to temporal compared to nasal stimulation (see also figure 7.6).

Taken together, these data demonstrate directly for the first time that the human SC responds more strongly to temporal than to nasal contralateral visual stimulation. In contrast, no such difference was evident in the LGN or cortical areas V1-V3, which differed significantly from the SC in this respect.

7.4 Discussion

These results show that human SC responses, but not those of the LGN, V1, V2 or V3, were significantly greater for monocular visual stimuli presented in the temporal hemifield than in the nasal hemifield. This provides strong and direct evidence for a biased representation favoring the temporal hemifield within the human SC (although whether this arises solely from retinotectal, or also reflects some corticotectal influences upon the SC is not yet established). This bias may provide a neural substrate for temporal-nasal asymmetries observed in prior purely behavioral studies that had sought to examine putatively collicular-related aspects of visual behavior (e.g. saccades and orienting, see Posner and Cohen, 1984).

7.4.1 FMRI of human superior colliculus

In non-human primates, single-cell recording has shown that individual neurons in the superficial layers of the SC are highly responsive to visual stimuli and receive afferent inputs from the retina (Schiller and Malpeli, 1977), striate cortex (Wilson and Toyne, 1970), extrastriate cortex (Fries, 1984) and frontal eye fields (Fries, 1984;Kuypers and Lawrence, 1967). Within the superficial layers of each SC there is a systematic map of the contralateral visual field (Cynader and Berman, 1972;Goldberg and Wurtz, 1972). The central visual field is represented anteriorly while the periphery is represented posteriorly. The upper fields are represented medially and the lower fields laterally. The

central ten degrees of the visual field is expanded to represent more than 30% of the surface of the colliculus. The projection of the contralateral hemi-retina includes the entire colliculus while the projection of the ipsilateral hemi-retina is represented only in the anterior portion of the colliculus, leaving a monocular representation of the temporal hemifield at the posterior pole (Hubel et al 1975).

As far as can be ascertained, human SC seems to follow a similar anatomical pattern (Hilbig et al., 1999;Laemle, 1981;Tardif et al., 2005). However, it has been difficult to study human SC responses using neuroimaging techniques until recently, because of the small size of the SC, plus its deep location near to vascular structures that increase local physiological noise (Guimaraes et al., 1998). Previous attempts to image the superficial layers of the SC used cardiac triggering of image acquisition to reduce movement artefacts related to nearby pulsatile blood vessels (DuBois and Cohen, 2000); or used very high spatial resolution scanning (Schneider and Kastner, 2005). In this study both methods were combined by using 1.5x1.5x1.5mm voxels for fMRI; plus twelve analysis regressors related to the cardiac cycle (as measured with pulse oximetry) in order to reduce physiological noise related to blood flow (Glover et al., 2000). The data confirm (see also Schneider and Kastner, 2005) that neuroimaging of visual responses in the human SC with fMRI is now feasible, although technically demanding. Moreover, the present results reveal clear temporal-versus-nasal differences within the human SC for the first time, while showing a significantly contrasting pattern for the LGN and for visual cortex.

These findings can also be redescribed as reflecting a preference in the SC for stimulation of the contralateral hemifield in the contralateral eye, but no overall eye preference for the neuronal populations recorded from LGN or visual cortex. In those voxels in LGN and V1 that showed an eye bias there were no systematic preferences in the overall responses of either left or right LGN and V1 for stimulation of one eye compared to the other (Figure 7.9). This contrasts with the findings in SC, where there were strong and highly significant responses for stimulation of the contralateral hemifield in the contralateral eye (equivalent to the temporal hemifield). Of note, there did not seem to be

any consistent clustering of such voxels preferring stimulation of one eye within SC (Figure 7.10). However, caution is appropriate before concluding that human SC shows no monocular structure, due to the small size of the SC and comparatively coarse fMRI spatial resolution. In monkey, the SC largely comprises binocularly responsive neurons (as discussed above) but there is a monocular region at the posterior pole (which represents the far temporal periphery i.e. beyond 25 degrees). No consistent evidence for a posterior region showing monocular preference within the human SC was found (Figure 7.10). However, the lateral extent of temporal visual field stimulation in the fMRI scanner was limited by the head coil to 20 degrees. It may therefore have been unlikely that this putative monocular region representing very eccentric visual locations was stimulated. Further research with even higher spatial resolutions and visual stimulation at much greater eccentricities may therefore be necessary to resolve this remaining issue definitively.

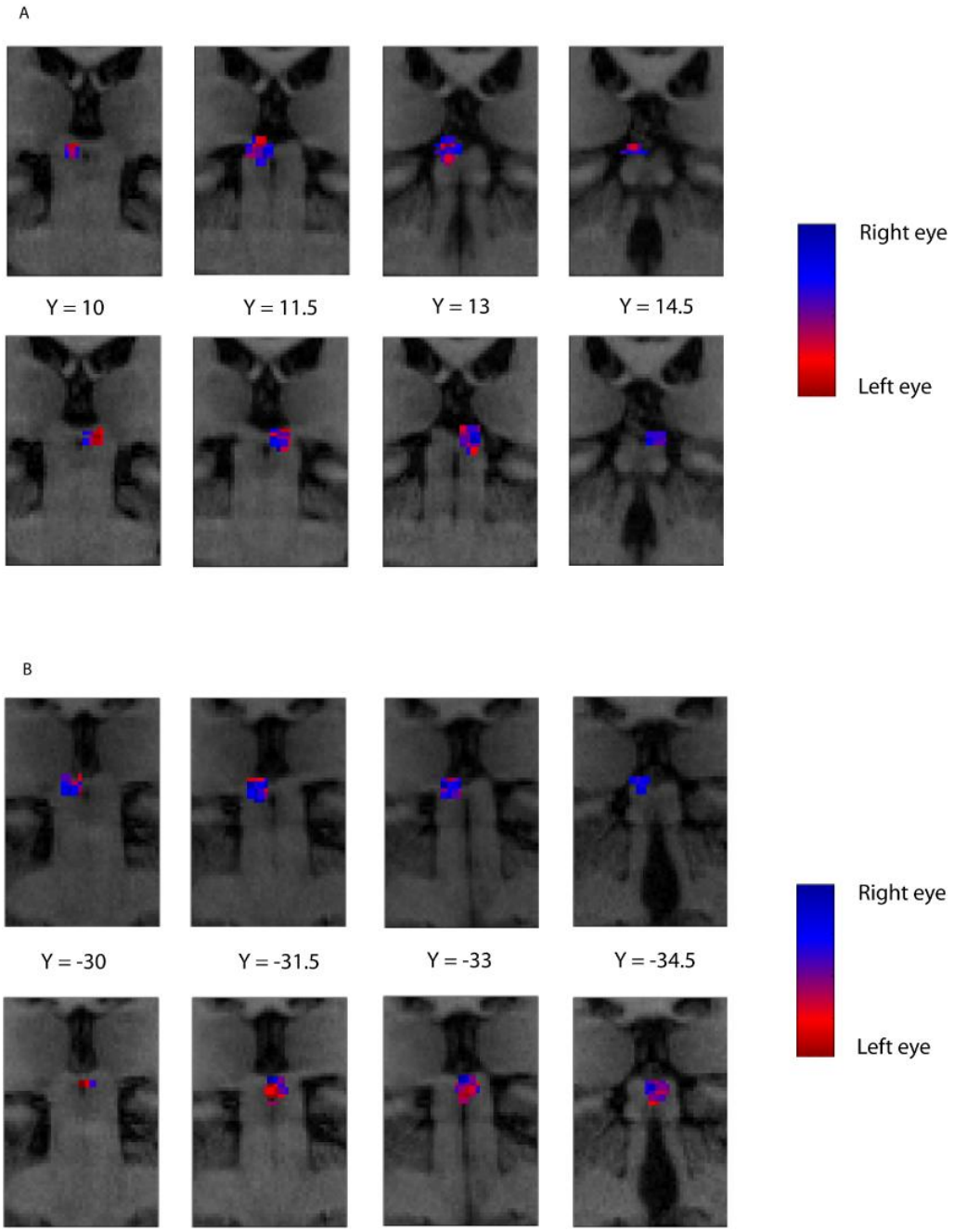

Figure 7.10. Left and right SC voxels plotted according to the degree to which they show eye preference to identical contralateral hemifield stimulation in two representative subjects.
Voxels are plotted for two subjects (A and B) in four consecutive slices through the region of the left (upper panel) and right (lower panel) SC. Voxels are colour coded to show the eye preference based on t-values of response to right eye stimulation greater than left eye. Voxels with a right eye preference are blue, while those with a left eye preference are red. Although there is no consistent pattern of eye dominance, overall each SC has more voxels that respond to the temporal than nasal hemifield (eg. left SC responds preferentially to right eye stimulation, right SC to left).

7.4.3 Possible neural substrate for behavioral temporal-hemifield advantages is confirmed in the collicular pathway

The retinotectal pathway is phylogenetically ancient and predates the geniculostriate system (see (Karten, 1989). It might have evolved to augment rapid orienting of the eyes and head to salient peripheral stimuli. In species where the eyes are positioned on or towards the side of the head, such a temporal hemifield advantage in the retinotectal pathway could convey a survival advantage by reducing the time required to orient to objects appearing in the periphery of vision. These data provide the first direct evidence that human SC responses are greater for stimuli presented in the temporal versus nasal visual field. The SC is considered intimately involved in orienting to salient stimuli through target selection (Ignashchenkova et al., 2004;McPeek and Keller, 2004b) and related shifts of visual attention (Muller et al., 2005a). Increased responses in the human SC for temporal hemifield stimuli, as observed here, might thus explain temporal-hemifield advantages previously observed in human visual orienting behavior (e.g. (Kristjansson et al., 2004;Posner and Cohen, 1984;Rafal et al., 1990). Indeed, such behavioral asymmetries have previously been tentatively attributed to the retintotectal pathway. However, hitherto such proposals had all been based on indirect speculation that temporal-nasal asymmetries might arise within the colliculus but not for the geniculate-striate pathway. Without direct evidence the opposite proposal, that any orientating biases arise from, could equally be made. Cortical influences on the deep SC (which is directly involved in saccade generation) could be better placed than retinal influences on the superficial SC (which has a largely sensory role) to cause biases in orientating behaviour. This study confirms that these asymmetries seem to be mediated by the retino-tectal but not the geniculo-striate pathway in the human brain for the first time. It remains uncertain whether the temporal-nasal asymmetries shown behaviorally, and now with fMRI, are merely a relic of evolution or continue to convey useful advantages in primates.

This study (and indeed any non-invasive imaging study of any stimulus property in humans) cannot distinguish whether any bias in fMRI responses evoked by a particular stimulus arises from an increased number of neurons responding to that stimulus; or to a

larger gain associated with neuronal responses to one particular stimulus. There are established anatomical asymmetries in temporal versus nasal hemifields in the retina (Stone and Johnston, 1981;Van Buren, 1963) and striate cortex in monkeys (LeVay et al., 1985), but only for retinal eccentricities of well beyond fifteen degrees. In the central fifteen degrees of the visual field, where temporal hemifield behavioural advantages occur (see Rafal et al 1991), and where the visual stimuli in this study were presented, there is no evidence for any anatomical asymmetry in either the retina or the retinotectal projection. In the macaque, there appears to be no numerical asymmetry in the temporal versus nasal projection from the retina to the SC (Williams et al 1995). But the present fMRI results accord with the human temporal nasal differences found behaviourally (Rafal et al., 1991).

BOLD contrast fMRI signals more closely correlate with local field potentials than with axonal spiking (Logothetis et al., 2001) and thus at a population level the BOLD signal cannot clearly distinguish between the effect of feedforward and feedback influences on a region. The temporal hemifield biases observed in SC responses could therefore in principle reflect either retinotectal or corticotectal influences. However, there were no differences in BOLD signal from V1 or other retinotopic cortical areas found when comparing temporal and nasal hemifield stimulation. This lack of temporal/nasal asymmetry in cortical structures may argue against the notion that the temporal biases that were observed in SC originate from the corticotectal pathway (see also e.g. Fries 1984). However these data cannot exclude the influence of corticotectal feedback on the SC. This might be examined in the future by imaging the SC in patients with cortical lesions.

7.5 Conclusion

In conclusion, this study provides direct evidence for a bias in the visual response of the human SC that favors the temporal over the nasal contralateral hemifield. No such bias is apparent in the geniculostriate pathway (LGN, V1-V3), which differed significantly from the SC in this respect. The collicular preference for the temporal hemifield shown here

may thus provide a neural substrate for analogous temporal-hemifield advantages in visual behaviour. These findings demonstrate that the interaction between the oculomotor and visual systems is reciprocal. Activity in early visual structures is profoundly influenced by oculomotor behaviour and leads to modulation of visual perception. While activity in oculomotor structures is influenced by visual conditions and this may lead to biases in oculomotor behaviour. Visual influences on oculomotor structures are not limited to the SC, indeed primate FEF encodes a visual salience map (Thompson and Bichot, 2005) that contributes to rapid covert or overt shifts of attention to salient locations in the visual field. However, the extent to which visual conditions modulate oculomotor activity throughout the oculomotor system remains to be seen.

CHAPTER 8: GENERAL DISCUSSION

8.1 Introduction

The experimental studies outlined in this thesis demonstrate that there is a significant interaction between visual and oculomotor processing at the neural level in the human brain. This general discussion will review these findings and the implications they have for our understanding of visual and oculomotor processing. In addition, I will explore the extent to which these findings can shed light on other brain processes and indeed abnormal visual perception or behaviour following damage to the brain. Finally, I will discuss further experimental studies that would test hypotheses generated from the experimental data presented in this thesis. The experimental studies can be grouped according to whether they examine the effect of dynamic oculomotor behaviour (Chapters 3,4,5) or static eye position (Chapter 6) on visual activity or the influence of varying visual context on oculomotor activity (Chapter 7).

8.2 The effects of dynamic oculomotor behaviour on human visual processing

Dynamic oculomotor behaviour includes a range of eye movements including saccades, microsaccades, smooth pursuit, accommodation, vergence and reflexes that limit retinal slip (such as the VOR). Each of these behaviours leads to perceptual consequences that potentially require compensation by the visual system. This issue is particularly important in the context of saccade where the high velocity and large amplitude of the eye movements leads to prolonged ‘gaps’ in visual experience. Why these gaps are not subjectively experienced has been the focus of much experimental research. While many groups have found significant perisaccadic decreases in human visual sensitivity

(saccadic suppression), (Burr et al., 1982;Riggs et al., 1974;Zuber and Stark, 1966) the precise nature and location of active saccadic influences on the human visual system are not clear. In monkeys, saccades have been shown to significantly modulate visually evoked neuronal responses in LGN, V1 and later visual areas (Duffy and Burchfiel, 1975;Ramcharan et al., 2001;Thiele et al., 2002) even when confounding visual effects of saccades are eliminated (Reppas et al., 2002). Three experimental chapters in this thesis were concerned with defining the neural substrates of saccadic modulation of visual processing:

Chapter 3 examined the effects of saccades on human LGN and V1-3 responses using BOLD contrast fMRI under a range of visual conditions (including darkness) in normal subjects. The major finding was that saccades altered activity in LGN and retinotopic visual cortex in two distinct ways. First, the presence (versus absence) of saccades was associated with significant modulation of activity in both the LGN and V1 (although to a significantly greater extent in LGN than V1). Second, this modulation differed depending on whether saccades were made in the presence or absence of visual stimulation. Visually evoked activity was reduced by saccades but in total darkness saccades led to increased activity in the same visual brain areas.

Chapter 4 outlined the results of a new analysis of the data from Chapter 3 which was carried out to characterize the underlying mechanisms that lead to saccadic modulation of visual brain areas in more detail. DCM, a method for modelling effective connectivity using fMRI data (Friston et al., 2003a), was used to examine changes in connectivity in a network of visual and oculomotor brain areas during saccades. The results of this analysis demonstrate that saccadic modulation of visual brain areas can be explained by changes in the effective connectivity between LGN, V1 and FEF. Specifically, saccades modulate LGN activity rather than later visual areas (which are modulated through decreased feedforward effective connectivity). Second, the differential modulation of visual areas during saccades made in darkness and light can be explained by changes in the effective connectivity between FEF and V1 under these different states of visual stimulation.

Chapter 5 explored the nature of the increased activity seen in visual areas during saccades in darkness by examining the effect of systematically manipulating the strength of visual stimulation on saccadic modulation of LGN and V1 responses. The findings suggest that the motor component of saccades alone can lead to increased activity in retinotopic visual areas. This activity can be measured directly in darkness using fMRI, but only inferred during visual stimulation (by the absence of suppression of visual activity at low levels of visual stimulation).

Taken together, these findings provide insight into both the mechanisms of saccadic suppression and more general principles concerning the neural basis of visual and occulomotor interactions. Saccadic modulation of visual processing is a more complex process than one might imagine. Saccadic effects are not confined to a single location and do not only result in suppression of activity in visual structures. Instead saccades act on a distributed network of subcortical and cortical visual areas and have different effects on these structures depending on the concurrent state of visual stimulation (suppression of visually evoked responses and increased activity in darkness representing a corollary discharge). This differential effect is consistent with the notion that the perceptual phenomenon of saccadic suppression results from an interaction of oculomotor and visual signals (Diamond et al., 2000). My results also suggest that LGN has a crucial role in relaying oculomotor information to later visual areas. LGN activity is modulated to a greater extent than cortical visual areas and the connectivity analysis suggests that modulation of cortical activity occurs *because* of changes in LGN activity. To examine whether LGN is necessary for saccadic modulation of later visual areas one could examine saccadic modulation of V1 in darkness using subjects with hemianopia due to optic radiation damage. If modulation of V1 activity by saccades is dependant on LGN then one would see modulation of V1 activity in the intact hemisphere but not in the damaged hemisphere.

The mechanism for changes in human LGN activity during saccades is not clear but may arise from areas involved in occulomotor planning and execution (such as FEF) directly or via brainstem oculomotor structures that have direct connections to the LGN. Intriguingly, concurrent single cell recordings at multiple sites within the pigeon visual system suggest that saccadic effects on visual activity arise from modulation of visual thalamus by oculomotor brainstem nuclei including omnipause and optinokinetic neurons (Yang et al., 2008). It is tempting to speculate that a similar mechanism in humans can account for the interaction between oculomotor structures and the LGN during saccades (and given the range of brainstem structures involved also during other types of dynamic oculomotor behaviour), but there is currently no direct evidence for this. Although combined TMS / fMRI studies have shown that FEF stimulation can influence V1 activity (Ruff et al., 2006), exploring brainstem and subcortical interactions would be very difficult given the current technology available.

There are a number of related areas that further studies could meaningfully address. First, whether corollary discharge related to saccades in early visual cortex is functionally relevant. If this extraretinal signal has a significant functional role, one would expect it to encode information about the saccade metrics that lead to its generation (such as direction and amplitude). Therefore one prediction that could be tested is that V1 activity related to saccades made in darkness can be differentiated on the basis of saccade direction alone (for example saccades to the left will cause a different pattern of V1 activity than those to the right). Second, the perceptual phenomenon of peri-saccadic mislocalization (Ross et al., 1997) could be explored. Here visual stimuli presented prior to saccade initiation are mislocalized towards the target of the upcoming saccade. This phenomenon is thought to arise from peri-saccadic remapping of visual receptive fields (although there is currently no human physiological evidence for this assertion). If this is the case the early cortical retinotopic maps may be altered prior to saccade onset and this could be examined by defining the spatial pattern of V1 activity elicited by the presentation of brief visual stimuli prior to saccade initiation. One might expect to see predictable differences in the spatial pattern of activation from an identical stimulus prior to initiation of saccades of

different amplitude and direction if saccade if this interpretation of the psychophysiacal results is correct.

8.3 The effects of static eye position on human visual processing

It is clear that dynamic oculomotor behaviour leads to significant modulation of activity in visual brain areas. This modulation represents compensation for the disruptive visual consequences of eye movements but also may contain information directly related to oculomotor behaviour. While altering the direction of gaze fixation leads to minimal disruption of perceptual continuity, extraretinal signals encoding eye position could provide potentially useful information for the visual system. In particular, such information could be used in the transformation of the contents of visual perception into a form that could guide motor behaviour. Psychophysical studies have shown that static eye position modulates human perception of stimuli that are processed early in the visual system (Nieman et al., 2005;Nishida et al., 2003) and monkey V1 single cell responses are modulated by gaze (Trotter and Celebrini, 1999). Therefore Chapter 6 examined whether human V1 responses are modulated by gaze direction when the visual environment is unchanged. The main finding was that gaze direction did not modulate visual cortical activity when the data was analysed using conventional univariate analysis. However, significant gaze effects were found when multivariate analysis was used. This result is consistent with a distributed representation of horizontal gaze direction being present at the earliest anatomical stages of cortical visual processing (V1-3). Therefore, static in addition to dynamic oculomotor behaviour seems to modulate activity in visual brain structures. However, this result raises important methodological and conceptual issues.

From the methodological viewpoint, the use of multivariate rather than mass univariate analysis requires further validation. The multivariate technique is a very sensitive method

for finding differences between sets of data, but the physiological basis and functional significance of these differences is not yet clear. Further work to clarify the underlying basis for this relatively new form of fMRI analysis is needed. My results suggest that it is not just the retinal location of a stimulus that is encoded in visual cortex, but the study did not distinguish between egocentric and world-centred representations which were both altered in the two different gaze conditions. Additionally whether this information is actually used by the brain in visiomotor transformations is uncertain. Finally, the source of eye position signals in visual cortex is unknown. One possibility is that higher areas involved in occulomotor control (such as parietal and frontal areas) send information about gaze direction to visual cortex but equally proprioceptive information from the eye itself could play a role.

8.4 The effect of varying visual stimulation on oculomotor brain responses

Rather than examining the effect of eye movements on visual structures when visual conditions remain constant, the experiment outlined in Chapter 7 examined the effect of altering visual conditions on oculomotor structures with the eyes fixated centrally. Specifically monocular responses in the SC, a structure that receives both visual and oculomotor input were examined when the visual hemifield that stimuli were presented in was varied. The experiment utilized eye patching to reverse which visual hemifield (left or right) is temporal or nasal, a technique that has uncovered pronounced behavioural advantages for orienting towards visual stimuli in the temporal versus the nasal hemifield, in newborns (Lewis and Maurer, 1992;Rothbart et al., 1990) and adults (Kristjansson et al., 2004;Rafal et al., 1991). The results suggested that human SC responses, but not those of the LGN or V1-V3, were significantly greater for monocular visual stimuli presented in the temporal hemifield than in the nasal hemifield.

These results provide evidence for a biased representation favouring the temporal hemifield within the human SC and may be the neural substrate for the behavioural effects described above in both normals and hemianopic subjects with blindsight. Similar behavioural biases have recently been shown audio-visual crossmodal integration (Bertini

et al., 2008), this could provide the basis for an interesting follow up study. However, there is growing evidence that temporal/nasal biases in visual orientating may not be mediated by the SC in either of these subject groups (Bompas et al., 2008;Walker et al., 2000). Further studies are needed to asses the behavioural significance of the biased hemifield representation found in SC. These would involve imaging studies of visual orientating behaviour in addition to passive viewing of visual stimuli.

Animal studies using single cell recording or targeted lesions have found that the SC has an important role in integrating visual and oculomotor information, and in behaviours that utilize such information such as visual orientating and covert shifts of attention (Ignashchenkova et al., 2004). The role of human SC in similar behaviours has not been extensively studied, largely because its small size and location make it technically difficult to study using non-invasive methods. The study presented in this thesis is one of the first to successfully use fMRI to examine human SC responses directly by utilizing ultra high resolution fMRI. Similar methods should allow the investigation of other roles of human SC to be performed.

Visual influences on oculomotor structures are not limited to the SC, indeed primate FEF encodes a visual salience map (Thompson and Bichot, 2005) that contributes to rapid covert or overt shifts of attention to salient locations in the visual field. However, the extent to which visual conditions modulate human oculomotor activity at other locations within the oculomotor system remains to be seen. Further studies could examine visual responses in higher oculomotor areas in parietal and frontal regions (such as FEF). One method that may be usefully employed in such studies is cortical flattening which allows precise delineation of functional brain areas and generation of accurate topographic maps of function. This method is used to define retinotopic visual areas, but more recently has been used in frontal cortex (Soon et al., 2008), although in a completely different context. It would be interesting to examine whether visual responses in human FEF are retinotopically organised and whether they show temporal/nasal asymmetry suggesting top-down, rather than bottom-up influences drive the behavioural hemifield biases. In addition, the neural basis for top down influences on visual orientating could be explored using such methods.

8.5 Conclusion

In summary, my findings provide direct evidence of visual and oculomotor interactions within human brain structures that are primarily thought of as either visual or oculomotor. Activity in early visual structures, both subcortically (LGN) and cortically (V1-V3) is profoundly influenced by different types of oculomotor behaviour. This interaction acts to both compensate for the visual effects of oculomotor behaviour and also to transform visual information into a form that can be used for action by the motor system. Saccadic eye movements modulate early stages in visual processing (particularly LGN) through the influence of an efference copy of the saccade motor plan (generated by oculomotor planning structures such as FEF). My findings suggest that this limits the disruptive perceptual effects of rapid eye movements. However, emerging animal evidence suggests that signals from occulomotor structures directly modify the receptive field properties of neurons in visual structures, a process that may mediate attentional shifts to salient locations in the visual field. The use of effective connectivity modelling and/or concurrent TMS/fMRI will allow these issues to be investigated in human subjects. Whether other types of eye movement, such as smooth pursuit or microsaccades, lead to similar modulation of visual structures has received minimal attention and could be studied using similar methods to those presented in this thesis.

In addition to eye movements, static oculomotor behaviour, such as the direction of gaze fixation also modulates human visual cortex. This may be important in the early stages of transformation of visual information from retinotopic to egocentric coordinates that can then guide motor behaviour. The underlying mechanisms that cause gaze modulation of visual responses are not clear and require further study. Finally, I have demonstrated that visual activity in an ‘oculomotor’ structure, the SC, shows a significant bias towards the periphery of the visual field. This may lead to biases in oculomotor behaviour that have been consistently demonstrated in a range of normal and brain damaged subjects. Additionally, the technical advances that enabled fMRI to be used in imaging SC can now be implemented to further explore the varied functions of SC. These include

crossmodal integration, a putative role in reward based learning as well as a crucial role in visual and occulomotor interactions.

The neural machinery that underpins human vision has been extensively studied. This thesis started by asserting that visual processing does not occur in isolation, but takes place within the context of dynamic oculomotor behaviour and then postulated that the physiological processes underlying visual processing and oculomotor behaviour must be highly integrated. The studies presented in this thesis add weight to this assertion. I have demonstrated profound oculomotor influences in primarily visual brain structures and visual influences in primarily oculomotor structures. The consequences of these interactions and the underlying mechanisms require further study. However, the existence of such interactions adds depth to models of the neural mechanisms of visual behaviour and perception and should be considered carefully when looking at other areas of human cognition that have traditionally been studied in isolation.

References

Adler R.J. (1981). The geometry of random fields (New York.

Andersen,R.A., Essick,G.K., and Siegel,R.M. (1985). Encoding of spatial location by posterior parietal neurons. Science *230*, 456-458.

Andersen,R.A., Essick,G.K., and Siegel,R.M. (1987). Neurons of area 7 activated by both visual stimuli and oculomotor behavior. Exp. Brain Res. *67*, 316-322.

Andersen,R.A., and Mountcastle,V.B. (1983). The influence of the angle of gaze upon the excitability of the light-sensitive neurons of the posterior parietal cortex. J. Neurosci. *3*, 532-548.

Anderson,T.J., Jenkins,I.H., Brooks,D.J., Hawken,M.B., Frackowiak,R.S., and Kennard,C. (1994). Cortical control of saccades and fixation in man. A PET study. Brain *117 (Pt 5)*, 1073-1084.

Andersson,F., Etard,O., Denise,P., and Petit,L. (2004). Early visual evoked potentials are modulated by eye position in humans induced by whole body rotations. BMC. Neurosci. *5*, 35.

Anstis,S.M. (1974). Letter: A chart demonstrating variations in acuity with retinal position. Vision Res. *14*, 589-592.

Ashburner,J., Neelin,P., Collins,D.L., Evans,A., and Friston,K. (1997). Incorporating prior knowledge into image registration. Neuroimage. *6*, 344-352.

Attwell,D., and Laughlin,S.B. (2001). An energy budget for signaling in the grey matter of the brain. J Cereb Blood Flow Metab *21*, 1133-1145.

Azzopardi,P., and Cowey,A. (1996). The overrepresentation of the fovea and adjacent retina in the striate cortex and dorsal lateral geniculate nucleus of the macaque monkey. Neuroscience *72*, 627-639.

Baker,J.T., Donoghue,J.P., and Sanes,J.N. (1999). Gaze direction modulates finger movement activation patterns in human cerebral cortex. J. Neurosci. *19*, 10044-10052.

Bartlett,J.R., Doty,R.W., Lee,B.B., Sr., and Sakakura,H. (1976). Influence of saccadic eye movements on geniculostriate excitability in normal monkeys. Exp. Brain Res. *25*, 487-509.

Berman,N., Blakemore,C., and Cynader,M. (1975). Binocular interaction in the cat's superior colliculus. J. Physiol *246*, 595-615.

Berman,R.A., Colby,C.L., Genovese,C.R., Voyvodic,J.T., Luna,B., Thulborn,K.R., and Sweeney,J.A. (1999). Cortical networks subserving pursuit and saccadic eye movements in humans: an FMRI study. Hum. Brain Mapp. *8*, 209-225.

Bertini,C., Leo,F., and Ladavas,E. (2008). Temporo-nasal asymmetry in multisensory integration mediated by the Superior Colliculus. Brain Res.

Bisley,J.W., and Goldberg,M.E. (2003b). Neuronal activity in the lateral intraparietal area and spatial attention. Science *299*, 81-86.

Bisley,J.W., and Goldberg,M.E. (2003a). Neuronal activity in the lateral intraparietal area and spatial attention. Science *299*, 81-86.

Blatt,G.J., Andersen,R.A., and Stoner,G.R. (1990). Visual receptive field organization and cortico-cortical connections of the lateral intraparietal area (area LIP) in the macaque. J. Comp Neurol. *299*, 421-445.

Bodis-Wollner,I., Bucher,S.F., and Seelos,K.C. (1999). Cortical activation patterns during voluntary blinks and voluntary saccades. Neurology *53*, 1800-1805.

Bodis-Wollner,I., Bucher,S.F., Seelos,K.C., Paulus,W., Reiser,M., and Oertel,W.H. (1997). Functional MRI mapping of occipital and frontal cortical activity during voluntary and imagined saccades. Neurology *49*, 416-420.

Bompas,A., Sterling,T., Rafal,R.D., and Sumner,P. (2008). Naso-temporal asymmetry for signals invisible to the retinotectal pathway. J. Neurophysiol.

Brainard,D.H. (1996). Cone contrast and opponent modulation color spaces. In Human Color Vision, Kaiser and Boynton, ed. (Washington: Optical Siciety of America).

Brenner,E., Smeets,J.B., and van den Berg,A.V. (2001). Smooth eye movements and spatial localisation. Vision Res. *41*, 2253-2259.

Bridgeman,B., Hendry,D., and Stark,L. (1975). Failure to detect displacement of the visual world during saccadic eye movements. Vision Res. *15*, 719-722.

Bridgeman,B., and Stark,L. (1991). Ocular proprioception and efference copy in registering visual direction. Vision Res. *31*, 1903-1913.

Bristow,D., Haynes,J.D., Sylvester,R., Frith,C.D., and Rees,G. (2005). Blinking suppresses the neural response to unchanging retinal stimulation. Curr. Biol. *15*, 1296-1300.

Brotchie,P.R., Andersen,R.A., Snyder,L.H., and Goodman,S.J. (1995). Head position signals used by parietal neurons to encode locations of visual stimuli. Nature *375*, 232-235.

Bruce,C.J., and Goldberg,M.E. (1985). Primate frontal eye fields. I. Single neurons discharging before saccades. J Neurophysiol. *53*, 603-635.

Bruce,C.J., Goldberg,M.E., Bushnell,M.C., and Stanton,G.B. (1985). Primate frontal eye fields. II. Physiological and anatomical correlates of electrically evoked eye movements. J Neurophysiol. *54*, 714-734.

Burr,D.C., Holt,J., Johnstone,J.R., and Ross,J. (1982). Selective depression of motion sensitivity during saccades. J. Physiol *333*, 1-15.

Burr,D.C., Morgan,M.J., and Morrone,M.C. (1999). Saccadic suppression precedes visual motion analysis. Curr. Biol. *9*, 1207-1209.

Burr,D.C., Morrone,M.C., and Ross,J. (1994). Selective suppression of the magnocellular visual pathway during saccadic eye movements. Nature *371*, 511-513.

Burr,D.C., and Ross,J. (1982). Contrast sensitivity at high velocities. Vision Res. *22*, 479-484.

Bushnell,M.C., Goldberg,M.E., and Robinson,D.L. (1981). Behavioral enhancement of visual responses in monkey cerebral cortex. I. Modulation in posterior parietal cortex related to selective visual attention. J. Neurophysiol. *46*, 755-772.

Buxton,R.B., and Frank,L.R. (1997). A model for the coupling between cerebral blood flow and oxygen metabolism during neural stimulation. J Cereb Blood Flow Metab *17*, 64-72.

Campos,M., Cherian,A., and Segraves,M.A. (2006). Effects of eye position upon activity of neurons in macaque superior colliculus. J. Neurophysiol. *95*, 505-526.

Carpenter,R.H.S. (1988). Movements of the Eyes (London: Pion).

Castet,E., and Masson,G.S. (2000). Motion perception during saccadic eye movements. Nat. Neurosci. *3*, 177-183.

Cavanaugh,J., and Wurtz,R.H. (2004). Subcortical modulation of attention counters change blindness. J. Neurosci. *24*, 11236-11243.

Cholet,N., Seylaz,J., Lacombe,P., and Bonvento,G. (1997). Local uncoupling of the cerebrovascular and metabolic responses to somatosensory stimulation after neuronal nitric oxide synthase inhibition. J Cereb Blood Flow Metab *17*, 1191-1201.

Christianini,N.S.-T.J. (2000). Support vector machines and other kernel based learning methods (Cambridge: Cambridge University Press).

Colby,C.L., Duhamel,J.R., and Goldberg,M.E. (1996). Visual, presaccadic, and cognitive activation of single neurons in monkey lateral intraparietal area. J Neurophysiol. *76*, 2841-2852.

Connolly,J.D., Goodale,M.A., Goltz,H.C., and Munoz,D.P. (2005). fMRI activation in the human frontal eye field is correlated with saccadic reaction time. J. Neurophysiol. *94*, 605-611.

Connolly,M., and Van Essen,D. (1984). The representation of the visual field in parvicellular and magnocellular layers of the lateral geniculate nucleus in the macaque monkey. J Comp Neurol. *226*, 544-564.

Cox,D.D., and Savoy,R.L. (2003). Functional magnetic resonance imaging (fMRI) "brain reading": detecting and classifying distributed patterns of fMRI activity in human visual cortex. Neuroimage. *19*, 261-270.

Cynader,M., and Berman,N. (1972). Receptive-field organization of monkey superior colliculus. J. Neurophysiol. *35*, 187-201.

Darby,D.G., Nobre,A.C., Thangaraj,V., Edelman,R., Mesulam,M.M., and Warach,S. (1996). Cortical activation in the human brain during lateral saccades using EPISTAR functional magnetic resonance imaging. Neuroimage. *3*, 53-62.

Davis,T.L., Kwong,K.K., Weisskoff,R.M., and Rosen,B.R. (1998). Calibrated functional MRI: mapping the dynamics of oxidative metabolism. Proc Natl Acad Sci U S A *95*, 1834-1839.

DeSouza,J.F., Dukelow,S.P., Gati,J.S., Menon,R.S., Andersen,R.A., and Vilis,T. (2000). Eye position signal modulates a human parietal pointing region during memory-guided movements. J. Neurosci. *20*, 5835-5840.

DeSouza,J.F., Dukelow,S.P., and Vilis,T. (2002). Eye position signals modulate early dorsal and ventral visual areas. Cereb. Cortex *12*, 991-997.

Deubel,H., Bridgeman,B., and Schneider,W.X. (1998). Immediate post-saccadic information mediates space constancy. Vision Res. *38*, 3147-3159.

Deutschlander,A., Marx,E., Stephan,T., Riedel,E., Wiesmann,M., Dieterich,M., and Brandt,T. (2005). Asymmetric modulation of human visual cortex activity during 10 degrees lateral gaze (fMRI study). Neuroimage. *28*, 4-13.

Diamond,M.R., Ross,J., and Morrone,M.C. (2000). Extraretinal control of saccadic suppression. J. Neurosci. *20*, 3449-3455.

Dickinson,A.R., Calton,J.L., and Snyder,L.H. (2003). Nonspatial saccade-specific activation in area LIP of monkey parietal cortex. J. Neurophysiol. *90*, 2460-2464.

Dodds,C., Machado,L., Rafal,R., and Ro,T. (2002). A temporal/nasal asymmetry for blindsight in a localisation task: evidence for extrageniculate mediation. Neuroreport *13*, 655-658.

Dodge,R. (1905). The illusion of clear vision during eye movement. Psychological Bulletin *3*, 193-199.

Dougherty,R.F., Koch,V.M., Brewer,A.A., Fischer,B., Modersitzki,J., and Wandell,B.A. (2003). Visual field representations and locations of visual areas V1/2/3 in human visual cortex. J. Vis. *3*, 586-598.

Dragoi,V., Sharma,J., and Sur,M. (2000). Adaptation-induced plasticity of orientation tuning in adult visual cortex. Neuron *28*, 287-298.

DuBois,R.M., and Cohen,M.S. (2000). Spatiotopic organization in human superior colliculus observed with fMRI. Neuroimage. *12*, 63-70.

Duffy,F.H., and Burchfiel,J.L. (1975). Eye movement-related inhibition of primate visual neurons. Brain Res. *89*, 121-132.

Duhamel,J.R., Colby,C.L., and Goldberg,M.E. (1992). The updating of the representation of visual space in parietal cortex by intended eye movements. Science *255*, 90-92.

Duhamel,J.R., Colby,C.L., and Goldberg,M.E. (1998). Ventral intraparietal area of the macaque: congruent visual and somatic response properties. J Neurophysiol. 79(1):126-36.

Dumoulin,S.O., Bittar,R.G., Kabani,N.J., Baker,C.L., Jr., Le,G.G., Bruce,P.G., and Evans,A.C. (2000). A new anatomical landmark for reliable identification of human area V5/MT: a quantitative analysis of sulcal patterning. Cereb. Cortex *10*, 454-463.

Duvernoy,H.M. (1999). The Human Brain (New York.

Engel,S., Zhang,X., and Wandell,B. (1997). Colour tuning in human visual cortex measured with functional magnetic resonance imaging. Nature *388*, 68-71.

Engel,S.A., Rumelhart,D.E., Wandell,B.A., Lee,A.T., Glover,G.H., Chichilnisky,E.J., and Shadlen,M.N. (1994). fMRI of human visual cortex. Nature *369*, 525.

Everling,S., and Munoz,D.P. (2000). Neuronal correlates for preparatory set associated with pro-saccades and anti-saccades in the primate frontal eye field. J. Neurosci. *20*, 387-400.

Felisberti,F., and Derrington,A.M. (1999). Long-range interactions modulate the contrast gain in the lateral geniculate nucleus of cats. Vis. Neurosci. *16*, 943-956.

Felleman,D.J., and Van Essen,D.C. (1991). Distributed hierarchical processing in the primate cerebral cortex. Cereb Cortex *1*, 1-47.

Fischer,W.H., Schmidt,M., and Hoffmann,K.P. (1998). Saccade-induced activity of dorsal lateral geniculate nucleus X- and Y-cells during pharmacological inactivation of the cat pretectum. Vis. Neurosci. *15*, 197-210.

Fjeld,I.T., Ruksenas,O. and Heggelund,P. (2002). Brainstem modulation of visual response properties of single cells in the dorsal lateral geniculate nucleus of cat. J Physiol. 1;543(Pt 2):541-54.

Fox,P.T., and Raichle,M.E. (1986). Focal physiological uncoupling of cerebral blood flow and oxidative metabolism during somatosensory stimulation in human subjects. Proc. Natl. Acad. Sci. U. S. A *83*, 1140-1144.

Fox,P.T., Raichle,M.E., Mintun,M.A., and Dence,C. (1988). Nonoxidative glucose consumption during focal physiologic neural activity. Science *241*, 462-464.

Frassinetti,F., Angeli,V., Meneghello,F., Avanzi,S., and Ladavas,E. (2002). Long-lasting amelioration of visuospatial neglect by prism adaptation. Brain *125*, 608-623.

Fries,W. (1984). Cortical projections to the superior colliculus in the macaque monkey: a retrograde study using horseradish peroxidase. J. Comp Neurol. *230*, 55-76.

Friston,J.A. (1995). Spatial registration and normalization of images. Human Brain Mapping *3*, 165-189.

Friston,K.J., Buechel,C., Fink,G.R., Morris,J., Rolls,E., and Dolan,R.J. (1997). Psychophysiological and modulatory interactions in neuroimaging. Neuroimage. *6*, 218-229.

Friston,K.J., Harrison,L., and Penny,W. (2003b). Dynamic causal modelling. Neuroimage. *19*, 1273-1302.

Friston,K.J., Harrison,L., and Penny,W. (2003a). Dynamic causal modelling. Neuroimage. *19*, 1273-1302.

Friston,K.J., Josephs,O., Rees,G., and Turner,R. (1998). Nonlinear event-related responses in fMRI. Magn Reson. Med. *39*, 41-52.

Friston,K.J., Mechelli,A., Turner,R., and Price,C.J. (2000). Nonlinear responses in fMRI: the Balloon model, Volterra kernels, and other hemodynamics. Neuroimage. *12*, 466-477.

Friston,K.J., Williams,S., Howard,R., Frackowiak,R.S., and Turner,R. (1996). Movement-related effects in fMRI time-series. Magn Reson Med *35*, 346-355.

Funke,K. and Eysel,U.T. (1998). Inverse correlation of firing patterns of single topographically matched perigeniculate neurons and cat dorsal lateral geniculate relay cells. Vis Neurosci. 15(4):711-29.

Garcia-Perez,M.A., and Peli,E. (2001). Intrasaccadic perception. J. Neurosci. *21*, 7313-7322.

Gauthier,G.M., Nommay,D., and Vercher,J.L. (1990). The role of ocular muscle proprioception in visual localization of targets. Science *249*, 58-61.

Gilbert,C.D., Das,A., Ito,M., Kapadia,M., and Westheimer,G. (1996). Spatial integration and cortical dynamics. PNAS *93*, 615-622.

Gilchrist,I.D., Brown,V., and Findlay,J.M. (1997). Saccades without eye movements. Nature *390*, 130-131.

Glover,G.H., Li,T.Q., and Ress,D. (2000). Image-based method for retrospective correction of physiological motion effects in fMRI: RETROICOR. Magn Reson. Med. *44*, 162-167.

Gnadt,J.W., and Andersen,R.A. (1988). Memory related motor planning activity in posterior parietal cortex of macaque. Exp. Brain Res. *70*, 216-220.

Goldberg,M.E., Bisley,J., Powell,K.D., Gottlieb,J., and Kusunoki,M. (2002). The role of the lateral intraparietal area of the monkey in the generation of saccades and visuospatial attention. Ann. N. Y. Acad. Sci. *956*, 205-215.

Goldberg,M.E., and Wurtz,R.H. (1972). Activity of superior colliculus in behaving monkey. I. Visual receptive fields of single neurons. J. Neurophysiol. *35*, 542-559.

Goodale,M.A. (1998). Visuomotor control: Where does vision end and action begin? Current Biology *8*, R489-R491.

Grosbras,M.H., Laird,A.R., and Paus,T. (2005). Cortical regions involved in eye movements, shifts of attention, and gaze perception. Hum. Brain Mapp. *25*, 140-154.

Guimaraes,A.R., Melcher,J.R., Talavage,T.M., Baker,J.R., Ledden,P., Rosen,B.R., Kiang,N.Y., Fullerton,B.C., and Weisskoff,R.M. (1998). Imaging subcortical auditory activity in humans. Hum. Brain Mapp. *6*, 33-41.

Guitton D (1992). Control of saccadic eye and gaze movements by the superior colliculus and basal ganglia. In Eye Movements, Carpenter RHS, ed. (London: Macmillan), pp. 244-276.

Hagler,D.J., Jr., and Sereno,M.I. (2006). Spatial maps in frontal and prefrontal cortex. Neuroimage. *29*, 567-577.

Hanes,D.P., Patterson,W.F., and Schall,J.D. (1998). Role of frontal eye fields in countermanding saccades: visual, movement, and fixation activity. J Neurophysiol. *79*, 817-834.

Hanes,D.P., and Wurtz,R.H. (2001). Interaction of the frontal eye field and superior colliculus for saccade generation. J Neurophysiol. 85(2):804-15.

Hanes,D.P., and Schall,J.D. (1996). Neural control of voluntary movement initiation. Science *274*, 427-430.

Haynes,J.D., Deichmann,R., and Rees,G. (2005). Eye-specific effects of binocular rivalry in the human lateral geniculate nucleus. Nature *438*, 496-499.

Haynes,J.D., Lotto,R.B., and Rees,G. (2004). Responses of human visual cortex to uniform surfaces. Proc. Natl. Acad. Sci. U. S. A *101*, 4286-4291.

Haynes,J.D., and Rees,G. (2005). Predicting the orientation of invisible stimuli from activity in human primary visual cortex. Nat. Neurosci. *8*, 686-691.

Haynes,J.D., and Rees,G. (2006). Decoding mental states from brain activity in humans. Nat. Rev. Neurosci. *7*, 523-534.

Hilbig,H., Bidmon,H.J., Zilles,K., and Busecke,K. (1999). Neuronal and glial structures of the superficial layers of the human superior colliculus. Anat. Embryol. (Berl) *200*, 103-115.

Hoge,R.D., Atkinson,J., Gill,B., Crelier,G.R., Marrett,S., and Pike,G.B. (1999). Investigation of BOLD signal dependence on cerebral blood flow and oxygen consumption: the deoxyhemoglobin dilution model. Magn Reson Med *42*, 849-863.

Holt,E.B. (1901). Eye-movement and central anaesthesia. Harvard Psychological Studies *1*, 3-45.

Honda,H. (1993). Saccade-contingent displacement of the apparent position of visual stimuli flashed on a dimly illuminated structured background. Vision Res. *33*, 709-716.

Honda,H. (1995). Visual mislocalization produced by a rapid image displacement on the retina: examination by means of dichoptic presentation of a target and its background scene. Vision Res. *35*, 3021-3028.

Hubel,D.H., LeVay,S., and Wiesel,T.N. (1975). Mode of termination of retinotectal fibers in macaque monkey: an autoradiographic study. Brain Res. *96*, 25-40.

Huerta,M.F., Krubitzer,L.A., and Kaas,J.H. (1986). Frontal eye field as defined by intracortical microstimulation in squirrel monkeys, owl monkeys, and macaque monkeys: I. Subcortical connections. J Comp Neurol. *253*, 415-439.

Huerta,M.F., Krubitzer,L.A., and Kaas,J.H. (1987). Frontal eye field as defined by intracortical microstimulation in squirrel monkeys, owl monkeys, and macaque monkeys. II. Cortical connections. J Comp Neurol. *265*, 332-361.

Hyder,F., Rothman,D.L., Mason,G.F., Rangarajan,A., Behar,K.L., and Shulman,R.G. (1997). Oxidative glucose metabolism in rat brain during single forepaw stimulation: a spatially localized 1H[13C] nuclear magnetic resonance study. J. Cereb. Blood Flow Metab *17*, 1040-1047.

Hyder,F., Shulman,R.G., and Rothman,D.L. (1998). A model for the regulation of cerebral oxygen delivery. J Appl Physiol *85*, 554-564.

Ignashchenkova,A., Dicke,P.W., Haarmeier,T., and Thier,P. (2004). Neuron-specific contribution of the superior colliculus to overt and covert shifts of attention. Nat. Neurosci. *7*, 56-64.

Janssen,P., and Shadlen,M.N. (2005). A representation of the hazard rate of elapsed time in macaque area LIP. Nat. Neurosci. *8*, 234-241.

Johnson MH (1990). Cortical maturation and the development of visual attention in early infancy. Journal of Cognitive Neuroscience *2*, 81-95.

Josephs,O., Houseman,A.M., Friston,K., Turner,R. (1997). Physiological noise modelling for multi-slice EPI fMRI using SPM. Proceedings, Fifth Annual Meeting of the ISMRM, 1682.

Kamitani,Y., and Tong,F. (2005). Decoding the visual and subjective contents of the human brain. Nat. Neurosci. *8*, 679-685.

Kamitani,Y., and Tong,F. (2006). Decoding seen and attended motion directions from activity in the human visual cortex. Curr. Biol. *16*, 1096-1102.

Karten,H.J.(1989). The origins of neocortex. Connections and laminations as distinct events in evolution. Journal of Cognitive Neuroscience *1*, 291-301.

Kastner,S., O'Connor,D.H., Fukui,M.M., Fehd,H.M., Herwig,U., and Pinsk,M.A. (2004). Functional imaging of the human lateral geniculate nucleus and pulvinar. J. Neurophysiol. *91*, 438-448.

Kastner,S., De,W.P., Desimone,R., and Ungerleider,L.G. (1998). Mechanisms of directed attention in the human extrastriate cortex as revealed by functional MRI. Science *282*, 108-111.

King AJ. (2004). The superior colliculus. Curr Biol. 14(9):R335-8.

Kleiser,R., Seitz,R.J., and Krekelberg,B. (2004). Neural correlates of saccadic suppression in humans. Curr. Biol. *14*, 386-390.

Kristjansson,A., Vandenbroucke,M.W., and Driver,J. (2004). When pros become cons for anti- versus prosaccades: factors with opposite or common effects on different saccade types. Exp. Brain Res. *155*, 231-244.

Kuypers,H.G., and Lawrence,D.G. (1967). Cortical projections to the red nucleus and the brain stem in the Rhesus monkey. Brain Res. *4*, 151-188.

Kwong,K.K., Belliveau,J.W., Chesler,D.A., Goldberg,I.E., Weisskoff,R.M., Poncelet,B.P., Kennedy,D.N., Hoppel,B.E., Cohen,M.S., Turner,R., and . (1992). Dynamic magnetic resonance imaging of human brain activity during primary sensory stimulation. Proc. Natl. Acad. Sci. U. S. A *89*, 5675-5679.

Laemle,L.K. (1981). A Golgy study of cellular morphology in the superficial layers of superior colliculus man, Saimiri, and Macaca. J. Hirnforsch. *22*, 253-263.

Lamme,V.A., and Roelfsema,P.R. (2000). The distinct modes of vision offered by feedforward and recurrent processing. Trends Neurosci *23*, 571-579.

LeVay,S., Connolly,M., Houde,J., and Van Essen,D.C. (1985). The complete pattern of ocular dominance stripes in the striate cortex and visual field of the macaque monkey. J. Neurosci. *5*, 486-501.

Lewis,T.L., and Maurer,D. (1992). The development of the temporal and nasal visual fields during infancy. Vision Res. *32*, 903-911.

Lie,C., Specht,K., RitzlA., Eickhoff,S., Stephan,K.E., Meinke,A., Ziles,K., Fink,G.R (2004). fMRI delineates asymmetrical representation of nasotemporal visual hemifields in human cortex - a neural substrate for functional lateralization in the visual system. Proceedings 10th Meeting OHBM.

Logothetis,N.K., Pauls,J., Augath,M., Trinath,T., and Oeltermann,A. (2001). Neurophysiological investigation of the basis of the fMRI signal. Nature *412*, 150-157.

Luck,S.J., Chelazzi,L., Hillyard,S.A., and Desimone,R. (1997). Neural mechanisms of spatial selective attention in areas V1, V2, and V4 of macaque visual cortex. J. Neurophysiol. *77*, 24-42.

Luna,B., Thulborn,K.R., Strojwas,M.H., McCurtain,B.J., Berman,R.A., Genovese,C.R., and Sweeney,J.A. (1998). Dorsal cortical regions subserving visually guided saccades in humans: an fMRI study. Cereb. Cortex *8*, 40-47.

Lynch,J.C., Graybiel,A.M., and Lobeck,L.J. (1985). The differential projection of two cytoarchitectonic subregions of the inferior parietal lobule of macaque upon the deep layers of the superior colliculus. J. Comp Neurol. *235*, 241-254.

Magistretti,P.J., and Pellerin,L. (1999). Cellular mechanisms of brain energy metabolism and their relevance to functional brain imaging. Philos Trans R Soc Lond B Biol Sci *354*, 1155-1163.

Malpeli,J.G., and Baker,F.H. (1975). The representation of the visual field in the lateral geniculate nucleus of Macaca mulatta. J Comp Neurol. *161*, 569-594.

Mateeff,S., Yakimoff,N., and Dimitrov,G. (1981). Localization of brief visual stimuli during pursuit eye movements. Acta Psychol. (Amst) *48*, 133-140.

McPeek,R.M., and Keller,E.L. (2004a). Deficits in saccade target selection after inactivation of superior colliculus. Nat. Neurosci. *7*, 757-763.

McPeek,R.M., and Keller,E.L. (2004b). Deficits in saccade target selection after inactivation of superior colliculus. Nat. Neurosci. *7*, 757-763.

Merriam,E.P., Genovese,C.R., and Colby,C.L. (2003). Spatial updating in human parietal cortex. Neuron *39*, 361-373.

Michels,L., and Lappe,M. (2004). Contrast dependency of sacadic compression and suppression. Vision Res. *44*, 2327-2336.

Milner,A.D., and Goodale,M.A. (1995). The Visual Brain in Action (Oxford: Oxford University Press).

Mintun,M.A., Lundstrom,B.N., Snyder,A.Z., Vlassenko,A.G., Shulman,G.L., and Raichle,M.E. (2001). Blood flow and oxygen delivery to human brain during functional activity: theoretical modeling and experimental data. Proc Natl Acad Sci U S A *98*, 6859-6864.

Moore,T., and Armstrong,K.M. (2003a). Selective gating of visual signals by microstimulation of frontal cortex. Nature *421*, 370-373.

Moore,T., and Armstrong,K.M. (2003b). Selective gating of visual signals by microstimulation of frontal cortex. Nature *421*, 370-373.

Moore,T., and Fallah,M. (2001). Control of eye movements and spatial attention. Proc. Natl. Acad. Sci. U. S. A *98*, 1273-1276.

Moore,T., and Fallah,M. (2004). Microstimulation of the frontal eye field and its effects on covert spatial attention. J. Neurophysiol. *91*, 152-162.

Moors,J., and Vendrik,A.J. (1979). Responses of single units in the monkey superior colliculus to stationary flashing stimuli. Exp. Brain Res. *35*, 333-347.

Moran,J., and Desimone,R. (1985). Selective attention gates visual processing in the extrastriate cortex. Science *229*, 782-784.

Morrone,M.C., Ross,J., and Burr,D. (2005). Saccadic eye movements cause compression of time as well as space. Nat. Neurosci. *8*, 950-954.

Morrone,M.C., Ross,J., and Burr,D.C. (1997). Apparent position of visual targets during real and simulated saccadic eye movements. J. Neurosci. *17*, 7941-7953.

Movshon,J.A., and Lennie,P. (1979). Pattern-selective adaptation in visual cortical neurones. Nature *278*, 850-852.

Muller,J.R., Philiastides,M.G., and Newsome,W.T. (2005b). Microstimulation of the superior colliculus focuses attention without moving the eyes. Proc. Natl. Acad. Sci. U. S. A *102*, 524-529.

Muller,J.R., Philiastides,M.G., and Newsome,W.T. (2005a). Microstimulation of the superior colliculus focuses attention without moving the eyes. Proc. Natl. Acad. Sci. U. S. A *102*, 524-529.

Munoz,D.P., and Wurtz,R.H. (1993). Fixation cells in monkey superior colliculus. I. Characteristics of cell discharge. J. Neurophysiol. *70*, 559-575.

Munoz,D.P., Wurtz,R.H. (1993). Fixation cells in monkey superior colliculus. II. Reversible activation and deactivation. J Neurophysiol. 70(2):576-89.

Munoz,D.P., & Wurtz,R.H. (1995a). Saccade-related activity in monkey superior colliculus 1. Characteristics of burst and buildup cells. J Neurophysiol. 73(6), 2313-2333.

Munoz,D.P., & Wurtz,R.H. (1995b). Saccade-related activity in monkey superior colliculus 2. Spread of activity during saccades. J Neurophysiol. 73(6), 2334-2348.

Murata,A., Gallese,V., Kaseda,M., and Sakata,H. (1996). Parietal neurons related to memory-guided hand manipulation. J Neurophysiol. *75*, 2180-2186.

Nieman,D.R., Hayashi,R., Andersen,R.A., and Shimojo,S. (2005). Gaze direction modulates visual aftereffects in depth and color. Vision Res. *45*, 2885-2894.

Nishida,S., Motoyoshi,I., Andersen,R.A., and Shimojo,S. (2003). Gaze modulation of visual aftereffects. Vision Res. *43*, 639-649.

O'Connor,D.H., Fukui,M.M., Pinsk,M.A., and Kastner,S. (2002). Attention modulates responses in the human lateral geniculate nucleus. Nat. Neurosci. *5*, 1203-1209.

Obermayer,K., and Blasdel,G.G. (1993). Geometry of orientation and ocular dominance columns in monkey striate cortex. J Neurosci *13*, 4114-4129.

Ogawa,S., Lee,T.M., Nayak,A.S., and Glynn,P. (1990). Oxygenation-sensitive contrast in magnetic resonance image of rodent brain at high magnetic fields. Magn Reson. Med. *14*, 68-78.

Pauling,L., and Coryell,C.D. (1936). The Magnetic Properties and Structure of the Hemochromogens and Related Substances. Proc. Natl. Acad. Sci. U. S. A *22*, 159-163.

Paus,T., Marrett,S., Worsley,K.J., and Evans,A.C. (1995). Extraretinal modulation of cerebral blood flow in the human visual cortex: implications for saccadic suppression. J. Neurophysiol. *74*, 2179-2183.

Penny,W.D., Stephan,K.E., Mechelli,A., and Friston,K.J. (2004). Comparing dynamic causal models. Neuroimage. *22*, 1157-1172.

Perry,V.H., and Cowey,A. (1985). The ganglion cell and cone distributions in the monkey's retina: implications for central magnification factors. Vision Res. *25*, 1795-1810.

Perry,V.H., and Cowey,A. (1984). Retinal ganglion cells that project to the superior colliculus and pretectum in the macaque monkey. Neuroscience *12*, 1125-1137.

Pisella,L., Rode,G., Farne,A., Boisson,D., and Rossetti,Y. (2002). Dissociated long lasting improvements of straight-ahead pointing and line bisection tasks in two hemineglect patients. Neuropsychologia *40*, 327-334.

Platt,M.L., and Glimcher,P.W. (1999). Neural correlates of decision variables in parietal cortex. Nature *400*, 233-238.

Pollack,J.G., and Hickey,T.L. (1979). The distribution of retino-collicular axon terminals in rhesus monkey. J. Comp Neurol. *185*, 587-602.

Polyak,S.L. (1957). The vertebrate visual system. (Chicago: University of Chicago Press).

Porta,J.B. (1593). De refractione optices parte: Libri novem. (Naples: Carlinum & Pacem).

Posner M I Cohen Y (1984). Components of visual orientating. In Attention and performance X, Douma H Bouwhuis D, ed. (London: Lawrence Erlbaum), pp. 531-556.

Powers,W.J., Hirsch,I.B., and Cryer,P.E. (1996). Effect of stepped hypoglycemia on regional cerebral blood flow response to physiological brain activation. Am J Physiol *270*, H554-H559.

Przybyszewski,A.W., Gaska,J.P., Foote,W., and Pollen,D.A. (2000). Striate cortex increases contrast gain of macaque LGN neurons. Vis. Neurosci. *17*, 485-494.

Rafal,R., Henik,A., Smith,J. (1991). Extrageniculate contributions to reflex visual orientating in normal humans: A temporal hemifield advantage. Journal of Cognitive Neuroscience *3*, 322-328.

Rafal,R., Smith,J., Krantz,J., Cohen,A., and Brennan,C. (1990). Extrageniculate vision in hemianopic humans: saccade inhibition by signals in the blind field. Science *250*, 118-121.

Raichle,M.E., MacLeod,A.M., Snyder,A.Z., Powers,W.J., Gusnard,D.A., and Shulman,G.L. (2001). A default mode of brain function. Proc. Natl. Acad. Sci. U. S. A *98*, 676-682.

Rambold,H., El,B., I, and Helmchen,C. (2004). Differential effects of blinks on horizontal saccade and smooth pursuit initiation in humans. Exp. Brain Res. *156*, 314-324.

Ramcharan,E.J., Gnadt,J.W., and Sherman,S.M. (2001). The effects of saccadic eye movements on the activity of geniculate relay neurons in the monkey. Vis. Neurosci. *18*, 253-258.

Rees,G., Friston,K., and Koch,C. (2000). A direct quantitative relationship between the functional properties of human and macaque V5. Nat Neurosci *3*, 716-723.

Rees,G., Frith,C.D., and Lavie,N. (1997). Modulating irrelevant motion perception by varying attentional load in an unrelated task. Science *278*, 1616-1619.

Reppas,J.B., Usrey,W.M., and Reid,R.C. (2002). Saccadic eye movements modulate visual responses in the lateral geniculate nucleus. Neuron *35*, 961-974.

Reynolds,J.H., and Desimone,R. (2003). Interacting roles of attention and visual salience in V4. Neuron *37*, 853-863.

Riggs,L.A., Merton,P.A., and Morton,H.B. (1974). Suppression of visual phosphenes during saccadic eye movements. Vision Res. *14*, 997-1011.

Rizzolatti,G., Riggio,L., Dascola,I., and Umilta,C. (1987). Reorienting attention across the horizontal and vertical meridians: evidence in favor of a premotor theory of attention. Neuropsychologia *25*, 31-40.

Robinson DL, McClurkin JW. (1989). The visual superior colliculus and pulvinar. Rev Oculomot Res. 3:337-60.

Roitman,J.D., and Shadlen,M.N. (2002). Response of neurons in the lateral intraparietal area during a combined visual discrimination reaction time task. J. Neurosci. *22*, 9475-9489.

Rosenbluth,D., and Allman,J.M. (2002). The effect of gaze angle and fixation distance on the responses of neurons in V1, V2, and V4. Neuron *33*, 143-149.

Ross,J., Morrone,M.C., and Burr,D.C. (1997). Compression of visual space before saccades. Nature *386*, 598-601.

Rossetti,Y., Rode,G., Pisella,L., Farne,A., Li,L., Boisson,D., and Perenin,M.T. (1998). Prism adaptation to a rightward optical deviation rehabilitates left hemispatial neglect. Nature *395*, 166-169.

Rothbart,M.K., Posner,M.I., Boylan,A. (1990). Regulatory mechanisms in infant development. In The development of attention: Research and theory, Enns J T, ed. (Amsterdam: Elsevier), pp. 139-160.

Ruff,C.C., Blankenburg,F., Bjoertomt,O., Bestmann,S., Freeman,E., Haynes,J.D., Rees,G., Josephs,O., Deichmann,R., and Driver,J. (2006). Concurrent TMS-fMRI and psychophysics reveal frontal influences on human retinotopic visual cortex. Curr. Biol. *16*, 1479-1488.

Sato,M., and Uchikawa,K. (1999). Increment-threshold spectral sensitivity during saccadic eye movements in uniform visual field. Vision Res. *39*, 3951-3959.

Saul,A.B., and Cynader,M.S. (1989). Adaptation in single units in visual cortex: the tuning of aftereffects in the spatial domain. Vis. Neurosci. *2*, 593-607.

Schall,J.D., Morel,A., King,D.J., and Bullier,J. (1995). Topography of visual cortex connections with frontal eye field in macaque: convergence and segregation of processing streams. J Neurosci *15*, 4464-4487.

Schall,J.D., and Thompson,K.G. (1999). Neural selection and control of visually guided eye movements. Annu. Rev. Neurosci *22*, 241-259.

Schiller,P.H., and Malpeli,J.G. (1977). Properties and tectal projections of monkey retinal ganglion cells. J. Neurophysiol. *40*, 428-445.

Schneider,K.A., and Kastner,S. (2005). Visual responses of the human superior colliculus: a high-resolution functional magnetic resonance imaging study. J. Neurophysiol. *94*, 2491-2503.

Schneider,K.A., Richter,M.C., and Kastner,S. (2004). Retinotopic organization and functional subdivisions of the human lateral geniculate nucleus: a high-resolution functional magnetic resonance imaging study. J Neurosci *24*, 8975-8985.

Schwartz,W.J., Smith,C.B., Davidsen,L., Savaki,H., Sokoloff,L., Mata,M., Fink,D.J., and Gainer,H. (1979). Metabolic mapping of functional activity in the hypothalamo-neurohypophysial system of the rat. Science *205*, 723-725.

Segraves,M.A. (1992). Activity of monkey frontal eye field neurons projecting to oculomotor regions of the pons. J Neurophysiol. *68*, 1967-1985.

Segraves,M.A., and Goldberg,M.E. (1987). Functional properties of corticotectal neurons in the monkey's frontal eye field. J Neurophysiol. *58*, 1387-1419.

Sereno,M.I., Dale,A.M., Reppas,J.B., Kwong,K.K., Belliveau,J.W., Brady,T.J., Rosen,B.R., and Tootell,R.B. (1995). Borders of multiple visual areas in humans revealed by functional magnetic resonance imaging. Science *268*, 889-893.

Sereno,M.I., Pitzalis,S., and Martinez,A. (2001). Mapping of contralateral space in retinotopic coordinates by a parietal cortical area in humans. Science *294*, 1350-1354.

Sherman,S.M., and Guillery,R.W. (2002). The role of the thalamus in the flow of information to the cortex. Philos. Trans. R. Soc. Lond B Biol. Sci. *357*, 1695-1708.

Shulman,R.G., Hyder,F., and Rothman,D.L. (2001). Cerebral energetics and the glycogen shunt: neurochemical basis of functional imaging. Proc Natl Acad Sci U S A *98*, 6417-6422.

Shulman,R.G., and Rothman,D.L. (1998). Interpreting functional imaging studies in terms of neurotransmitter cycling. Proc Natl Acad Sci U S A *95*, 11993-11998.

Sibson,N.R., Dhankhar,A., Mason,G.F., Rothman,D.L., Behar,K.L., and Shulman,R.G. (1998). Stoichiometric coupling of brain glucose metabolism and glutamatergic neuronal activity. Proc Natl Acad Sci U S A *95*, 316-321.

Sillito,A.M., and Jones,H.E. (2002). Corticothalamic interactions in the transfer of visual information. Philos. Trans. R. Soc. Lond B Biol. Sci. *357*, 1739-1752.

Smith,A.T., Singh,K.D., Williams,A.L., and Greenlee,M.W. (2001). Estimating receptive field size from fMRI data in human striate and extrastriate visual cortex. Cereb. Cortex *11*, 1182-1190.

Snyder,L.H., Batista,A.P., and Andersen,R.A. (1997). Coding of intention in the posterior parietal cortex. Nature *386*, 167-170.

Sommer,M.A., and Tehovnik,E.J. (1997). Reversible inactivation of macaque frontal eye field. Exp. Brain Res. *116*, 229-249.

Sommer,M.A., and Wurtz,R.H. (1998). Frontal eye field neurons orthodromically activated from the superior colliculus. J Neurophysiol. *80*, 3331-3335.

Sommer,M.A., and Wurtz,R.H. (2001). Frontal eye field sends delay activity related to movement, memory, and vision to the superior colliculus. J Neurophysiol. *85*, 1673-1685.

Sommer,M.A., and Wurtz,R.H. (2006). Influence of the thalamus on spatial visual processing in frontal cortex. Nature. 16;444(7117):374-7.

Soon,C.S., Brass,M., Heinze,H.J., and Haynes,J.D. (2008). Unconscious determinants of free decisions in the human brain. Nat. Neurosci. *11*, 543-545.

Sparks,D.L. (2002). The brainstem control of saccadic eye movements. Nat. Rev. Neurosci. *3*, 952-964.

Sparks DL, Hartwich-Young R. (1989). The deep layers of the superior colliculus. Rev Oculomot Res. 3:213-55.

Stanton,G.B., Bruce,C.J., and Goldberg,M.E. (1995). Topography of projections to posterior cortical areas from the macaque frontal eye fields. J Comp Neurol. *353*, 291-305.

Stephan,K.E., Harrison,L.M., Penny,W.D., and Friston,K.J. (2004b). Biophysical models of fMRI responses. Curr. Opin. Neurobiol. *14*, 629-635.

Stephan,K.E., Harrison,L.M., Penny,W.D., and Friston,K.J. (2004a). Biophysical models of fMRI responses. Curr. Opin. Neurobiol. *14*, 629-635.

Sterling,P. (1973). Quantitative mapping with the electron microscope: retinal terminals in the superior colliculus. Brain Res. *54*, 347-354.

Stettler,D.D., Das,A., Bennett,J., and Gilbert,C.D. (2002). Lateral connectivity and contextual interactions in macaque primary visual cortex. Neuron *36*, 739-750.

Stone,J., and Johnston,E. (1981). The topography of primate retina: a study of the human, bushbaby, and new- and old-world monkeys. J. Comp Neurol. *196*, 205-223.

Sumner,P., Adamjee,T., and Mollon,J.D. (2002). Signals invisible to the collicular and magnocellular pathways can capture visual attention. Curr. Biol. *12*, 1312-1316.

Super,H., van der,T.C., Spekreijse,H., and Lamme,V.A. (2004). Correspondence of presaccadic activity in the monkey primary visual cortex with saccadic eye movements. Proc. Natl. Acad. Sci. U. S. A *101*, 3230-3235.

Sylvester,R., Haynes,J.D., and Rees,G. (2005). Saccades differentially modulate human LGN and V1 responses in the presence and absence of visual stimulation. Curr. Biol. *15*, 37-41.

Tardif,E., Delacuisine,B., Probst,A., and Clarke,S. (2005). Intrinsic connectivity of human superior colliculus. Exp. Brain Res. *166*, 316-324.

Taylor,P.C., Nobre,A.C., and Rushworth,M.F. (2006). FEF TMS Affects Visual Cortical Activity. Cereb. Cortex.

Tehovnik,E.J., Sommer,M.A., Chou,I.H., Slocum,W.M., and Schiller,P.H. (2000b). Eye fields in the frontal lobes of primates. Brain Res. Brain Res. Rev. *32*, 413-448.

Tehovnik,E.J., Sommer,M.A., Chou,I.H., Slocum,W.M., and Schiller,P.H. (2000a). Eye fields in the frontal lobes of primates. Brain Res. Brain Res. Rev. *32*, 413-448.

Teo,P.C., Sapiro,G., and Wandell,B.A. (1997). Creating connected representations of cortical gray matter for functional MRI visualization. IEEE Trans. Med. Imaging *16*, 852-863.

Thiele,A., Henning,P., Kubischik,M., and Hoffmann,K.P. (2002). Neural mechanisms of saccadic suppression. Science *295*, 2460-2462.

Thilo,K.V., Santoro,L., Walsh,V., and Blakemore,C. (2004). The site of saccadic suppression. Nat. Neurosci. *7*, 13-14.

Thompson,K.G., and Bichot,N.P. (2005). A visual salience map in the primate frontal eye field. Prog. Brain Res. *147*, 251-262.

Tolias,A.S., Moore,T., Smirnakis,S.M., Tehovnik,E.J., Siapas,A.G., and Schiller,P.H. (2001). Eye movements modulate visual receptive fields of V4 neurons. Neuron *29*, 757-767.

Trotter,Y., and Celebrini,S. (1999). Gaze direction controls response gain in primary visual-cortex neurons. Nature *398*, 239-242.

Turner,R., Howseman,A., Rees,G.E., Josephs,O., and Friston,K. (1998). Functional magnetic resonance imaging of the human brain: data acquisition and analysis. Exp. Brain Res. *123*, 5-12.

Turner,R., Le,B.D., Moonen,C.T., Despres,D., and Frank,J. (1991). Echo-planar time course MRI of cat brain oxygenation changes. Magn Reson. Med. *22*, 159-166.

Ungerleider,L.G., and Mishkin,M. (1982). Two cortical visual systems. In Analysis of Visual Behavior, D.J. Ingle, M.A. Goodale, and R.J.W. Mansfield, eds. (Cambridge, Massachusetts: MIT Press), pp. 549-586.

Vafaee,M.S., and Gjedde,A. (2000). Model of blood-brain transfer of oxygen explains nonlinear flow-metabolism coupling during stimulation of visual cortex. J Cereb Blood Flow Metab *20*, 747-754.

Vallines,I., and Greenlee,M.W. (2006). Saccadic suppression of retinotopically localized blood oxygen level-dependent responses in human primary visual area V1. J. Neurosci. *26*, 5965-5969.

Van Buren,J.M. (1963). The Retinal Ganglion Cell Layer (Springfield, IL: Charles C. Thomas Publishers).

Van Essen,D.C., Newsome,W.T., and Maunsell,J.H. (1984). The visual field representation in striate cortex of the macaque monkey: asymmetries, anisotropies, and individual variability. Vision Res. *24*, 429-448.

Vanzetta,I., and Grinvald,A. (1999). Increased cortical oxidative metabolism due to sensory stimulation: implications for functional brain imaging. Science *286*, 1555-1558.

Vapnik,V.N. (1995). The Nature of Statistical Learning Theory (New York.

Villringer,A., and Dirnagl,U. (1995). Coupling of brain activity and cerebral blood flow: basis of functional neuroimaging. Cerebrovasc. Brain Metab Rev. *7*, 240-276.

Volkmann,F.C. (1986). Human visual suppression. Vision Res. *26*, 1401-1416.

Volkmann,F.C., Riggs,L.A., and Moore,R.K. (1980). Eyeblinks and visual suppression. Science *207*, 900-902.

Vuilleumier,P., and Schwartz,S. (2001). Modulation of visual perception by eye gaze direction in patients with spatial neglect and extinction. Neuroreport *12*, 2101-2104.

Waitzman,D.M., Ma,T.P., Optican,L.M., and Wurtz,R.H. (1991). Superior colliculus neurons mediate the dynamic characteristics of saccades. J. Neurophysiol. *66*, 1716-1737.

Walker,R., Mannan,S., Maurer,D., Pambakian,A.L., and Kennard,C. (2000). The oculomotor distractor effect in normal and hemianopic vision. Proc. Biol. Sci. *267*, 431-438.

Wandell,B.A. (1995). Foundations of vision. Mass. Sinauer Associates.

Wandell,B.A. (1999). Computational neuroimaging of human visual cortex. Annu. Rev. Neurosci. *22*, 145-173.

Wandell,B.A., Chial,S., and Backus,B.T. (2000). Visualization and measurement of the cortical surface. J. Cogn Neurosci. *12*, 739-752.

Wardak,C., Ibos,G., Duhamel,J.R., and Olivier,E. (2006). Contribution of the monkey frontal eye field to covert visual attention. J. Neurosci. *26*, 4228-4235.

Wardak,C., Olivier,E., and Duhamel,J.R. (2002). Saccadic target selection deficits after lateral intraparietal area inactivation in monkeys. J. Neurosci. *22*, 9877-9884.

Weir,C.R., Knox,P.C., and Dutton,G.N. (2000). Does extraocular muscle proprioception influence oculomotor control? Br. J. Ophthalmol. *84*, 1071-1074.

Wenzel,R., Wobst,P., Heekeren,H.H., Kwong,K.K., Brandt,S.A., Kohl,M., Obrig,H., Dirnagl,U., and Villringer,A. (2000). Saccadic suppression induces focal hypooxygenation in the occipital cortex. J. Cereb. Blood Flow Metab *20*, 1103-1110.

Weyand,T.G., and Malpeli,J.G. (1993). Responses of neurons in primary visual cortex are modulated by eye position. J. Neurophysiol. *69*, 2258-2260.

Williams,C., Azzopardi,P., and Cowey,A. (1995). Nasal and temporal retinal ganglion cells projecting to the midbrain: implications for "blindsight". Neuroscience *65*, 577-586.

Wilson,M.E., and Toyne,M.J. (1970). Retino-tectal and cortico-tectal projections in Macaca mulatta. Brain Res. *24*, 395-406.

Wurtz,R.H., and Goldberg,M.E. (1972). Activity of superior colliculus in behaving monkey. 3. Cells discharging before eye movements. J. Neurophysiol. *35*, 575-586.

Yang,Y., Cao,P., Yang,Y., and Wang,S.R. (2008). Corollary discharge circuits for saccadic modulation of the pigeon visual system. Nat. Neurosci. *11*, 595-602.

Zuber,B.L., and Stark,L. (1966). Saccadic suppression: elevation of visual threshold associated with saccadic eye movements. Exp. Neurol. *16*, 65-79.